

1998

## CHARACTERIZATION OF GELLING PHENOMENON OF A LIPID BASED FORMULATION

Inayet Dumanli  
*University of Rhode Island*

Follow this and additional works at: <https://digitalcommons.uri.edu/theses>

Terms of Use

All rights reserved under copyright.

---

### Recommended Citation

Dumanli, Inayet, "CHARACTERIZATION OF GELLING PHENOMENON OF A LIPID BASED FORMULATION" (1998). *Open Access Master's Theses*. Paper 246.  
<https://digitalcommons.uri.edu/theses/246>

This Thesis is brought to you by the University of Rhode Island. It has been accepted for inclusion in Open Access Master's Theses by an authorized administrator of DigitalCommons@URI. For more information, please contact [digitalcommons-group@uri.edu](mailto:digitalcommons-group@uri.edu). For permission to reuse copyrighted content, contact the author directly.

CHARACTERIZATION OF GELLING PHENOMENON

OF A LIPID BASED FORMULATION

BY

INAYET DUMANLI

A THESIS SUBMITTED IN PARTIAL FULFILLMENT OF THE

REQUIREMENTS FOR THE DEGREE OF

MASTER OF SCIENCE

IN

APPLIED PHARMACEUTICAL SCIENCES

UNIVERSITY OF RHODE ISLAND

1998

MASTER OF SCIENCE THESIS

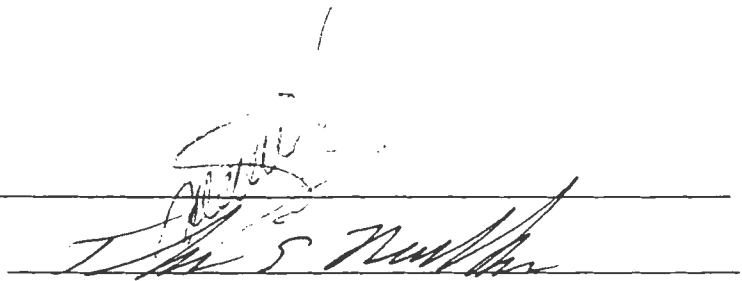
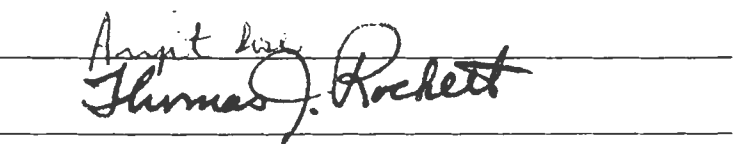
OF

INAYET DUMANLI

APPROVED:

Thesis Committee

Major Professor

  
\_\_\_\_\_  
  
\_\_\_\_\_

DEAN OF THE GRADUATE SCHOOL

UNIVERSITY OF RHODE ISLAND

1998

## ABSTRACT

In this study, gelling which occurred during the processing of a peptide drug formulation was investigated. The formulation was prepared by dissolving the drug in a lipid vehicle, composed of mono-, di- and triglycerides of Caprylic (C<sub>8</sub>) and Capric (C<sub>10</sub>) Acids (MCM). Gelling was observed during high shear mixing of the formulation. Therefore, to evaluate the gelled material, a solution of the drug in MCM was sheared at 3000 rpm until it turned into an opaque gel. The rheology, thermodynamic properties, chemical structure, polymorphism, particle size, moisture content and stability of the vehicle and pre- and post-sheared formulation were evaluated. The factors such as shear rate, temperature, time, humidity and solution concentration that may affect the development of a gel structure were investigated.

While rheograms of the vehicle and the drug solution showed Newtonian behavior, oscillatory measurements showed that there is a structure build up in the system. This interaction of the drug and the vehicle was postulated to occur via hydrogen bonds, and was shown by a Differential Scanning Calorimeter (DSC) and Fourier Transform Infrared (FT-IR).

It was determined that prolonged shearing changed the rheological behavior of the system from Newtonian to pseudoplastic. Shearing also caused physical modification of the system which was verified with FT-IR studies and X-Ray diffraction. Gelling was found to be a physical phenomenon and was shown to be reversible by heating.

Shear rate, shearing time, temperature and humidity were found to be the critical parameters that affect the gelation of the system. Gelling also was found to be highly concentration dependent. As the concentration increases, zero shear viscosity of the solution increases. The slope of the curve of zero shear viscosity vs. concentration changes sharply at a concentration above 17% (w/v) at which gelling starts. At a concentration of 15% (w/v) and below, a gel structure did not form. In addition, appearance of particles above 1 nm starts at 10% (w/v) concentration and the particle size increases as the concentration increases. DSC studies of the different solution concentrations suggest that the drug at increased concentrations interacts with a vehicle component. The solution reaches saturation at a concentration of 17% (w/v), and addition of the drug beyond this level may increase particle formation which acts as gel nuclei by interaction of the drug with vehicle components. Particle size increases at 40°C and disappears at 80°C. These temperature sensitive particles may cause phase transition upon shearing.

In order to avoid this gelling phenomenon during processing of the formulation of the drug, the vehicle components should be thoroughly characterized. The use of high shear should be avoided. If possible, all processing should be conducted at or above 60°C at low humidity levels.

## ACKNOWLEDGEMENTS

I would like to express my gratitude to my major professor, Dr. Serpil M. Kislalioglu, for her support in guiding this research.

I also would like to thank Dr. Waseem Malick for giving me the opportunity to use Hoffmann-La Roche Pharmaceutical Research facilities including the use of all instrumentation and materials and for financial support. I am very grateful to Drs. Navnit Shah, Wantanee Phuapradit and Martin Infeld for their valuable assistance in guiding me throughout this research.

I am thankful to Mr. Michael Lanyi for helping me in FT-IR studies, and to Mr. Renee Kirsch for assistance in X-Ray experiments. I am sincerely grateful to Dr. Fang-Chung Chen for his guidance in Laser Light experiments and to Dr. Rodolfo Pinal for valuable discussions regarding DSC studies.

I also wish to thank Drs. Thomas E. Needham and Arijit Bose, thesis committee members, for spending their valuable time on my thesis.

Finally, my warmest feelings and regards go to my parents, my family and friends for their endless moral support and full trust that enabled me to go through all the challenges in an environment of love.

## PREFACE

A model peptide drug is formulated as a lipid solution and encapsulated in soft-gel capsules. The drug has poor bioavailability and low aqueous solubility (0.03 mg/mL). It is a highly lipophilic drug with two pKas ( $pK_{a1} = 1.1$  and  $pK_{a2} = 7.1$ ) and with a partition coefficient of 3.34. The number of solvents that increase the solubility of the drug is very limited. Mono- di- and triglyceride of capric and caprylic acids (MCM) was selected for formulation development because of its suitable solvent properties. The final formulation contains 20% active substance in MCM. In preparing the formulation, the vehicle is heated and the drug is then added and stirred using a high shear mixer until a clear solution is obtained. The solution is cooled to 25°C. The formulation is encapsulated into soft-gel capsules at room temperature.

In order to improve patient compliance, the reduction of number of dosing units to be administrated is always desirable. This can be achieved by increasing the drug loading in the vehicle and thus reducing the number of capsules to be administrated. However, higher drug loading is extremely challenging because of the occurrence of gelling during processing.

It was observed that during processing, the formulation had a tendency to gel due to high shear mixing. Gelation can reduce the dissolution rate of the drug from the capsule, although it appears that gelling does not have a significant effect on drug bioavailability. However, during processing, the capsule fill formulation should remain as a solution and

preferably stay as such in the soft-gel capsule throughout the product shelf life. Gelation can also change the appearance of the formulation. In order to resolve this situation, complete characterization of the gelling mechanism and the formulation is necessary. This study characterizes the changes occurred which in the formulation and suggests a potential solution to minimize or overcome the gelling.



## TABLE OF CONTENTS

ABSTRACT.....	ii
ACKNOWLEDGMENTS.....	iv
PREFACE.....	v
TABLE OF CONTENTS.....	vii
LIST OF TABLES.....	x
LIST OF FIGURES.....	xii
I. INTRODUCTION.....	1
1.1 OVERVIEW OF THE DRUG.....	1
1.2 PHYSICAL CHEMICAL PROPERTIES AND DESCRIPTION OF DQAIC.....	1
1.3 RATIONALE FOR DEVELOPING SOFT-GEL CAPSULE FORMULATION.....	2
1.4 STATEMENT OF THE PROBLEM.....	4
1.5 OVERVIEW OF THE ANALYTICAL METHODS USED TO CHARACTERIZE GELLING.....	5
1.5.1 Rheological Investigations.....	5
1.5.2 Thermoanalysis.....	7
1.5.3 FT-IR and Raman Analysis.....	8
1.5.4 X-Ray Diffraction.....	9
1.5.5 Dynamic Light Scattering.....	12
II. OBJECTIVE.....	14

III. EXPERIMENTAL.....	15
3.1 MATERIALS USED.....	15
3.1.1 The Vehicle.....	15
3.2 INSTRUMENTS USED.....	18
3.3 METHODOLOGY.....	18
3.3.1 Preparation of the Formulation.....	18
3.3.2 Characterization of the Drug, Vehicle and the Formulation.....	22
3.3.2.1 Rheological Investigations.....	22
3.3.2.2 Thermal Analysis.....	23
3.3.2.3 Chemical Analysis.....	24
3.3.2.4 Morphological Analysis.....	25
3.3.2.5 Particle Size Determination.....	25
3.3.2.6 Effect of Storage Time Measurements.....	26
3.3.2.7 Measurements of Moisture Content.....	27
IV. RESULTS AND DISCUSSION.....	28
4.1 CHARACTERIZATION OF MCM.....	28
4.2 CHARACTERIZATION OF THE DRUG.....	43
4.3 CHARACTERIZATION OF THE DRUG SOLUTION IN	
MCM.....	51
4.3.1 Rheological Characterization .....	51
4.3.2 Solution Morphology and Physicochemical Characteristic	
of DQAIC.....	54

4.4 CHARACTERIZATION OF SOLUTION AFTER SHEAR.....	59
4.4.1 Rheological Investigations.....	59
4.4.2 Morphological and Physicochemical Characterization of the Gelled DQAIC Solution.....	63
4.5 DETERMINATION OF INDIVIDUAL VARIABLES THAT AFFECT GELLING.....	69
4.5.1 Combined Effects of Shear and Temperature.....	69
4.5.2 Effect of Humidity.....	69
4.5.3 Effect of Storage Time.....	71
4.5.4 Effect of The Drug Concentrations.....	71
4.5.5 Reversibility of Gelling Structure.....	81
4.6 POSSIBLE EXPLANATIONS FOR GELATION.....	84
4.6.1 Studies to Correct Gelling.....	85
V. CONCLUSION.....	88
REFERENCES.....	90
APPENDIX.....	91
BIBLIOGRAPHY.....	111

## LIST OF TABLES

Table I :	Solubility of DQAIC in Various Solvents at 21°C.....	3
Table II :	List of Chemicals Used.....	16
Table III :	Specification of MCM as Provided by the Manufacturer .....	17
Table IV :	Instruments Used in This Study .....	19
Table V :	DSC Traces of MCM in temperature range of (-70°)-(150°) C during heating.....	37
Table VI :	DSC Traces of MCM in temperature range of (-70°)-(150°) C during cooling.....	37
Table VII :	DSC Performances of the Drug Scanned Between 20°-150°C ; Heating and Cooling Curves.....	46
Table VIII :	Microscopic and Visual Observation for the Drug Solution During Shear.....	60
Table IX :	Effect of Shear on the Thermodynamic Properties of the Solution as Determined by Heating Cycles Between -70°C and 150°C.....	64
Table X :	Effect of Shear on the Thermodynamic Properties of the Solution as Determined by Cooling Cycles Between -70°C and 150°C.....	64
Table XI :	The Variables That Affect Gelling Time of the Formulation.....	70
Table XII :	Particle Size Measurements of DQAIC Solution at Different Concentrations at 25°C.....	76

Table XIII :	DSC Traces During Heating Curve of the Drug Solution in MCM at 10% and 25% (w/v) Concentrations.....	79
Table XIV :	Gelling Time and Activation Energy for 20% (w/w) DQAIC Solution with Different Vehicles.....	87

## LIST OF FIGURES

Figure 1 :	Diffraction of X-rays by a Crystal.....	11
Figure 2 :	Schematic View of a Typical Light Scattering.....	13
Figure 3 :	The Rheological Characteristic of MCM and 20% (w/w) DQAIC Solution Obtained at a Shear Rate 1-500 1/sec, 4-2050 dyne/cm <sup>2</sup> Shear Stress with a 0.053 mm gap at 25°C.....	29
Figure 4 :	Frequency Sweep of MCM and 20 % (w/w) DQAIC Solution with a 6 cm Parallel Plate and 1 mm Gap at 25°C.....	30
Figure 5 :	Temperature Sweep of MCM and 20% (w/w) Drug Solution at 0.5 Hz Frequency, 1 Strain obtained with 6 cm Parallel Plate and 1 mm gap between 4°C and 80°C.....	31
Figure 6 :	DSC Traces of MCM During Heating and Cooling between 20°C and 65°C at a Rate of 0.33°C /min.....	33
Figure 7 :	DSC Traces of MCM During Heating and Cooling between -70°C and 150°C at a Rate of 5°C /min.....	34
Figure 8 :	DSC Traces of Mono-, Di- and Triglyceride of Caprylic Acid.....	35
Figure 9 :	FT-IR Spectrum of MCM at 4 cm <sup>-1</sup> Resolution.....	40
Figure 10:	FT-Raman Spectrum of MCM at 4 cm <sup>-1</sup> Resolution.....	41
Figure 11:	The X-Ray Pattern of MCM Taken from 1 to 45 2-θ at 0.75 deg/min Rate Before and After Shear and 3 Times Heating and Shear.....	42

Figure 12:	Microscopic Image of Powder DQAIC with 20 x 25 Magnification.....	44
Figure 13:	DSC Traces of DQAIC Powder During Heating and Cooling Between 20°C and 150°C.....	45
Figure 14:	X-Ray Pattern of DQAIC Taken at 0.75 deg/min in a 2-θ range of 1-45.....	46
Figure 15 :	FT-IR Spectrum of DQAIC at 4 cm <sup>-1</sup> Resolution.....	48
Figure 16:	FT-Raman Spectrum of DQAIC at 4 cm <sup>-1</sup> Resolution.....	49
Figure 17:	Strain Sweep for MCM and 20% (w/w) Drug Solution with 6 cm parallel plate and 1 mm gap.....	52
Figure 18 :	DSC Traces of 20% DQAIC Solution During Heating and Cooling Between 20°C and 65°C at a Rate of 0.33°C/min.....	55
Figure 19:	Comparison of DSC of MCM and 20% (w/w) DQAIC solution between -70°C and 150°C.....	56
Figure 20:	FT-IR Spectrum of 20% (w/w) DQAIC at 4 cm <sup>-1</sup> Resolution.....	58
Figure 21:	Microscopic Image of DQAIC Solution After Shearing 12 hr at 25 x 20 Magnification under Cross Polar.....	60
Figure 22:	Frequency Sweep for Sheared Solution with 6 cm Parallel Plate and 1 mm gap at 25°C.....	61
Figure 23:	Effect of Shearing Time on G'' of 20% (w/w) Drug Solution and MCM with 6 cm Parallel Plate and 1 mm gap at 25°C.....	62
Figure 24:	DSC Heating Curves of Non-Sheared and Sheared Samples Between -70°C and -150°C.....	65

Figure 25:	Comparison of FT-IR Spectra of Non-Gelled Solution and Gelled Solution at $4\text{ cm}^{-1}$ Resolution.....	66
Figure 26:	X-Ray Diffraction of MCM, 20% (w/w) DQAIC Solution Before Shearing, After 6 hr and 12 hr Shearing.....	68
Figure 27:	G'' Profiles with time for MCM and 20% (w/w) DQAIC Solution at 40 % and 60 % RH with 6 cm Parallel Plate and 1 mm Gap.....	72
Figure 28:	G'' Profiles with time for MCM and 20% (w/w) DQAIC Solution at 4°C, 25°C and 50°C obtained with 6 cm Parallel Plate and 1 mm Gap.....	73
Figure 29:	Effect of the Drug Concentration on Zero Shear Viscosity and Particle Size of the Solution at 25°C.....	75
Figure 30:	Effect of Shearing Time on Particle Size of 20% and 15% (w/v) DQAIC Solution.....	76
Figure 31 :	Comparison of DSC Heating of 10% and 25% (w/v) DQAIC Solution in MCM between -70°C and 150°C.....	78
Figure 32 :	DSC Traces of 20% DQAIC Solution with 2.4% Glycerin and 2.4% Water During Heating Between -70°C and 150°C.....	80
Figure 33:	Frequency Sweeps of Pre-sheared, Sheared and Recovered Solutions.....	82
Figure 34:	FT-IR Spectra of 20% (w/w) DQAIC Solution Before Shearing, After Shearing and Recovering at 65°C.....	83
Figure 35:	Correlation Between Activation Energy and Gelling Time of a Sample...	87



## I. INTRODUCTION

### 1.1 OVERVIEW OF THE DRUG

The drug used in this study is a peptide analogue and is used as a model drug to investigate the gelling phenomenon in a lipid vehicle.

The drug { N-tert-butyl-decahydro-2-[2(R)-hydroxy-4-phenyl-3(S)-[[ N-(2-quinolylylcarbonyl)-L-asparagynyl]amino]butyl]-(4aS,8aS)-isoquinoline-3(S)-carboxamide (DQAIC)} is a transition-state mimetic of the phenylalanine-proline (Phe-Pro) peptide cleavage site.

### 1.2. PHYSICAL CHEMICAL PROPERTIES AND DESCRIPTION OF DQAIC

DQAIC is a white, amorphous, micronized powder. It has a molecular weight of 670.86.

DQAIC has poor aqueous solubility (0.03 mg/ml). It is soluble in ethanol, propylene glycol and some lipid vehicles. It is a highly lipophilic drug with two pK<sub>as</sub> (pK<sub>a1</sub>= 1.1 and pK<sub>a2</sub> =7.1) and with a partition coefficient of 3.34. The melting range is 123.3°-124.6°C.

### 1.3 RATIONALE FOR DEVELOPING SOFT GEL CAPSULE FORMULATION

Due to lipophilic properties of the drug ( $\log P = 3.34$ ) and its limited solubility in the common solvents, Table I, an oil based solvent that would provide good solvent properties like MCM, a medium chain fatty acid ester was chosen that dissolve DQAIC with 400 mg/mL solubility value and the solution can encapsulated.

Since the bioavailability of the drug is dissolution dependent, its solubility needs improvement. Several approaches were tested to improve its bioavailability. Salts of DQAIC were prepared which did not provide the required bioavailability. Micellar solubilization with Tween, Brij and Pluronic provided small improvements in solubility. Solid dispersions of the drug did not offer better dissolution due to poor drug loading. Enteric coated tablets did not provide adequate bioavailability.

Based on solubilization data, Table I, lipid based solvents were proposed as the reasonable vehicle to achieve a satisfactory formulation.

DQAIC due to its lipophilic character ( $\log P = 3.34$ ) dissolves in oil fractions and mixtures to a reasonable degree. MCM, mixture of mono-, di- and triglyceride, was used as the solvent due to its suitable solvent properties.

**Table I : Solubility of DQAIC in Various Solvents at 21°C**

<b>Solvent</b>	<b>Solubility (mg/mL)</b>
Ethanol	400
Water	0.03
Glycerol	< 1
Propylene Glycol	400
Mono- / di-glycerides of capric/ caprylic acids	400
PEG-6 caprylic and capric glycerides	400
Glycerol monocaprylate	388
Triglyceride of capric and caprylic acid	5

#### 1.4. STATEMENT OF THE PROBLEM

The selected formulation contains 20% (w/w) drug, dissolved in MCM (mixture of mono- di- and triglyceride of caprylic and capric acids). The formulation is a viscous solution with Newtonian properties.

The formulation is prepared as follow:

The processing unit includes a jacketed vessel, a mixer and a temperature regulator. The vehicle is then heated up to 65°C, the drug is added and the contents are thoroughly mixed until a clear solution is obtained by using high shear mixer. The liquid formulation is cooled down to room temperature, and encapsulated into soft-gel capsules.

During processing of DQAIC soft-gels, some formulations turn into a translucent mixture from a transparent clear solution. Former investigations demonstrated that the shearing stress applied during the mixing and encapsulation stages were responsible for these changes that occurred. The gelling tendency was observed to be more pronounced in the high shear mixing.

## **1.5 OVERVIEW OF ANALYTICAL METHODS USED TO CHARACTERIZE GELLING**

### **1.5.1 Rheological Investigations**

Rheology is the study of the flow and deformation of materials. Studying rheology will be extremely beneficial for characterization of fluids and semi solids specially when other properties such as molecular weight can also be well defined. The rheology of a particular product, which can range in consistency from liquid to solid, drug dissolution, physical stability and even bioavailability. In this case, rheological measurements will provide important information about effects of processing factors.

Rheological measurements can be carried out either by measuring flow properties under continue shear or oscillatory disturbance. Continuous shear measurements provide information about apparent yield stress, viscosity, shear thinning and thixotropic behavior and good correlation with real processes such as pumping, stirring and extrusion through a nozzle. However, continuous shear during flow measurements alters a material's ground state. On the other hand, oscillatory measurement is designed not to destroy the structure, so that these measurements can provide information on the intermolecular and interparticle forces of the material and measures both viscous and elastic behavior of a sample. The stress or shear rate is applied in a sinusoidal manner and hence the sample is simple "wobbled". In oscillation measurements, it is important to find the viscoelastic linear region since it is a non-destructive test. In oscillatory tests, the elastic ( $G'$ ) and

viscous moduli ( $G''$ ) and the complex viscosity ( $\eta^*$ ) are determined.  $G''$  represents viscous dissipation or loss of energy while  $G'$  elastic storage of energy. The more viscous the system, the more differences between the shear stress (input) and shear rate (output) will be observed. This differences is defined as delta ( $\delta$ ) which is related to elastic to viscous modulus by:

$$\tan(\delta) = G''/G' \dots\dots\dots(1)$$

where  $G'$  is elastic modulus and  $G''$  is viscous modulus. Their relationship to complex viscosity is demonstrated as:

$$\eta^* = (G' + iG'')/\omega \dots\dots\dots(2)$$

where  $\omega$  is angular frequency and  $i$  is imaginary root.

The phase angle ( $\delta$ ) indicates the elastic strength of the body. It changes from 0 to 90. At low values, the system is elastic at high values it is viscous (1, 2, 3).

Strain sweep, frequency sweep and temperature sweep are important experiments to be carried out. Strain is relative deformation to the initial length of material. Strain sweep is important to predict the strength of a samples internal structure. Frequency sweep is used to differentiate flow properties and structural differences. In oscillatory measurements, creep test can be carried out , which measures the slow deformation of a material under a small constant stress. In a creep test, retardation of the material is initially measured under constant stress, and then relaxation is measured by removing the stress and the material behavior is defined.

### 1.5.2 Thermoanalysis

Thermal analysis is useful to characterize materials and in this case may indicate the changes in the form. Determination of glass transition temperature ( $T_g$ ) which characterizes the amorphous phase, melting points ( $T_m$ ) and crystallization points provide an identification of the stability of the gels obtained. A Differential Scanning Calorimeter was used for thermodynamic characterization of the system. One of the most classical application of DSC is in the determination of possible interactions between a drug and the excipients in its formulation. In DSC technique, heat flow into a substance and reference are measured as a function of sample temperature while the two are subjected to a controlled temperature program.

At  $T_g$ , the heat capacity of the sample suddenly increases, requiring more power to maintain the same temperature as the reference temperature. This differential heat flow to the sample (endothermic) causes a drop in the DSC curve. At  $T_m$ , the sample crystals want to melt at a constant temperature, so that a sudden input of large amounts of heat is required to keep the sample temperature the same the reference temperature. This results in a characteristic endothermic melting peak. Crystallization, in which large amounts of heat are given off at constant temperature, gives an exothermic peak.

Glass transition is defined as the temperature at which the heat capacity is midway between the liquid and glassy states. Determination of the  $T_g$  of a material is important

since it characterizes the amorphous phase which has improved dissolution rates and bioavailability over the crystalline state (1, 4).

### **1.5.3 FT-IR and Raman Analysis**

In order to understand whether the changes occurring in the system are chemical or physico-chemical in nature and the type of interaction between the vehicle and the drug molecules, FT-IR equipped with Raman accessory can be useful. In IR technique, a molecule must undergo a net change in dipole moment as a consequence of its vibrational or rotational motion in order to absorb infrared radiation. The types of molecular vibrations are stretching and bending. A stretching vibration involves a continuous change in the interatomic distance along the axis of bond between the two atoms. Bending vibrations are characterized by a change in the angle between the two bonds and are of four types: scissoring, rocking, wagging and twisting. FT-IR technique has three major advantages over regular IR techniques. First advantage is called Jacquinot advantage where the power of the radiation reaching the detector is much greater than conventional dispersive IR spectrophotometer, and much greater signal-to-noise ratios are observed which improves certainty of the structural conformation. The second advantage of FT-IR instruments is their high wavelength accuracy and precision. This leads to improved signal-to-noise ratios. The third advantage is called the multiplex or Fellgett advantage, where all the elements of the source reach the detector in a few nanoseconds to provide fast accurate results (5, 6).



In Raman Spectroscopy, the radiation is scattered as the result of vibrational-energy-level transitions occurring in the molecule as a consequence of the polarization process. Therefore, this technique is complementary to the infrared spectroscopy technique. The intensity of a normal Raman peak depends on polarizability of the molecule, the intensity of the source, and the concentration of the active groups.

#### 1.5.4 X-Ray Diffraction

Polymorphism is one of the important factors that affect solubility of a drug in a particular solvent. Different polymorphs may exhibit different solubilities. For poorly soluble drugs, among others, polymorphism may affect the rate of solidification and dissolution. X-Ray diffraction is used to determine any polymorphic changes that may occur in the systems studied.

X-Rays are electromagnetic radiation of short wavelength and therefore high energy. X-Rays used for diffraction studies have wavelengths in the 0.1-1 Å range. Like all electromagnetic radiations, X-Rays are absorbed, scattered, and diffracted by matter. The scattering and diffraction X-Rays is caused by the interaction with electrons. Electrons of the molecules in gases, liquids, or disordered solids states scatter X-Rays. However, electrons in the ordered arrays of atoms in crystals scatter X-Rays only in particular

directions. Diffraction is the scattering of X-Rays in a few specific directions by the crystals .

When an X-Ray beam hits a crystal surface at angle  $\theta$ , a portion of it is scattered by the layers of atoms at the surface. The unscattered portion of the beam penetrates to the second layer of atoms where again a fraction is scattered, and the remainder passes on to the third layer (Figure 1). X-Rays appear to be reflected from the crystals only if the angle of incidence satisfies the following condition:

$$\sin\theta = n\lambda/2d.....(3)$$

where n is order of reflection (an integer),  $\lambda$  is wavelength of X-Rays source, d is the interplanar spacing of the crystal. This equation is called Bragg Equation, and is used to determine d value of crystals (6).

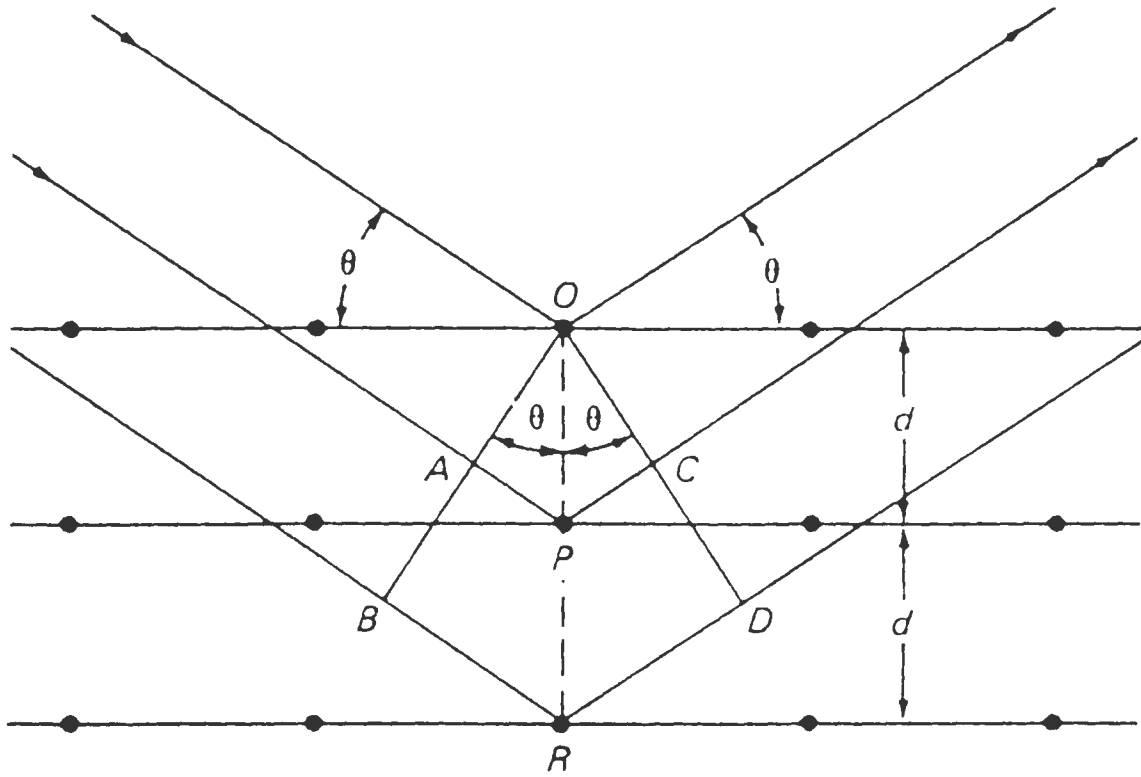


Figure 1: Diffraction of X-Rays by a Crystal

### 1.5.5 Dynamic Light Scattering

In Dynamic Light Scattering (DLS), the temporal variation of the intensity is measured. Diffusion coefficients of the particles, particle size, and size distribution can be obtained from such measurements. A DLS apparatus contains a laser light source, a spectrometer (containing the optical components for defining the scattering angle volume), a detector, a correlator and a computer with software for analysis. A schematic representation of a typical arrangement is shown in Figure 2.

Once the diffusion coefficient of a the particle is found, the particle size can be calculated from the Stokes-Einstein equation

$$D = (k_B T) / (6 \pi \eta R_H) \dots\dots\dots(4)$$

where  $\eta$  is the viscosity of the fluid,  $k_B$  is the Boltzman constant, and  $T$  is the absolute temperature of the system. The radius  $R_H$  measured in this manner is usually known as the hydrodynamic radius (7).

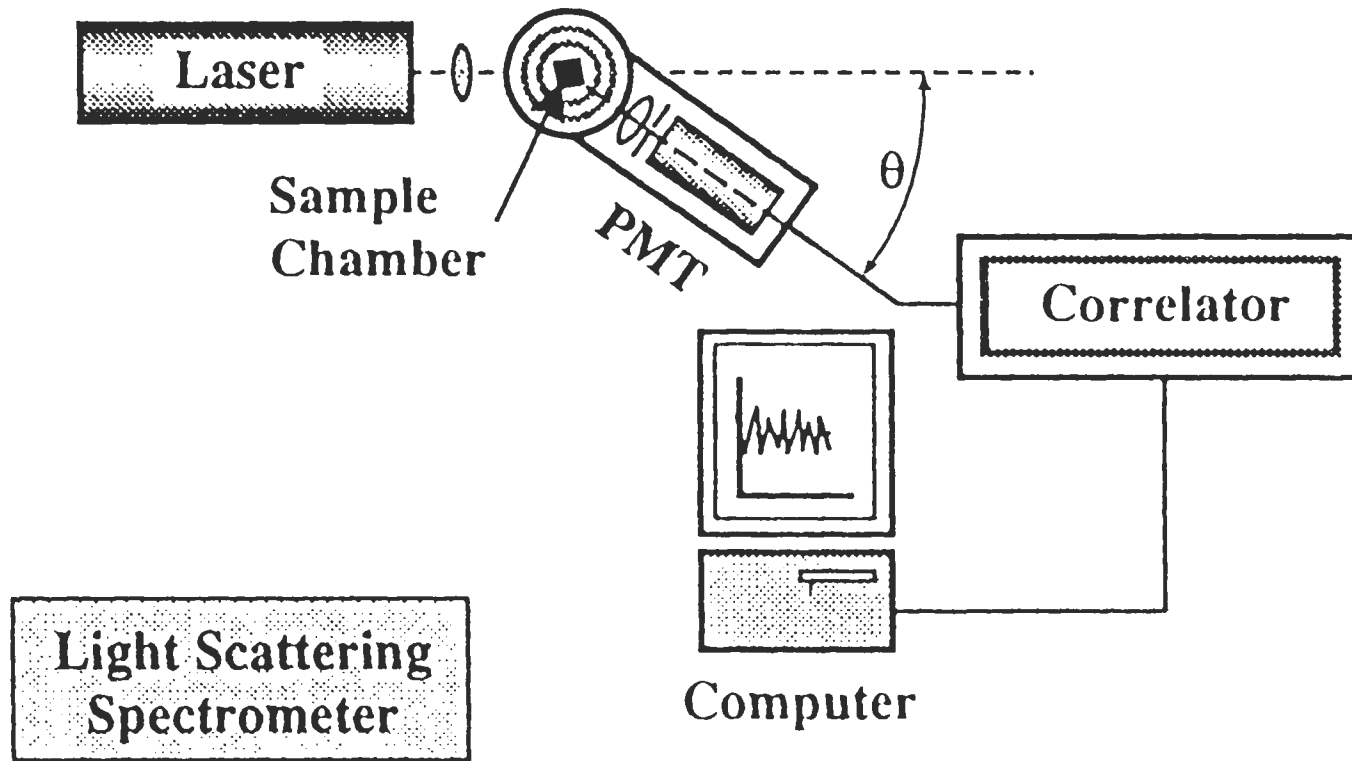


Figure 2: Schematic View of a Typical Light Scattering Instrument

## II. OBJECTIVES

The formulation under investigation is a relatively high concentration drug solution in MCM encapsulated in soft-gel capsules. Occasional gelation occurs during processing of the dosage form making high drug loading a difficult process. The occurrence of gelation can potentially reduce dissolution rate of the drug. Ideally, during processing, the capsule fill formulation should remain as a solution and preferable stay as a liquid through the product shelf-life. Gelation can also change the appearance of the formulation.

In order to come up with an acceptable remedy to gelling, full characterization of the system is necessary. The aim of this study is to characterize the shear, temperature and concentration dependent changes occurring in the system during processing. Determination and characterization of the rheological, thermoanalytical and chemical changes that occur in the system by aforementioned variables is the main goal of this study. Combined effects of the factors such as the shear, temperature, time and humidity that may have an effect on the processing of the formulation will also be determined in order to explain gelling phenomenon.

### **III. EXPERIMENTAL**

#### **3.1 MATERIALS USED**

All the main chemicals used in this study are listed in Table II. The properties of the drug used has been already described in Section 1.2. and MCM, used as the vehicle, in Section 3.1.1.

##### **3.1.1 The Vehicle**

MCM was used as the solvent in soft-gel formulation. The reasons for its selection were discussed in Sections 1.3 and 1.4. MCM is mixture of mono-, di- and triglyceride of dominantly caprylic (C<sub>8</sub>) and capric (C<sub>10</sub>) acids. It has an approximate molecular weight of 250. The specifications of MCM are given in Table III (8).

MCM is processed by the reaction of glycerin or propylene glycol with fatty acids obtained from palm, kernel and coconut oils in the presence of an alkaline catalyst. The products are further purified to obtain a mixture of glycerides, free fatty acids, free glycerin that contains at least 90 % by-weight glycerides. The ingredients meet the specifications of the Food Chemical Codex, 3d Ed. (1981), p 201. The affirmation of this ingredient is generally recognized as safe (GRAS) (9).

**Table II: List of Chemicals Used**

<b>CHEMICALS</b>	<b>LOT NO.</b>	<b>MANUFACTURES</b>
DQAIC	-	-
MCM (mono- di and triglyceride of Caprylic and Capric Acid)	60111-6	Abitec Corp. Columbus, OH 43216
MCM D (mono- di and triglyceride of Caprylic and Capric Acid)	JLW-61-25B	Abitec Corp. Columbus, OH 43216
PG-8 (Propylene glycol ester of Caprylic and Capric Acid)	80205	Abitec Corp. Columbus, OH 43216
Polyvinyl Pyrrolidone K30	960026	BASF Corp., Mount Olive, NJ
Propylene Glycol	20-652-930185	Dow Chemical, Midland, MI
Monoglyceride of Caprylic Acid	041H8431	Sigma-Aldrich, Inc., Saint Louis, MO
Diglyceride of Caprylic Acid	010H84466	Sigma-Aldrich, Inc., Saint Louis, MO
Triglyceride of Caprylic Acid	038H0651	Sigma-Aldrich, Inc., Saint Louis, MO
Karl Fisher Reagent (Diethylene glycol monoethyl ether, imidazole, sulfur dioxide, iodine, hydriodic acid )	70990	Allied Signal Inc., Morristown, NJ



**Table III : Specifications of MCM As Provided by the Manufacturer**

<b>Test</b>	<b>Test Result</b>	<b>Method</b>
Acid value (mg KOH/g sample)	<4	USP
Color	3.2R	AOCS Cc 13b-45
Free glycerol	0.86 %	NF
Water content	0.34 %	USP
Sulfated Ash	0.28 %	EP
Hydroxyl value	386	USP
Iodine value	0.1	EP
Saponification value	277	USP
Density at 30°C	0.995 g/mL	-
Viscosity at 30°C	64.6 cS	-
HLB	5.5	-
Glyceride composition		
Monoglyceride	68.57%	-
Diglyceride	25.95%	-
Triglyceride	2.65%	-
Alkyl chain distribution (%)		
C <sub>6</sub> (Caproic acid)	0.6	
C <sub>8</sub> (Caprylic acid)	86.1	
C <sub>10</sub> (Capric acid)	13.3	

MCM is a mixture of mono-, di- and triglyceride but mainly composed of monoglyceride, and is semisolid at ambient temperature. Its melting point is not specified and the final melting behavior is dependent on thermal pre-history and therefore it should be heated before use to obtain liquid. It was reported that the final melting point is also dependent on the grade of MCM. The grades used had a low acid glycerin values. Same MCM lot was used throughout the study. In addition to MCM, two more grades containing different ratios of ester components were used for comparisons. The one that contains 85 % mono-ester type is MCM(D) with a HLB value of 6.5, and the one with 90 % mono-ester is PG-8 with a HLB value of 2.5, which is propylene glycol esters of C<sub>8</sub>-C<sub>10</sub> fatty acids. They were used as controls to test their impact on the gelling phenomenon investigated.

## **3.2 INSTRUMENT USED**

The instruments used in this study are listed in Table IV.

## **3.3 METHODOLOGY**

### **3.3.1 Preparation of the Formulation**

In this study, a laboratory scale procedure to simulate processing conditions was set up. All the formulations except the ones that were used to investigate the effect of concentration were prepared by the following method. A water jacketed glass vessel (500

**Table IV: Instruments Used in This Study**

<b>Instruments</b>	<b>Model</b>	<b>Manufactures</b>
Silverson Homogenizer	L4R	Silverson Machines Ltd., England
Caframo Mixer	RZR 2000	Caframo Co., Canada
Temperature Regulator	9110	Fisher Scientific, Pittsburgh, PA
Rheometer	Carry-Med CSL 100	TA Ins., New Castle, DE
Differential Scanning Calorimeter	SII5200	Seiko Inc., Paramus, NJ
Fourier Transform Infrared Spectroscopy	FTS-60 A	Biorad Digilab, Cambridge, MA
Zeiss Polarizing Microscope	Axioplan	Carl Zeiss Inc., Thornwood, NY
Scintag 2000XDS X-Ray Diffractometer	ASC0012	Scintag Inc., Cupertino, CA
Dynamic Light Scattering	BI 200SM	Brookhaven Instrumens Corp., Holtsville, NY
Mettler Balance	PM480	Mettler-Toledo Inc., Hightstown, NJ
Mettler Electronic Balance	MT5 SNR P33594 FNR 211000165 04	Mettler-Toledo Inc., Hightstown, NJ

**Table IV (continuation)**

<b>Instrument</b>	<b>Model</b>	<b>Manufacturer</b>
Moisture Analyzer	Blending Karl Fisher Turbo2 Co-10	Orion Research Inc., Boston, MA
Incubator	3940	Forma Scientific Inc., Marietta, OH
Environmental Chamber	3852	Forma Scientific Inc., Marietta, OH
Incubator	3920	Forma Scientific Inc., Marietta, OH
Refrigerator		Fisher Scientific, Springfield, NJ

mL) was used for all sample preparations. The vehicle (400g) is weighted and transferred into the vessel connected with a temperature regulator. The vehicle was heated to 65°C. DQAIC (100 g) was added to the heated vehicle and mixed for 30 minutes at 3000 rpm using a Silverson L4R homogenizer that provided turbulent mixing until the drug was completely dissolved. The formulation was cooled down to 25°C at a cooling rate of 20°C /hour.

The formulation prepared was subjected to shear at 3000 rpm, 25°C until it was reverted to an opaque gel. To analyze the effect of shearing time, 20 g samples were withdrawn every 3 hours during shearing.

The same procedure was followed for the vehicle and all other sample preparations. The formulation was sheared at varying temperatures (40°, 60°, 80°C), shear rates (1500, 500 rpm) and humidity environments (50 and 30 % Relative Humidity). All experiments were carried out in triplicates.

The effect of drug concentrations investigated using the method described below: The vehicle (200mL) was heated up to 65°C, and the drug at various concentrations (2, 5, 7, 10, 12, 15, 17, 20, 22, 25% w/v) was added and mixed using a Caframo RZR 2000 mixer that provides impeller type mixing until the drug was completely dissolved. The mixer was changed to impeller type mixer because turbulent mixer was inoperable at high drug concentrations. The solution was cooled to 25°C at a cooling rate of 20°C /hour, and the

solution was transferred to a 250 mL volumetric flask and added up to final volume with MCM, heated up to 65°C for 30 minutes and cooled down to ambient temperature before used.

### **3.3.2 Characterization of the Drug, Vehicle and the Formulation**

#### **3.3.2.1 Rheological Investigations**

A Carri-Med CSL 100 Rheometer (TA Ins, New Castle, DE) is used for the rheological investigations. A cone and plate geometry for flow modes and a parallel plate geometry for oscillatory and creep measurements were chosen as the best modes to detect shear-dependent structural changes occurring in the system. The flow mode was investigated by using a 4 cm /2 degree cone and plate with a 0.053 mm gap. These arrangements were tested at 1-500 1/sec shear rate. 10 % significance tolerance was selected to obtain per data point. The creep mode was studied by using a 6 cm parallel plate with 1 mm gap. 0.5 dyne/cm<sup>2</sup> shear stress was applied to the system. It was sheared for 3 minutes and relaxed by omitting stress applied for 3 minutes. The oscillatory studies were conducted by the same parallel plate with 1 mm gap. The linear region was obtained in 0.1-10 strain range at 0.5 Hz frequency. Frequency sweep was carried out in a range of 0.1-0.5 Hz at 1 strain. 4-80°C temperature range, 0.5 Hz frequency and 1 strain was used in temperature sweeps. All experiments except temperature sweep was conducted at 25°C. Temperature sweep was conducted over a temperature range of 4-80°C with a 6 cm parallel plate and 1

mm gap. This temperature range was selected in order to mimic processing and storage conditions.

All the samples were tested for rheology within 3 days following preparation. The samples were equilibrated at 25°C for 20 minutes prior to rheological measurements.

### 3.3.2.2. Thermal Analysis

In order to follow the thermodynamic changes that occur in the system during shear, thermal analysis was conducted. A Differential Scanning Calorimeter (SII5200 DSC, Seiko Inc., Paramus, NJ) was used for thermodynamic characterization of the system.

The sample to be tested ( $10.000 \pm 0.050$  mg) was placed into a DSC pan. The pan was crimped with the instrument sealer for the solid samples, left uncrimped for liquid and semisolid samples. The preliminary runs at rates of 2, 5, 10°C/min showed the best rate was at 5°C/min. The vehicle and drug solution were heated and cooled in two different temperature ranges. First, they are heated from 20°C to 65°C at a rate of 0.33°C/min in order to follow thermodynamic changes during the production of the formulation. After holding 30 minutes at 65°C, the sample was cooled to 20°C at the same rate. The polymorphic reverses were investigated 3 heating and the cooling cycles between -70°C and 150°C at a rate of 5°C/min. A Seiko Inc., SSC 5200 disk station was used to collect and analyze the raw data.

In the thermoanalysis of the drug, the sample was placed into a DSC pan and crimped by the instrument sealer. The sample was heated from 20°C to 150°C at a rate of 5°C/min and cooled to 20°C at same rate.

### 3.3.2.3 Chemical Analysis

In order to understand further whether the changes occurring in the system are chemical or physico-chemical in nature and the type of interaction between the vehicle and the drug molecules, the samples were examined by Fourier Transform Infrared (FT-IR, Biorad-Digilab) equipped with FT-Raman accessory (FTS-60).

IR spectra was recorded at 4 cm<sup>-1</sup> resolution with 64 scans. Raman spectra was generated on the same instrument. All samples were run as they were without sample preparation. The laser used to illuminate the samples was a Neodymium-Yttrium Aluminum Garnet (Nd-YAG) laser operating at 9395 cm<sup>-1</sup>. A 900 mW power was used to run the samples. No thermal degradation was observed during measurements. 128 scans were collected at 4 cm<sup>-1</sup> resolution.

To investigate the interaction between the drug and the vehicle induced by shear, the spectra of the drug, the vehicle and the formulations before and after shear were obtained using FT-IR, equipped with Raman spectroscopy.



#### **3.3.2.4 Morphological Analyses**

In order to determine any polymorphic changes that may occur in the systems, microscopical and X-ray diffraction analysis were conducted at each stage of the formulation.

In this study, a Scintag 2000XDS X-ray Diffractometer, ASC0012 (Scintag Inc., Cupertino, CA) was used to obtain X-rays diffraction pattern of the drug, vehicle and solution before and after shearing. All samples were placed on a zero background plate, irradiated with X-rays from a copper target ( $\lambda = 1.54 \text{ \AA}$ ) and analyzed by X-ray powder diffraction from 0-45 degrees  $2\theta$  at  $19 \pm 2^\circ\text{C}$ .

Microscopical analysis was also conducted. A Zeiss Polarizing Microscopy (Carl Zeiss Inc., Thornwood, NY) was used to determine any crystal growth or change of crystalline state or liquid crystal formation. The samples were placed onto a microscope slide and observed with a microscope cover with 20x 25 magnification at  $19 \pm 2^\circ\text{C}$ .

#### **3.3.2.5 Particle Size Determination**

The presence of particles and the particle size changes of the solution at different concentrations was measured. A Dynamic Light Scattering (DLS) Apparatus BI 200MS (Brookhaven Instruments Corp., Holtsville, NY) was used for this purpose.

A Lexer Model 95 Argon Ion Laser source was used. The intensity measurements were obtained at  $90^\circ$  at 488 nm wavelength and with 200  $\mu\text{m}$  hole size. The sample in a scintillation vial was placed in the cell holder, which was controlled at  $25^\circ \pm 0.1^\circ\text{C}$ . Laser power was set in a manner to provide the measured intensity of approximately 70 Kcount/sec. Delay time was adjusted according to the size of the sample. First, a polystyrene dispersion, which has standard particle size of  $96 \pm 3$  nm, was used to check the instrumental setup. An average of three measurements were provided particle size of  $95 \pm 3$  nm. In order to calculate the particle size of a sample from the diffusion coefficient, zero shear viscosity should be known. Complex viscosity ( $\eta^*$ ) values from frequency sweep at low frequency range (0.01 - 1 Hz) can be accepted as zero-shear viscosity. Therefore, a frequency sweep was carried for each sample and  $\eta^*$  values were determined before the DLS measurements.

#### **3.3.2.6. Effect of Storage Time Measurements**

The formulations tested were kept at  $25^\circ\text{C}$  60% relative humidity,  $25^\circ\text{C}$  with 40% relative humidity,  $50^\circ\text{C}$  with 13% RH and  $4^\circ\text{C}$  with ambient humidity for 4 weeks in scintillation vials and their rheological properties were determined at  $25^\circ\text{C}$  every week.

### 3.3.2.7. Measurement of the Moisture Content

The USP Method I (Direct Titration) technique was used to determine the water content of the drug, MCM and the solution before and after shearing in order to determine the effect of water content on the gelling properties of the system. The principle of the titrimetric determination of water is based on the quantitative reaction of water with an anhydrous solution of sulfur dioxide and iodine in the presence of a buffer that reacts with hydrogen ions. In the original titrimetric solution, known as Karl Fisher Reagent, the sulfur dioxide and iodine are dissolved in pyridine and methanol (10).

A Karl Fisher Moisture Titrator, model Turbo2 Co-10 (Orion Research Inc., Boston, MA) was used for this purpose.  $1.000 \pm 0.150$  g sample was dissolved in anhydrous methanol solution, which was stirred for about 2 minutes and titrated with the reagent. The instrument calculates the water content in % w/w.

## **IV. RESULTS AND DISCUSSION**

### **4.1. CHARACTERIZATION OF MCM**

MCM is the mixture of mono-, di- and triglyceride of caprylic and capric acids. All known properties of MCM is discussed in Section 3.1.1. In order to understand gelling mechanism of the system, a placebo solution of only MCM was prepared under the same conditions used for the formulation preparation, and subjected to shear as explained in Section 3.3.1.

MCM did not show any detectable structures under regular and polarized light microscope before and after shearing at 3000 rpm for 3, 6, 9, 12 hours.

Data presented in Figure 3 demonstrates that MCM showed Newtonian characteristics having a viscosity of 83 cP at 25°C. When it contains 20% (w/w) drug, the viscosity increases 5-fold (411 cP). However, Newtonian characteristics remains the same with 0.1-500 1/sec shear rate range. No thixotropic properties were detected in time dependent shear studies.

On the other hand, the frequency sweep of the solvent at the linear region demonstrated that there is a slight structural build-up of MCM above frequencies of 0.35 Hz, which may indicate a very weak dilatant behavior that  $G''$  demonstrates (Figure 4). The

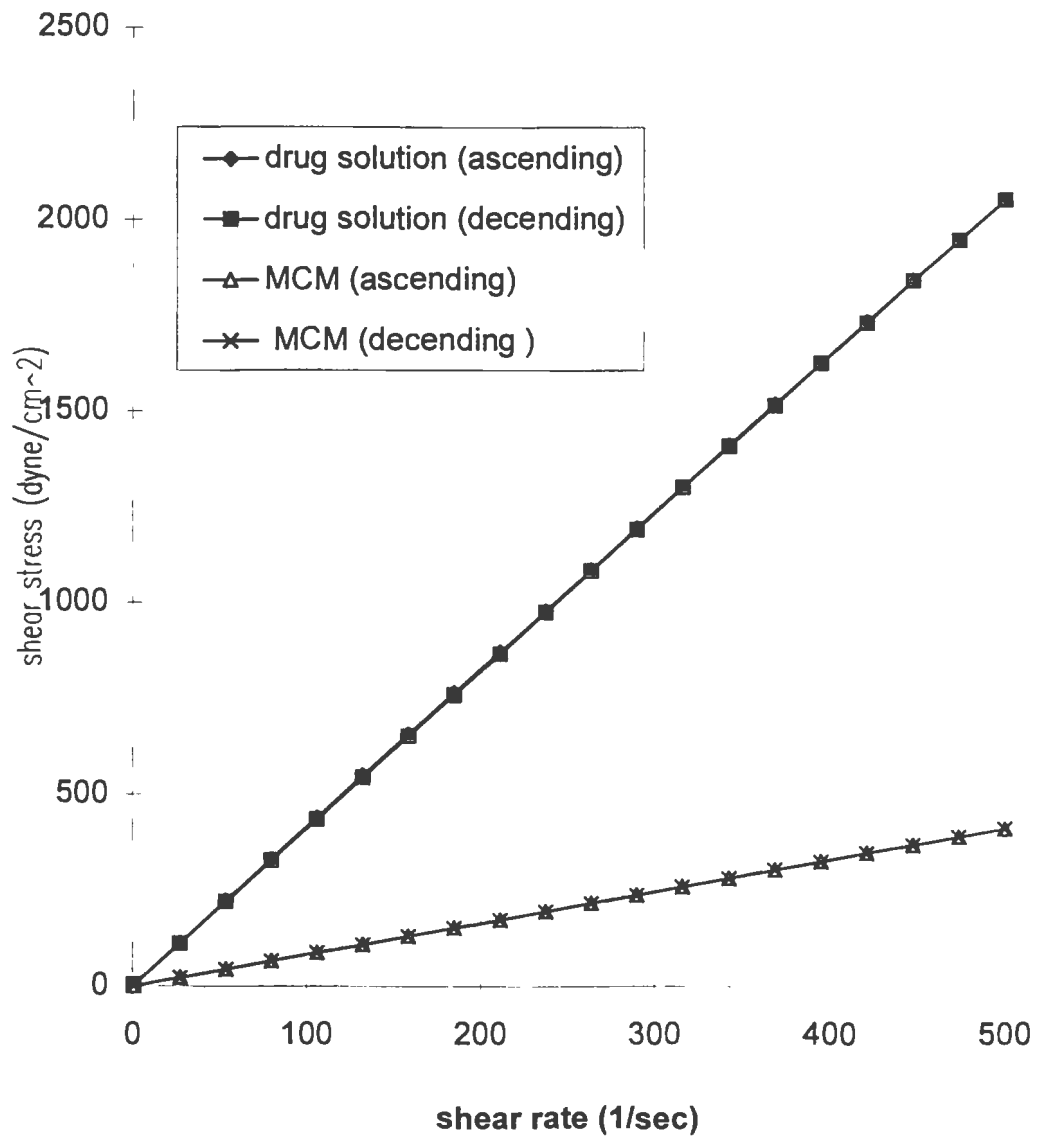


**Figure 3: The Rheological Characteristic of MCM and 20% (w/w) DQAIC Solution Obtained at a Shear Rate 1-500 1/sec, 4-2050 dyne/cm<sup>2</sup> Shear Stress with a 0.053 mm Gap at 25<sup>0</sup>C**

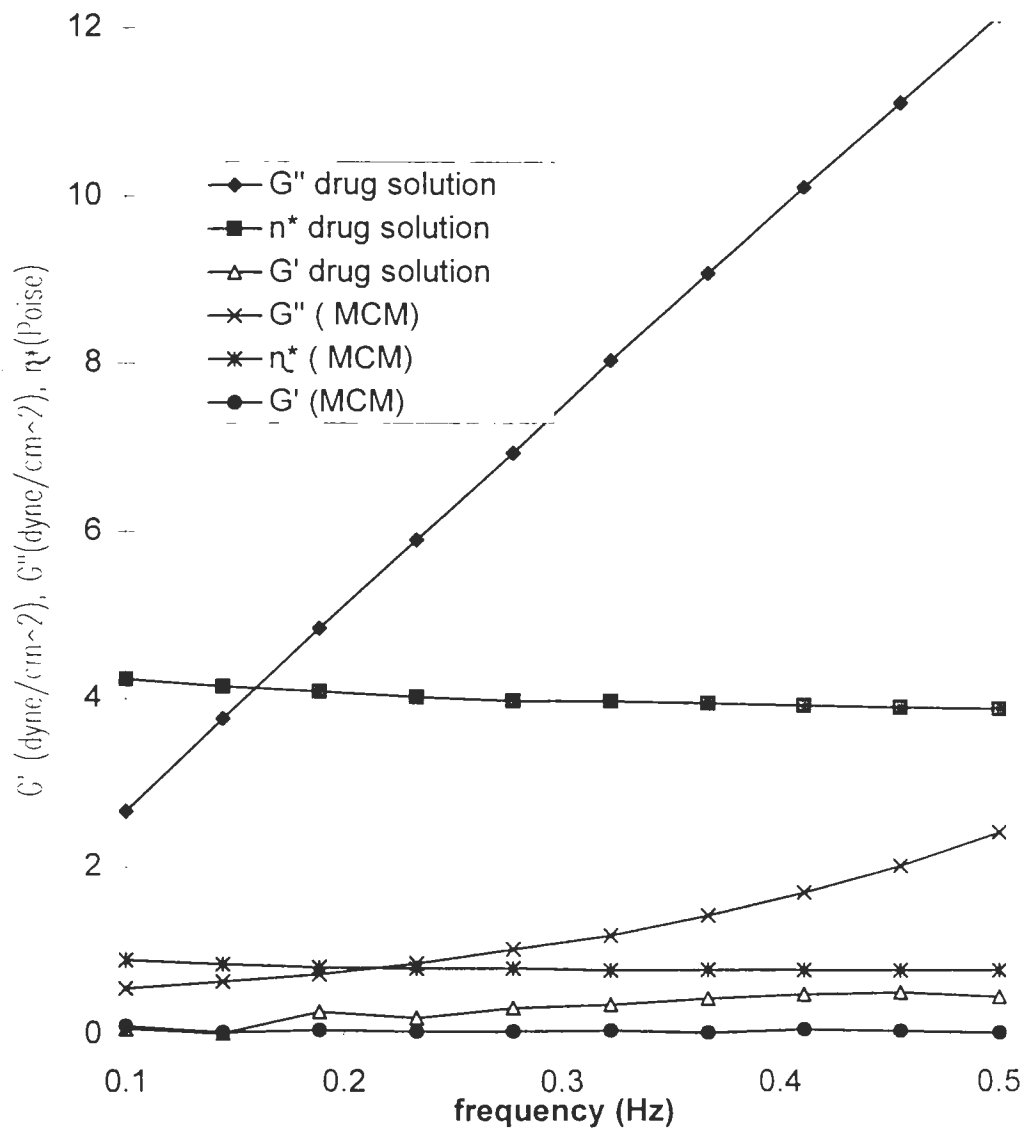


Figure 4: Frequency sweep of MCM and 20 % (w/w) the drug solution determined with a 6 cm parallel plate and 1 mm gap at 25<sup>0</sup>C

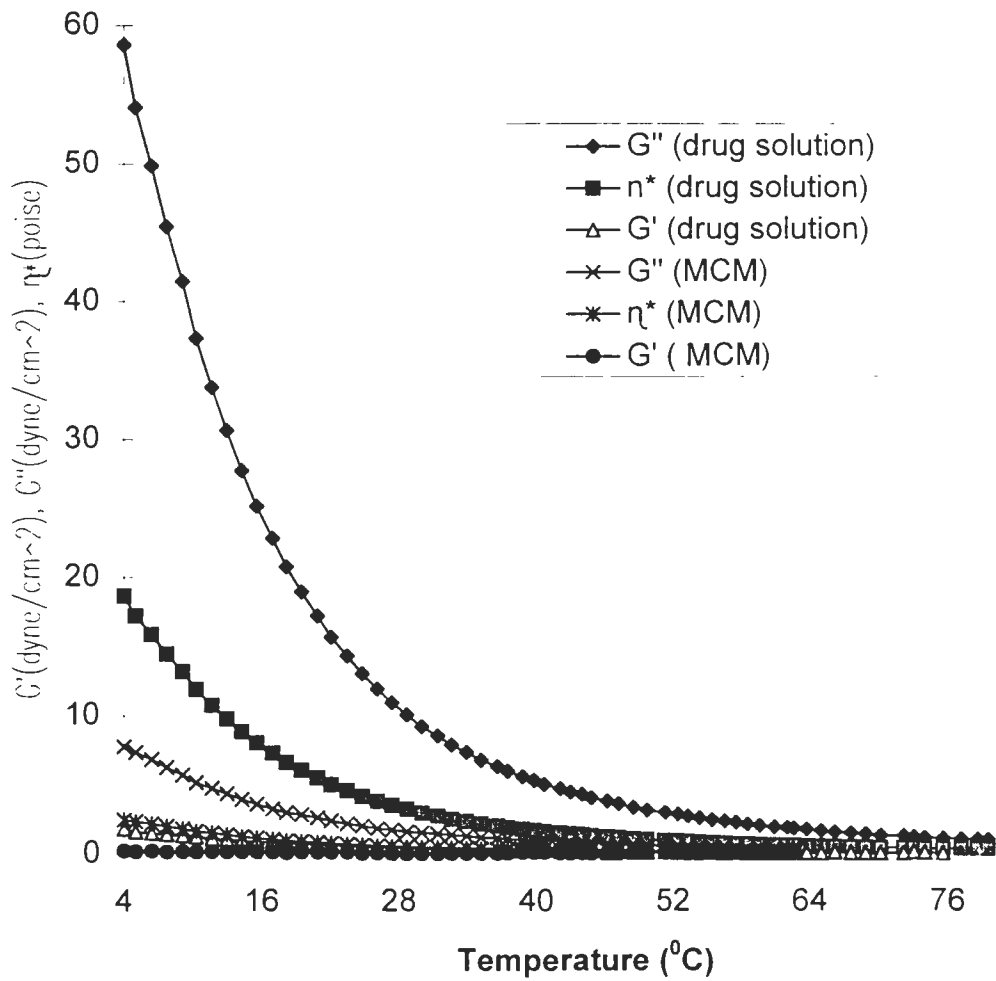
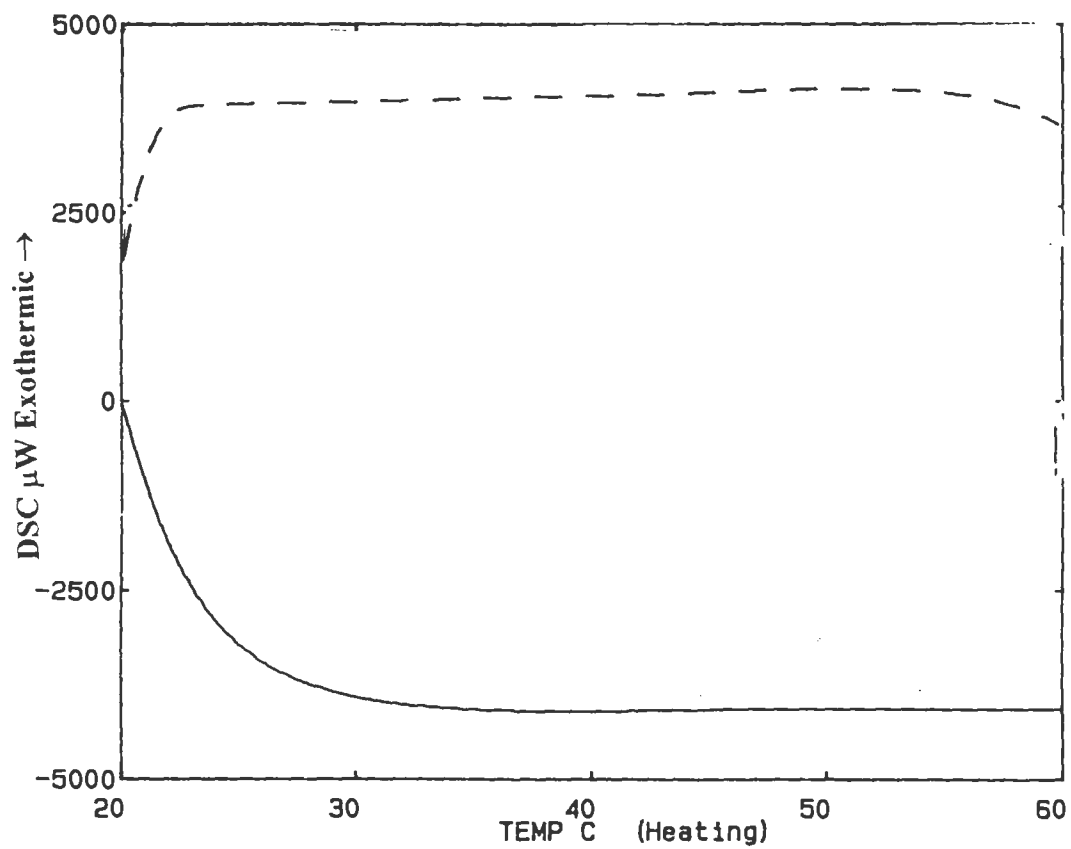


Figure 5: Temperature sweep of Capmul MCM and 20% (w/w) drug solution at 0.5 Hz frequency , 1 strain obtained with 6 cm parallel plate and 1 mm gap

rheological properties of the drug solution shown in Figure 3-5 will be discussed in 4.3.1. The temperature effect on the rheology is demonstrated in Figure 5. During heating from 4°C to 80°C, the  $G''$  is reduced from 7.75 dyne/cm<sup>2</sup> to 0.3 dyne/cm<sup>2</sup> between 4°C to 40°C and disappeared above 50°C. This may be liquefaction of the monoglyceride that tend to be at semisolid form at the ambient temperature.

Figure 6 demonstrates that the DSC curves of MCM provided thermodynamic changes. Two different temperature ranges were used. First, the sample was heated up from 25°C to 65°C at a rate of 0.33°C/min, after holding the sample at 65°C for 30 min., it was cooled down to 25°C at the same rate (Figure 6). The intention was to imitate processing conditions during which MCM is heated up to 65°C and mixed with the drug for 30 min and cooled down to 25°C. Under these conditions, no changes were detected in MCM. In a second set of experiments, MCM was cooled from 20°C to -70°C, was kept at this temperature for 10 minutes to equilibrate the targeted temperature, and was reheated up to 150°C and cooled down to -70°C at a rate of 5°C/min. This heating and cooling cycle was repeated 3 times to obtain an amorphous history of the material. In order to determine if any thermodynamic changes may occur during shear, this procedure was repeated for sheared MCM as well. All the exothermic and endothermic traces were collected using the instrument software and related enthalpies were calculated. Figure 7 A and B are examples of the heating and cooling performance of MCM. Their DSC were compared with the pure glyceride of Caprylic acid, Figure 8 A, B, C. Only Diglyceride has a crystallization peak.





**Figure 6 : DSC Traces of MCM During Heating (—) and Cooling (---) Between 20 $^{\circ}\text{C}$  and 65 $^{\circ}\text{C}$  at a Rate of 0.33 $^{\circ}\text{C}/\text{min}$ .**

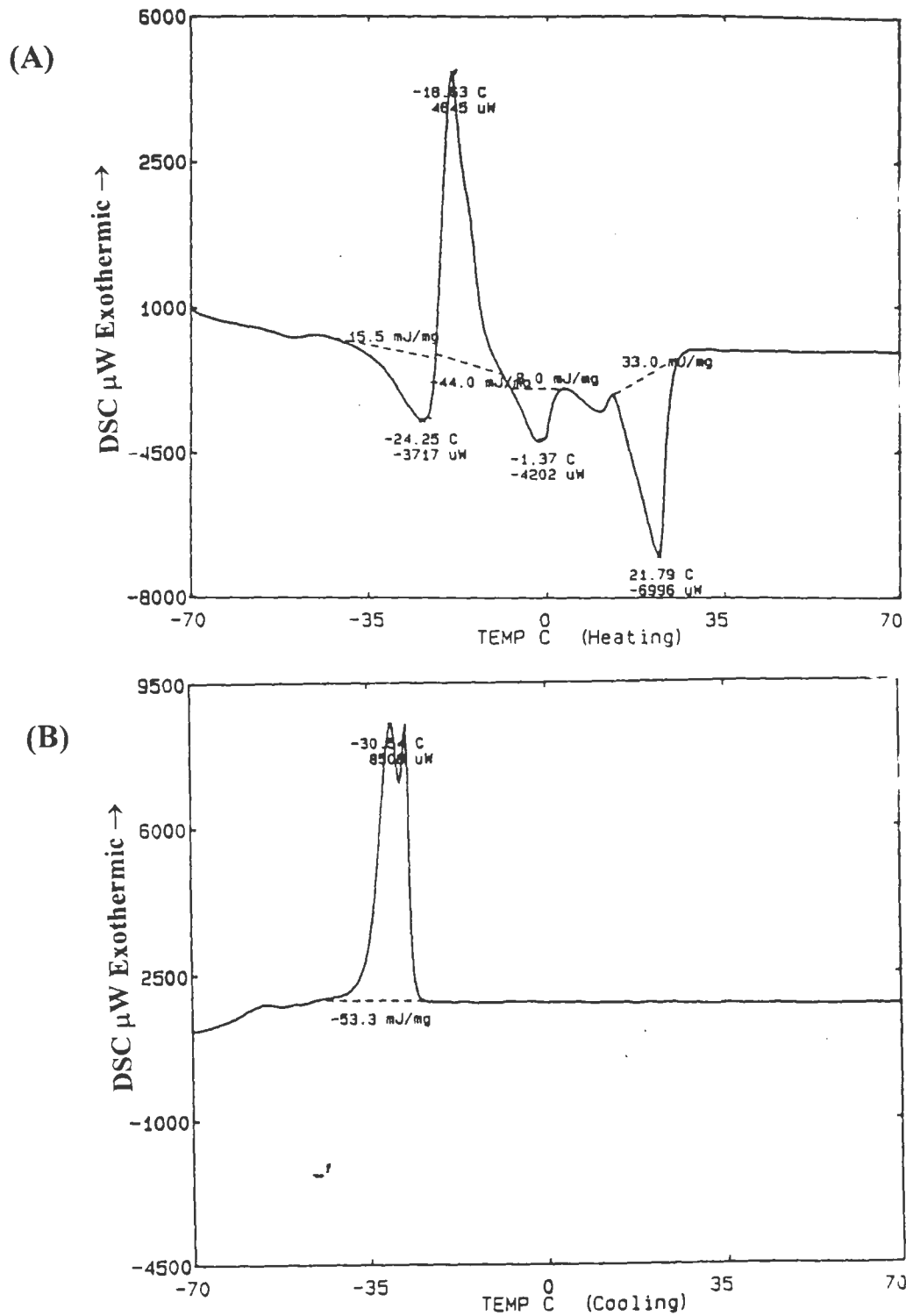


Figure 7 : DSC Traces of MCM During Heating (A) and Cooling (B) Between -70°C and 150°C at a Rate of 5°C/min.

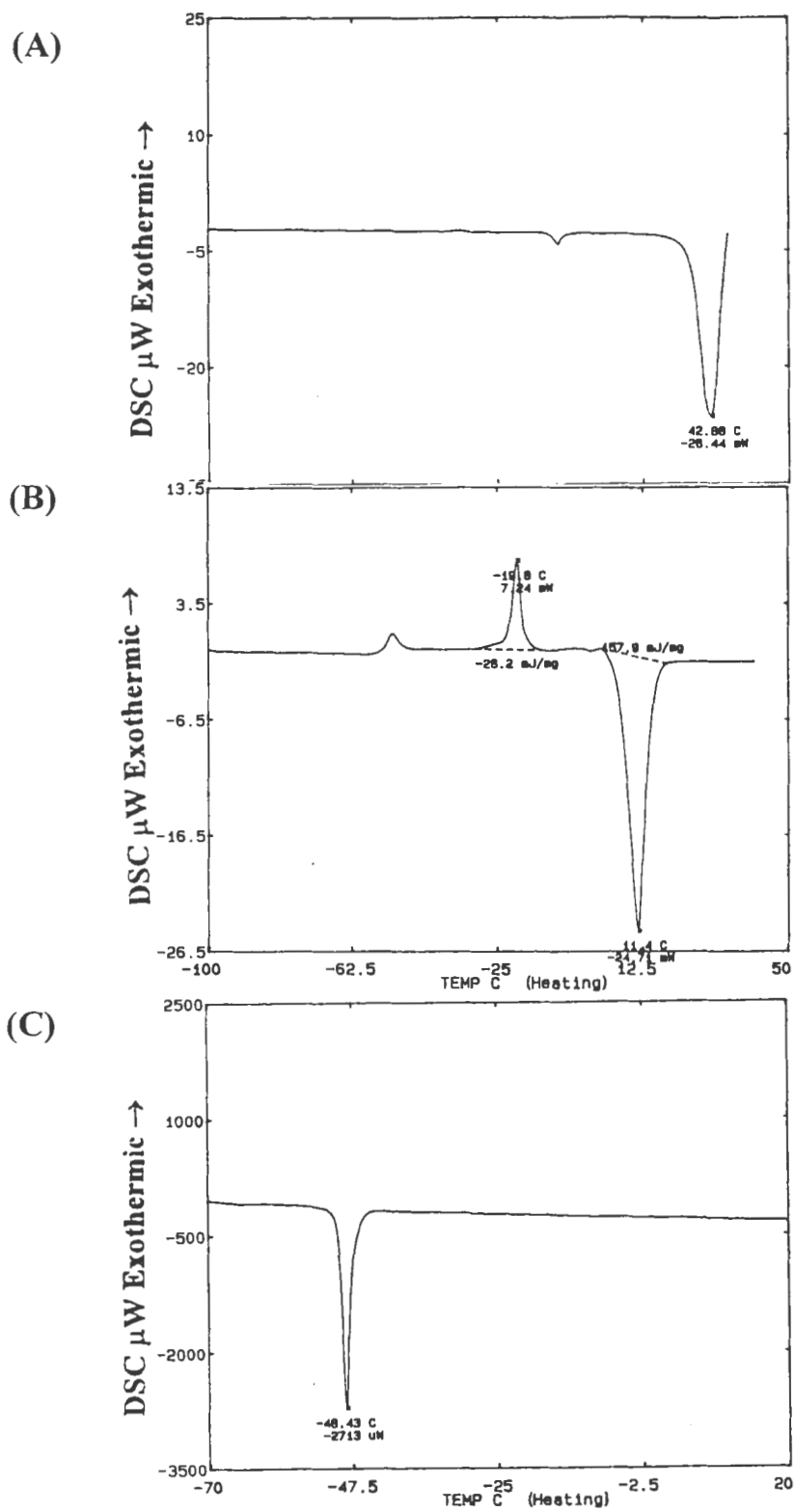


Figure 8: DSC Traces of Mono- (A), di- (B) and tri- (C) glyceride of Caprylic Acid

The sharp melting peak of monoglyceride is at 42.66°C, diglyceride at 11.4°C and triglyceride is at -48.43°C. Comparison of Figures 7 A, B and 8 A, B, C reveals the fact that the first peak that appear in 7A, the wide endothermic melting may be of triglyceride Caprylic and Capric Acids.

MCM was further heated to 150°C and cooled down to -70°C. The enthalpies calculated are given in Table V and Table VI. The first peak appeared at -24.25°C is the triglyceride of Caprylic and Capric Acids, at the third heating cycle, the melting peak of the triglyceride esters was shifted from -25.5°C to -23.92°C. There is little differences in  $\Delta H$  during cycle experiments. The second peak which occurs at -18.63°C is an exothermic crystallization trace of di-ester components of the vehicle. During the heating curves, the  $\Delta H$  value has changed from -35.2 to -40.4 mJ/mg (Table V). The third trace is the endothermic melting point of diglyceride component of MCM. The final trace is the melting point of monoglyceride component of the vehicle. There is a significant change in  $\Delta H$  value of the fourth peak which differs from the other traces. The value is decreased from 42.0 mJ/mg to 30.1mJ/mg. This decreasing in value of  $\Delta H$  can be explained by thermal decomposition of the sample. Heating may increase decomposition of the sample resulting in enthalpy changes.

Only one exothermic peak was seen during the cooling of the sample. There is no differences in temperature and  $\Delta H$  values while heat flow values is increasing from 8242  $\mu W$  to 8508  $\mu W$ . Since heat flow value is an instrumental parameter, this may not be a

**Table V: DSC Traces of MCM in Temperature Range of (-70°)-(150°)C During Heating**

Peak*	First Heating		Second Heating		Third Heating	
	Temp. (°C)	$\Delta H_{mJ/mg}$	Temp. (°C)	$\Delta H_{mJ/mg}$	Temp. (°C)	$\Delta H_{mJ/mg}$
1	-25.50	17.1	-24.25	15.5	-23.92	16.9
<i>1S</i>	-26.14	11.6	-22.70	11.7	-22.06	9.5
2	-19.87	-35.2	-18.63	-44.0	-18.29	-40.4
<i>2S</i>	-21.12	-43.0	-17.65	-41.4	-17.06	-41.7
3	-0.74	11.0	-1.37	8.0	-0.78	10.5
<i>3S</i>	-1.08	18.2	-0.74	9.4	-0.12	9.9
4	21.80	42.0	21.79	33.0	22.12	30.1
<i>4S</i>	18.65	43.9	23.36	30.6	23.04	28.2

\* the peak denoted S in *italic* form are for the sheared MCM samples

**Table VI: DSC Trace of MCM in Temperature Range of (-70°)-(150°) C During Cooling**

	Temperature (°C)	$\Delta H$ (mJ/mg)
First Cooling	-30.89	-53.2
<i>First Cooling</i>	-28.99	-51.9
Second Cooling	-30.54	-53.1
<i>Second Cooling</i>	-28.69	-51.1
Third Cooling	-30.54	-53.3
<i>Third Cooling</i>	-29.01	-48.9

sign of thermodynamic changes occurred in the sample. The cooling curves on the other hand, do not show a temperature dependent transformation between the fatty acid glycerides.

Overall, DSC results of MCM show that the vehicle is not thermostable.

DSC results for the sheared vehicle showed that shearing did not caused any significant effect on the thermodynamics of MCM (Table V). Although, there are differences in the location of the melting peaks caused by the first and second heating, these may be due to moisture uptake induced by shear which disappears after first heating.

Figure 9 demonstrates FT-IR of MCM. The broad band which appeared at  $3410\text{ cm}^{-1}$  is the hydrogen bond (O-H) stretching. The sharp bands between  $2957\text{-}2858\text{ cm}^{-1}$  corresponds to alkane (C-H) stretching. Carboxylic acid ester stretching can be seen at  $1741\text{ cm}^{-1}$ . The bands at between  $1470$  and  $1200\text{ cm}^{-1}$  correspond for C-H and O-H bending. C-O-C stretching can be seen at between  $1300$  and  $1050\text{ cm}^{-1}$ .

Raman spectrum was obtained on same instrument in order to get completed information about the chemical structure of MCM, Figure 10. The stretching vibrations at between  $2800$  and  $2940\text{ cm}^{-1}$  are for -CH- groups. The small and weak peak at  $1744\text{ cm}^{-1}$  corresponds for C=O groups. A -CH<sub>2</sub> bending vibration and CH<sub>3</sub> antisymmetric vibration can be seen at  $1445\text{ cm}^{-1}$ . The peak at  $1308\text{ cm}^{-1}$  is for CH<sub>3</sub> symmetric vibration. The

peaks at 1136, 845 and 725  $\text{cm}^{-1}$  correspond for antisymmetric C-O-C vibration, O-O stretching and C-C stretching vibrations, respectively.

X-ray Diffraction pattern of MCM was obtained at a scan rate of 0.75 deg/min. in the range of 0.00-45.00  $2\theta$  at room temperature ( $19.00 \pm 2.00^\circ\text{C}$ ) (Figure 11A). The vehicle showed amorphous behavior under given experimental conditions. X-ray studies was also conducted for sheared MCM (Figure 11B). The DSC results Table V, demonstrated that MCM showed unstable conditions when it was heated up and cooled 3 times. Therefore, X-ray pattern of MCM subjected to 3 heating cycles was taken (Figure 11C). Like shear, heating did not caused a detectable change in the structure of the vehicle within the measurable limits of the instrument.

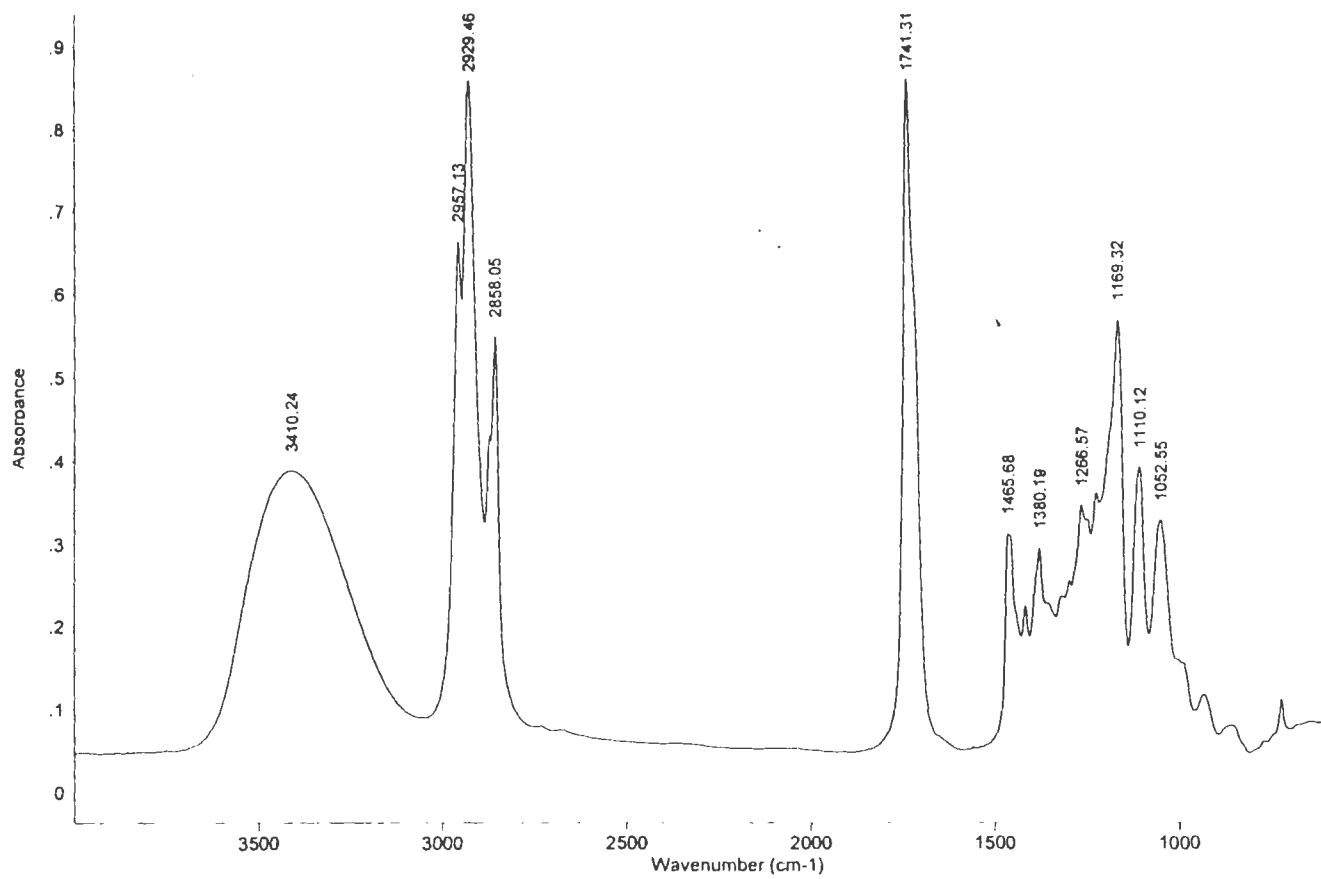
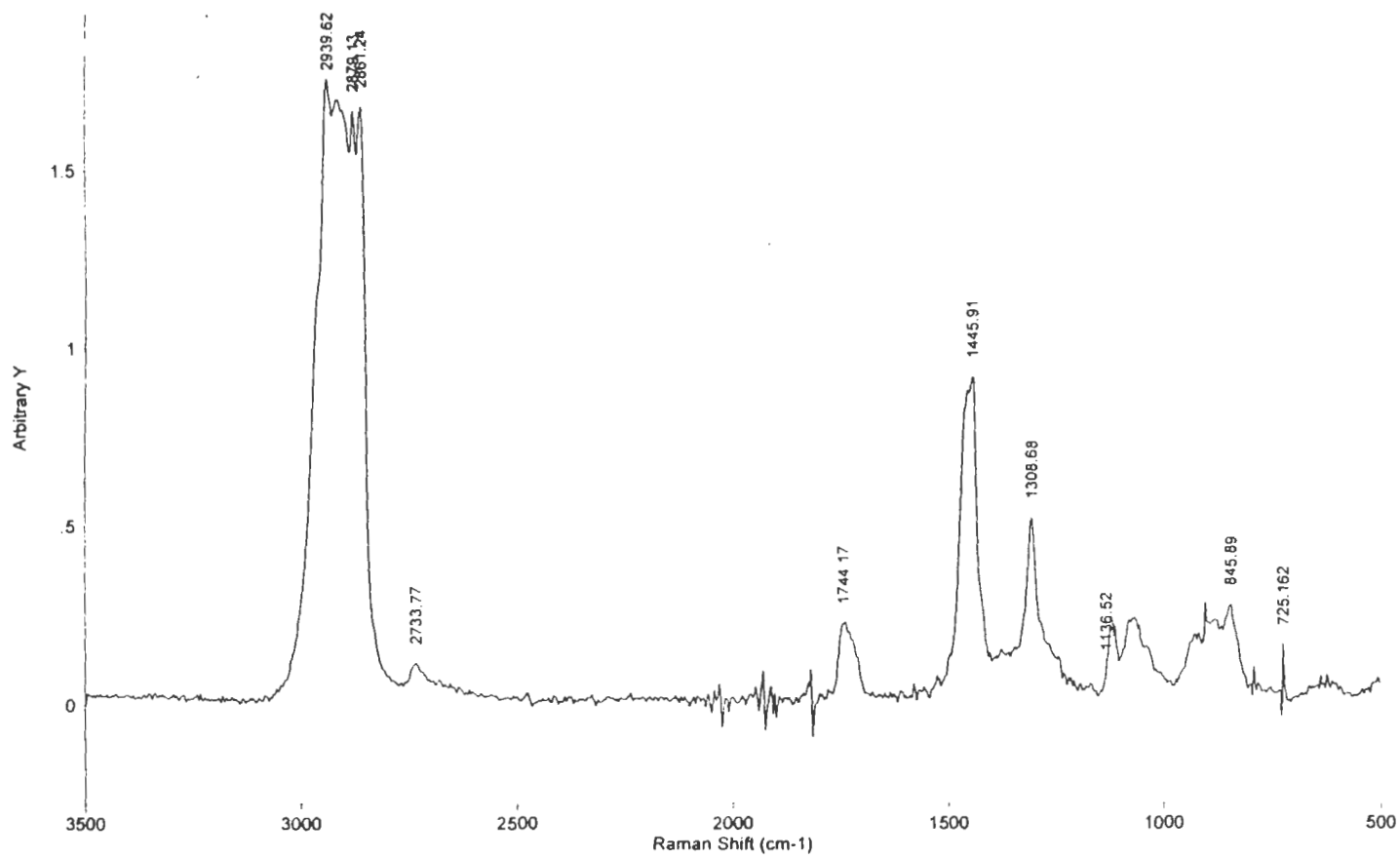
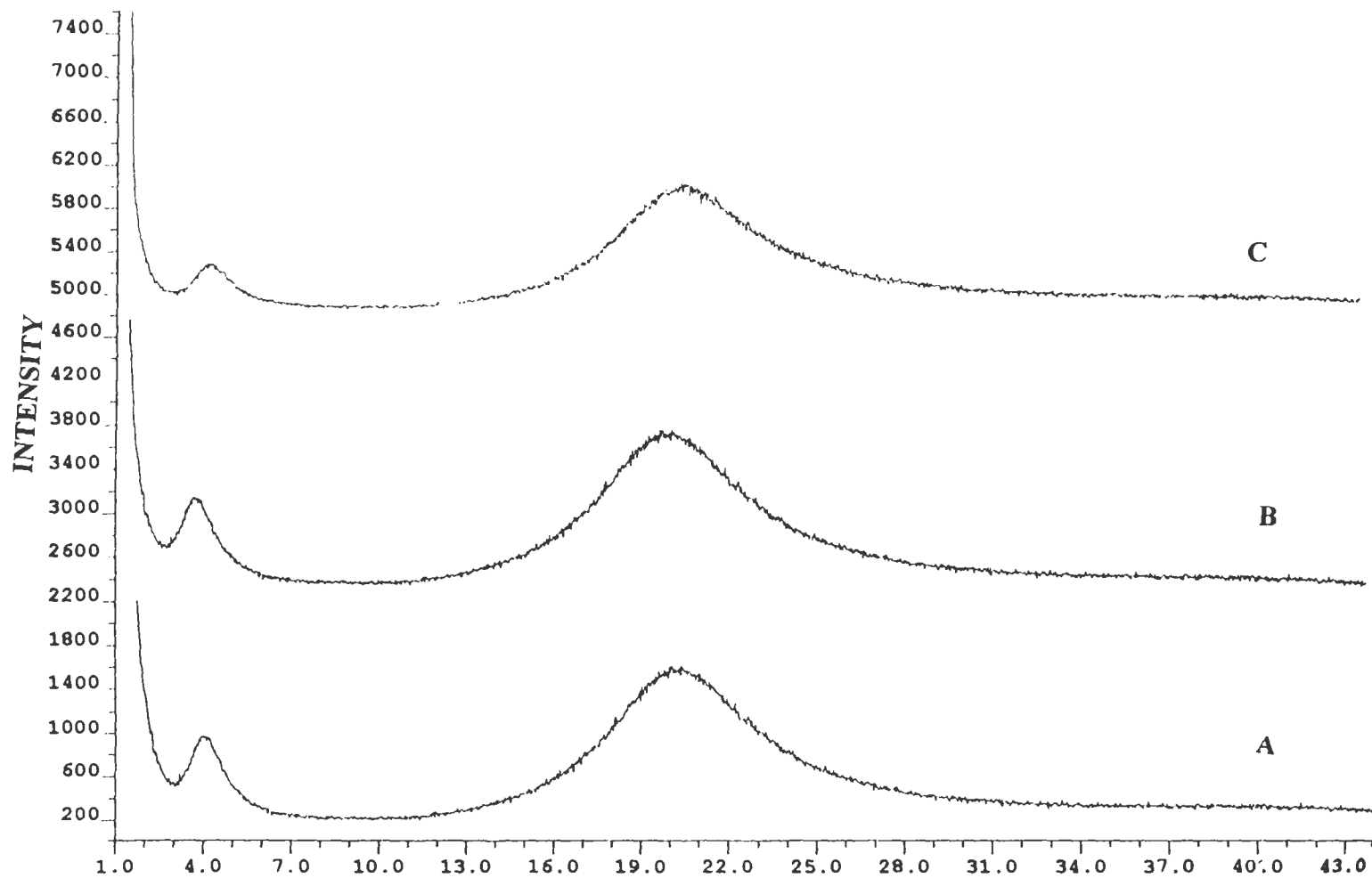


Figure 9: FT-IR Spectrum of MCM at 4 cm<sup>-1</sup> Resolution





**Figure 10: FT-Raman Spectrum of MCM at 4 cm<sup>-1</sup> Resolution**



**Figure 11 : The X-Ray Pattern of MCM Taken from 1 to 45  $2\theta$  ( $19 \pm 2.00$ ) at 0.75 deg/min Rate Before Shear (A), After shear (B) and After 3 Times Heating and Shear (C)**

## 4.2 CHARACTERIZATION OF THE DRUG

DQAIC used in this study is a peptide derivative. All the relevant properties of the drug were discussed in Sections 1.2 and 1.3. The amorphous form of the drug that was used in the study had 0.03 mg/mL water solubility and 400 mg/mL MCM solubility at 21°C. It decomposed above 200°C. In addition to these known properties, characterization of the drug by using DSC, FT-IR and X-Ray diffraction was conducted in order to understand changes occurring in the system.

Amorphous DQAIC is a white, powder which has average mean particle size of 5  $\mu\text{m}$  (Figure 12). It does not refract under polarizing light.

The moisture content of the drug was determined using the titration technique explained in Section 3.3.2.7. The average of three moisture content was  $1.135 \pm 0.002$  %w/w.

The results of thermodynamic screening of DQAIC is given in Figure 13. The heating curve of DQAIC provides a sharp endothermic peak at  $106.4^\circ \pm 0.015^\circ\text{C}$ . From the cooling curve, the glass transition temperature was calculated as  $104.9^\circ\text{C}$ . Enthalpies tabulated are given in Table VII.

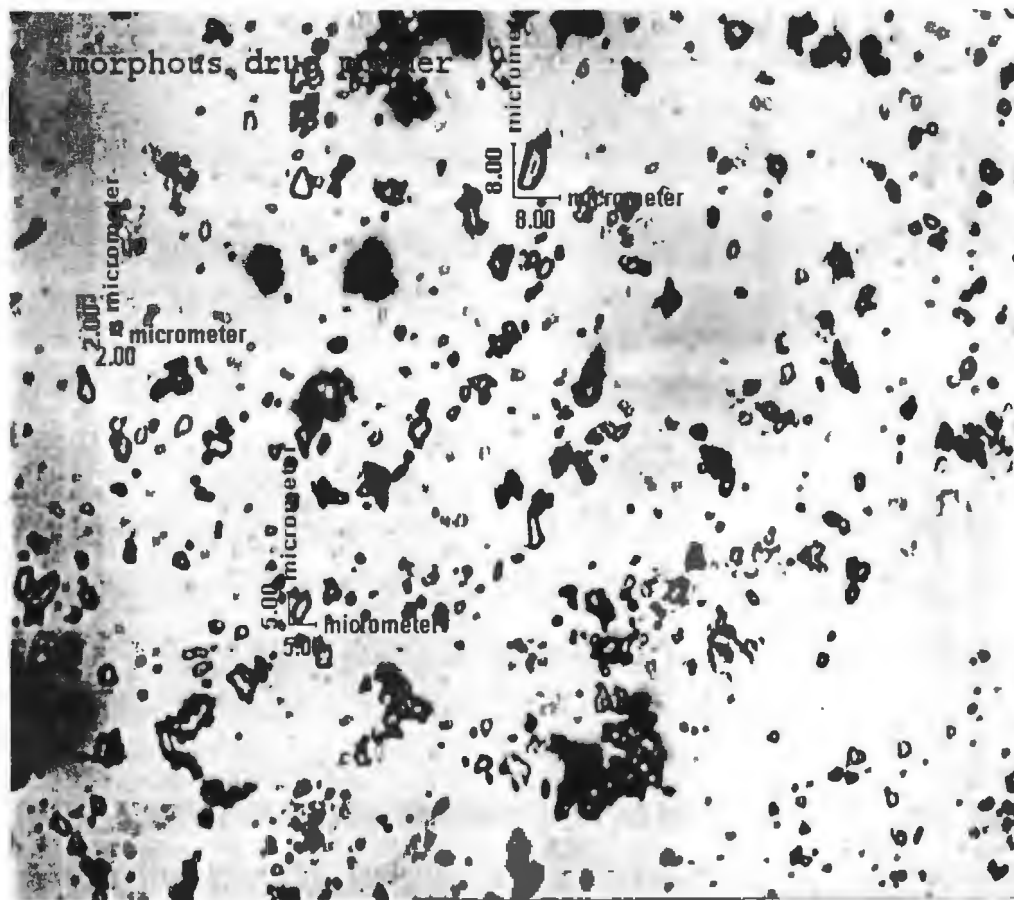


**Figure 12 : Microscopic Image of Powder DQAIC with 20 x 25 Magnification at  
19.00 ± 2.00°C.**

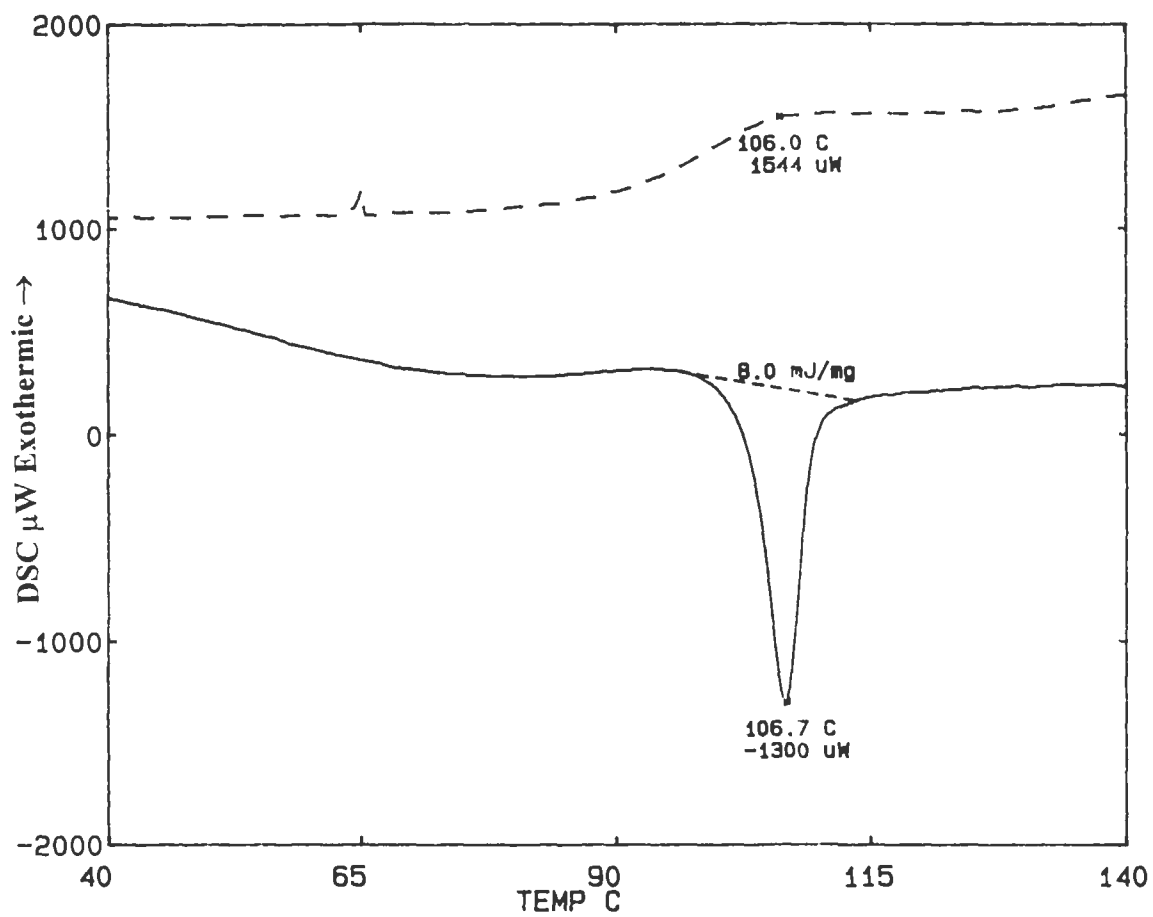
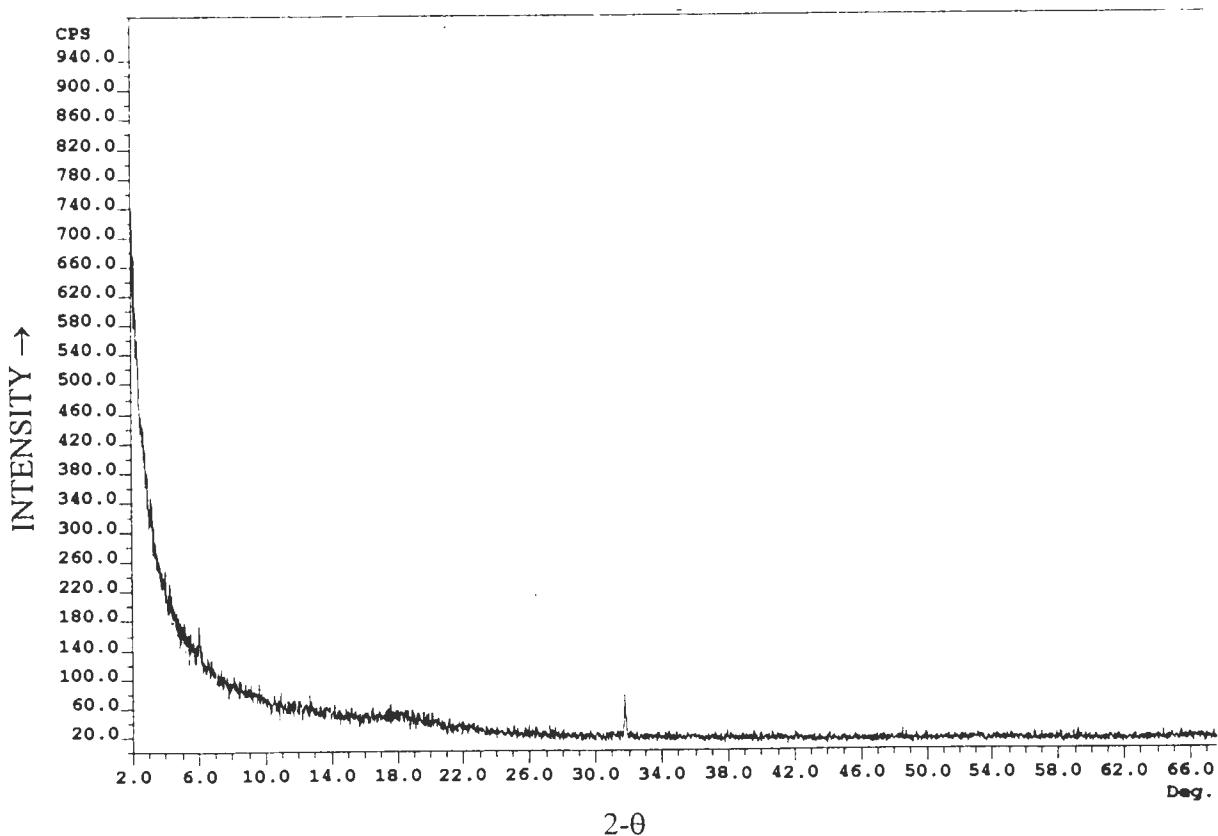


Figure 13 : DSC Traces of DQAIC Powder During Heating (—) and Cooling (----) Between 20°C and 150°C.

**Table VII: DSC Performance of the Drug Scanned Between 20°-150°C; Heating and Cooling Curves**

Cycle	Heating		Cooling	
	Temperature(°C)	Enthalpy (mJ/m)	Temperature(°C)	Enthalpy (mJ/m)
1	106.4	8.1	104.9 -82.1	-
2	105.6	2.3	106.2-82.5	-
3	105.4	2.5	106.2-81.4	-



**Figure 14 : X-ray Pattern of DQAIC Taken at 0.75 deg/min in a 2-θ Range of 1-70**

X-Ray Diffraction pattern of the drug is shown in Figure 14. The little peak occurred at  $32\ 2-\theta$  may be from the result of crystalline impurities or a minute portion of the drug that is crystallized.

FT-IR spectrums along with Raman spectrums were obtained as explained in section 3.3.2.3. O-H and N-H stretching were obvious between  $3500$  and  $3000\ \text{cm}^{-1}$  appeared as a broad band (Figure 15). The bands obtained at  $2924$  and  $2863\ \text{cm}^{-1}$  are representative of C-H aromatic rings stretching. The strong peak appeared at  $1659\ \text{cm}^{-1}$  can be for C=C, C=O and C=N stretching. N-H bending can be seen at  $1570\ \text{cm}^{-1}$ . Finally, C-H, and O-H bending can be seen at between  $1524$  and  $1456\ \text{cm}^{-1}$ .

In the Raman spectrum of the drug, Figure 16 a weak peak for O-H stretching vibration is found at  $3064\ \text{cm}^{-1}$ . -C-H stretching vibrations are seen at  $2931\ \text{cm}^{-1}$ . The peak at  $1674\ \text{cm}^{-1}$  corresponds to C=O vibration. The region between  $1600\ \text{cm}^{-1}$  and  $1435\ \text{cm}^{-1}$  exhibits -CH<sub>2</sub> and CC aromatics vibrations. The strongest peak at  $1384\ \text{cm}^{-1}$  shows that the compound has mainly aromatic C=C structures. The peak at  $1008\ \text{cm}^{-1}$  demonstrates C-C aromatic vibrations. C-O-C symmetric vibration peak can be seen at  $776\ \text{cm}^{-1}$  as one of the strongest peak of the spectrum.

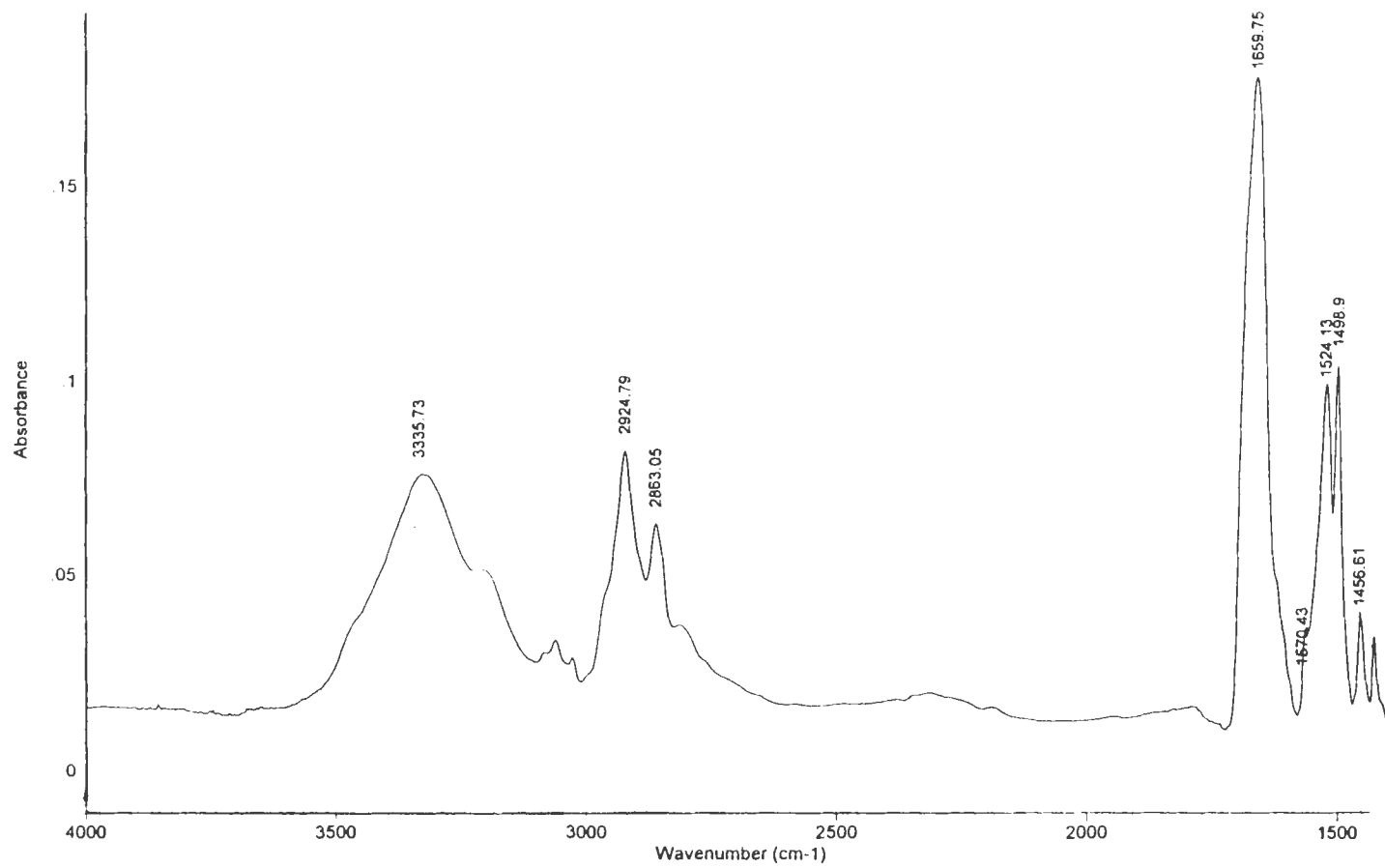


Figure 15: FT-IR spectrum of DQAIC at 4 cm<sup>-1</sup> resolution



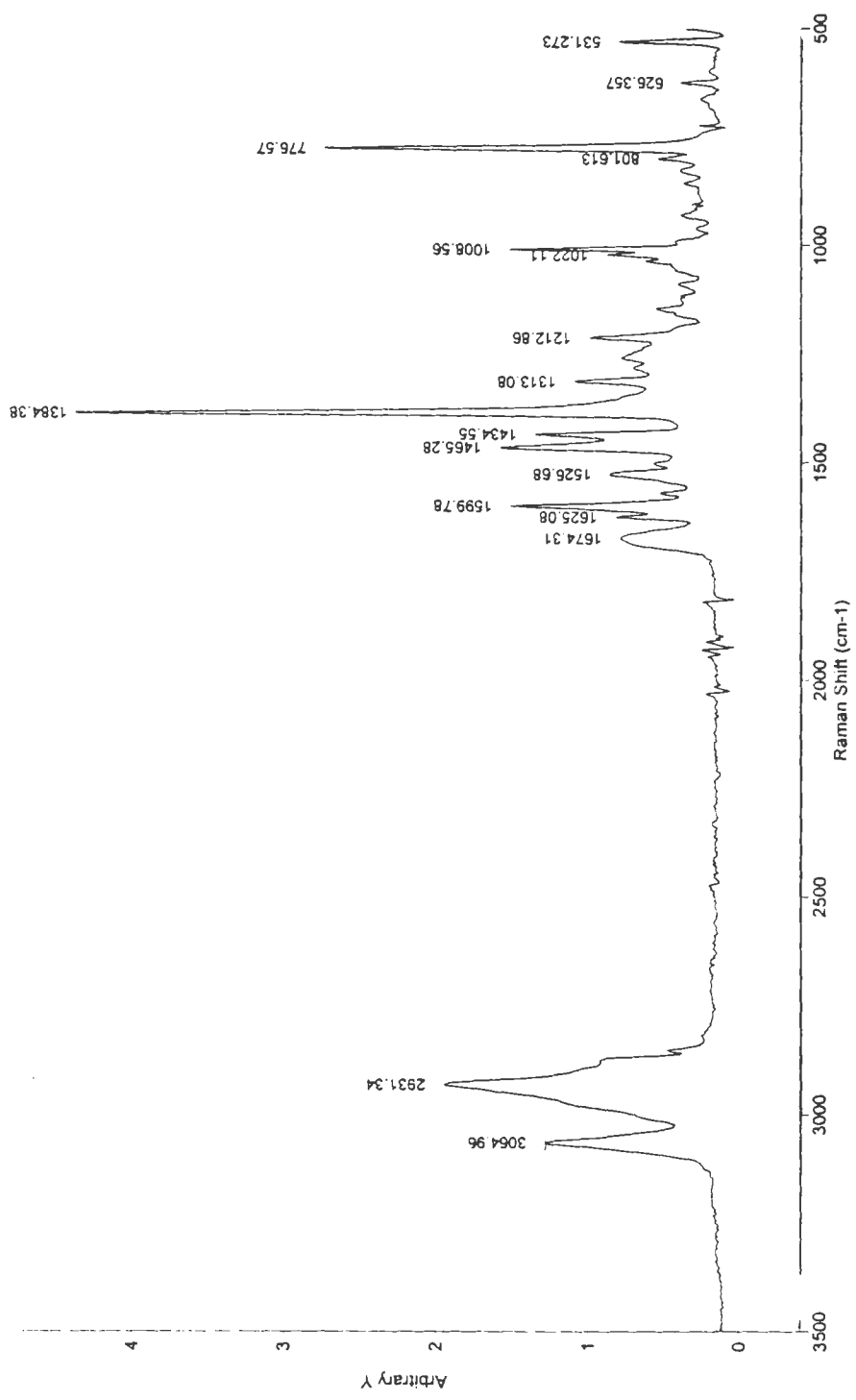


Figure 16: FT-Raman spectrum of DQAIC at 4 cm<sup>-1</sup> resolution

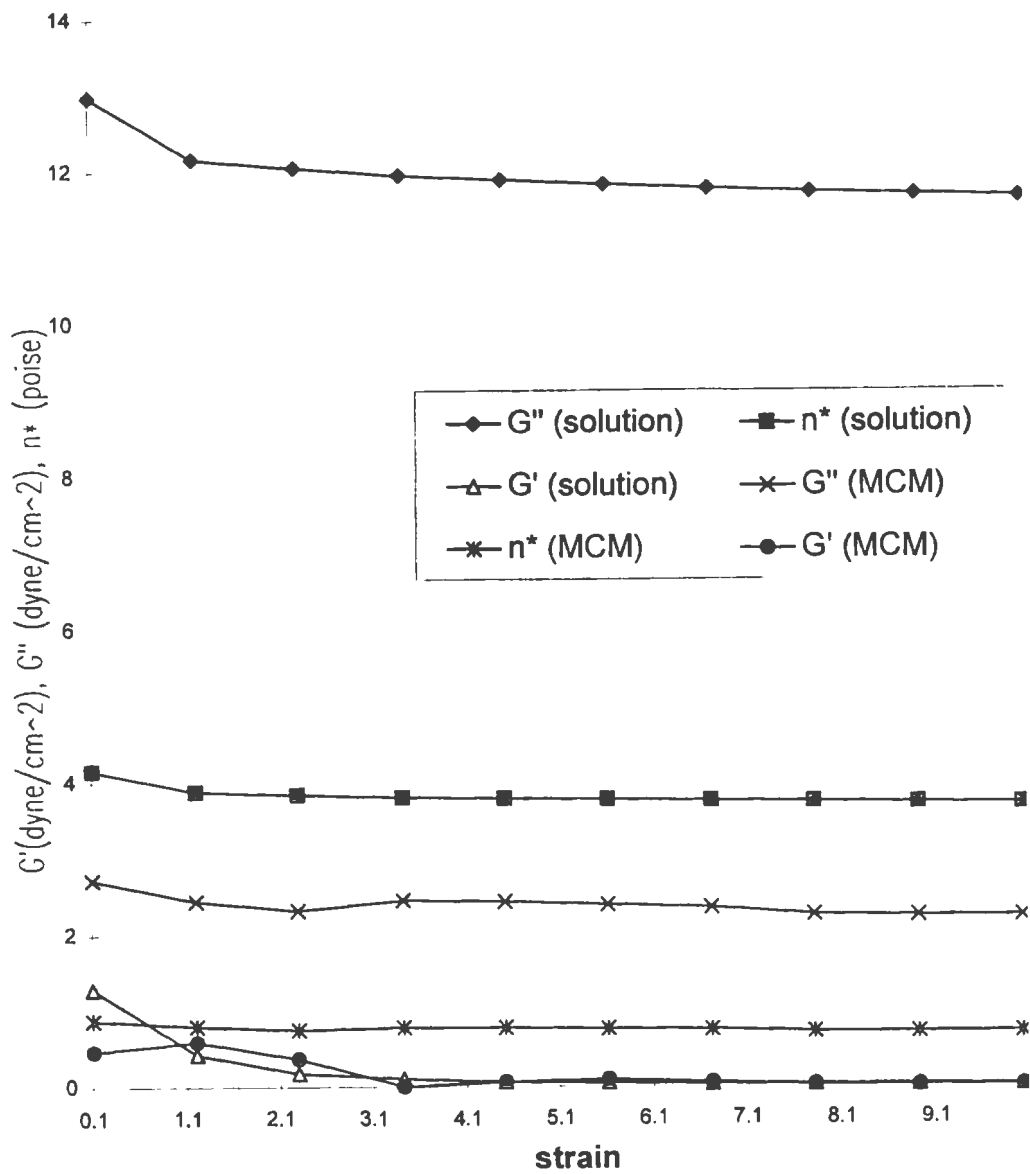
Overall, the drug used in this study is an amorphous drug. Therefore, it is in metastable state. Any processing condition may affect its morphological properties. The FT-IR and Raman studies, Figure 15 and 16 demonstrated that it can form hydrogen bonds, Van-der Waals as well as hydrophobic bonds. It may easily interact with suitable solvents.

### 4.3 CHARACTERIZATION OF THE DRUG SOLUTION IN MCM

In order to determine solvent- solute interaction, the rheological properties, DSC, FT-IR and X-Ray of the 20% (w/w) DQAIC solution in MCM were investigated. This concentration is the therapeutic concentration that is used per capsule.

#### 4.3.1 Rheological Characterization

Figure 3 demonstrates that the viscosity of the drug solution remained Newtonian although the viscosity increased from 83 cP to 411 cP at 25°C. The results demonstrate no changes in viscous pattern between 1-500 1/sec shear rate. Creep measurements (Appendix I, Figure 9) obtained showed there is no elastic component in the system. Both MCM and 20% (w/w) drug showed purely viscous behavior. The viscous modulus ( $G''$ ), elastic modulus ( $G'$ ) and complex viscosity ( $\eta^*$ ) of the solution and MCM were also studied with an oscillatory viscometer. The strain sweep, Figure 17, shows that all rheological parameters of the drug solution and MCM are linear in a strain range of 0.1-10. Therefore, any strain values between 0.1 and 10 can be used to carry out frequency and temperature sweeps. In the strain sweep experiment,  $G''$  of the drug solution was the highest with a value of 12 dyne/cm<sup>2</sup>. There was hardly any elasticity,  $G'$  value was found as 0.1 dyne/cm<sup>2</sup> and  $\eta^*$  at the zero shear was 380 Poise.



**Figur 17: Strain sweep for MCM and 20% (w/w) Drug Solution with 6 cm Parallel Plate and 1 mm Gap at 25°C**

Frequency sweep carried out in a frequency range of 0.1-0.5 Hz demonstrated an interesting phenomenon (Figure 4, Section 4.1.). Although the solution was characterized as a viscous system, and in a rotational viscometer, the rheogram indicates a Newtonian behavior, the oscillation dependent increase in the viscous modulus ( $G''$ ) demonstrated a structure built up in the system. The same property, in much lesser magnitude, exists in MCM, Figure 4. The findings demonstrate that, shear dependent intra molecular interaction is somewhat present in MCM, but increased greatly by the presence of the drug.

The temperature sweep (Figure 5) demonstrated that all the rheological parameters ( $G'$ ,  $G''$  and  $\eta^*$ ) decrease as the temperature increases. Among the all parameters,  $G''$  of the solution was found to be highly temperature dependent. The decrease in  $G''$  between 4°C and 10°C is linear, but it is the most critical between 10-40°C. The change in  $G'$  value of the solution and in all measured rheological components of MCM is much less critical again demonstrating the presence of DQAIC in MCM increased the temperature and shear dependence greatly.

Overall,  $G''$  was found to be a representative of the structural changes occurring in the drug solution and may be used as a critical parameter to investigate various experimental factors and to demonstrate gelling potential of a formulation.

#### 4.3.2 Solution Morphology and Physico-Chemical Characteristic of DQAIC

DSC of 20% (w/w) DQAIC studied between 20°C and 65 °C did not show any traces in during heating and cooling, Figure 18. DSCs of the solution obtained between -70°C and 150°C are given in Figure 19. Since the drug is amorphous, DSC of only MCM and drug solution was compared (Figure 19 A and B). The difference in MCM in the presence of DQAIC occurred is the peak of the monoglyceride appeared at 21°C. It is moved to 18.69°C indicating a weakened interaction of the chains. The melting point of diglyceride shifted from -1.37°C to -4.86°C indicating relatively weakened structure. In the solution form, the enthalpy of both monoglyceride and diglyceride are decreased as expected. Those may indicate an interaction of the drug with -OH groups of the vehicle. The presence of the drug also influences crystallizing ability of MCM as impurity.

In the drug solution, an insignificant peak occurs in the immediate left of the monoglyceride peak of MCM. In the presence of DQAIC, this peak is increased in intensity and the shape. It might indicate an interaction of the drug with component that is present in minimum amount in MCM.

A FT-IR difference spectrum was generated by subtracting the MCM spectrum from the solution spectrum in order to compare both spectra clearly because the peaks of MCM are very strong (Figure 20). In the spectrum of the solution, the region

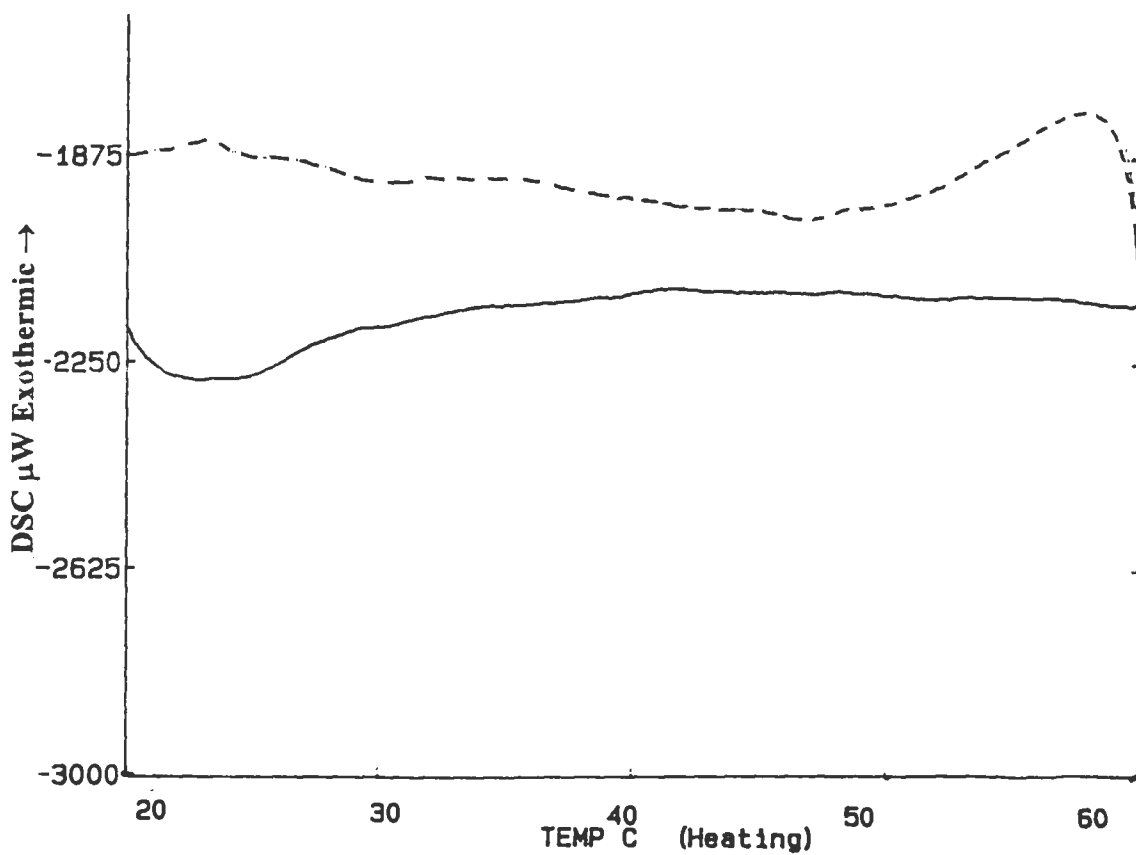


Figure 18: DSC Traces of 20% DQAIC Solution During Heating (—) and Cooling (----) Between 20°C and 65°C at a Rate of 0.33°C/min

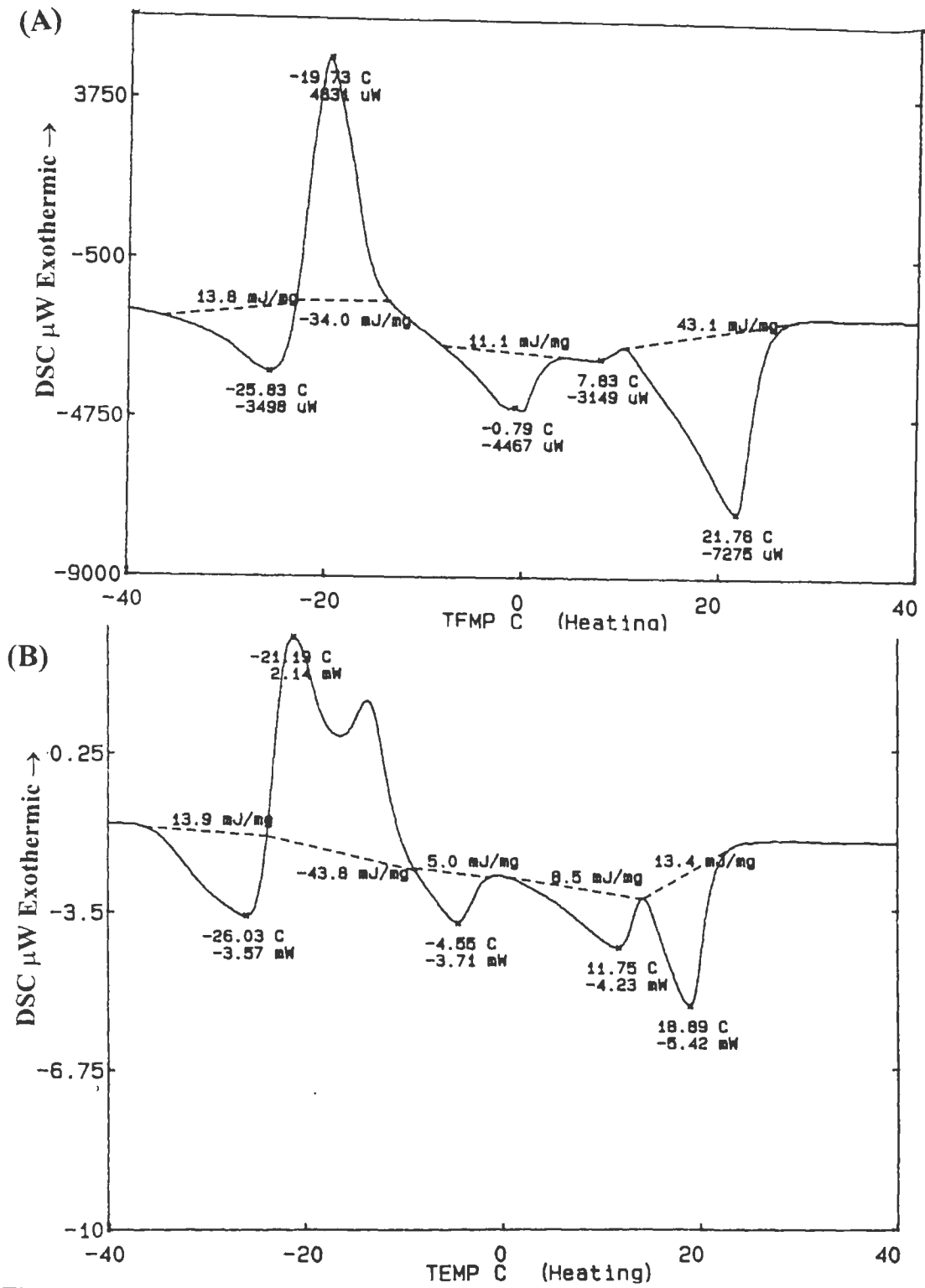


Figure 19: Comparison of DSC of MCM (A) and 20% (w/w) DQAIC solution (B); between -70°C and 150°C



between  $3600\text{ cm}^{-1}$  and  $3000\text{ cm}^{-1}$  exhibits O-H and N-H stretching. This band is similar to one that was seen in the drug powder (Figure 15). The only differences in this region is the appearance of an extra weak peak at around  $3600\text{ cm}^{-1}$  in the spectrum generated by the solution of the drug. This difference shows that there is little increase in the O-H bonding between the drug and MCM. The other difference observed is the weak peak at around  $2800\text{ cm}^{-1}$  which corresponds to C-H stretching in the solution spectrum. The weak band seen at around  $1700\text{ cm}^{-1}$  can be due to C=O stretching which was not seen in the drug molecule. Other traces such as the one at  $1667\text{ cm}^{-1}$  for C=C, C=O and C=N stretching and at  $1500\text{ cm}^{-1}$  for C-H and O-H bending are the same peaks seen in the spectrum of the drug.

There were no changes in Raman spectra of the solvent, drug and the drug solution, (Appendix I, Figure 14).

The particle size determination was also carried out on the solution using Dynamic Light Scattering (DLS). As explained in Section 3.3.2.5, first zero shear viscosity was found from the frequency sweep. Complex viscosity ( $\eta^*$ ) with a value of 338.92 cP was accepted as a zero shear viscosity. Particle size of the solution was found to be  $8.85 \pm 0.30\text{ nm}$  with polydispersity of 0.218. The data indicate that the drug at 20% concentration is not a true solution.

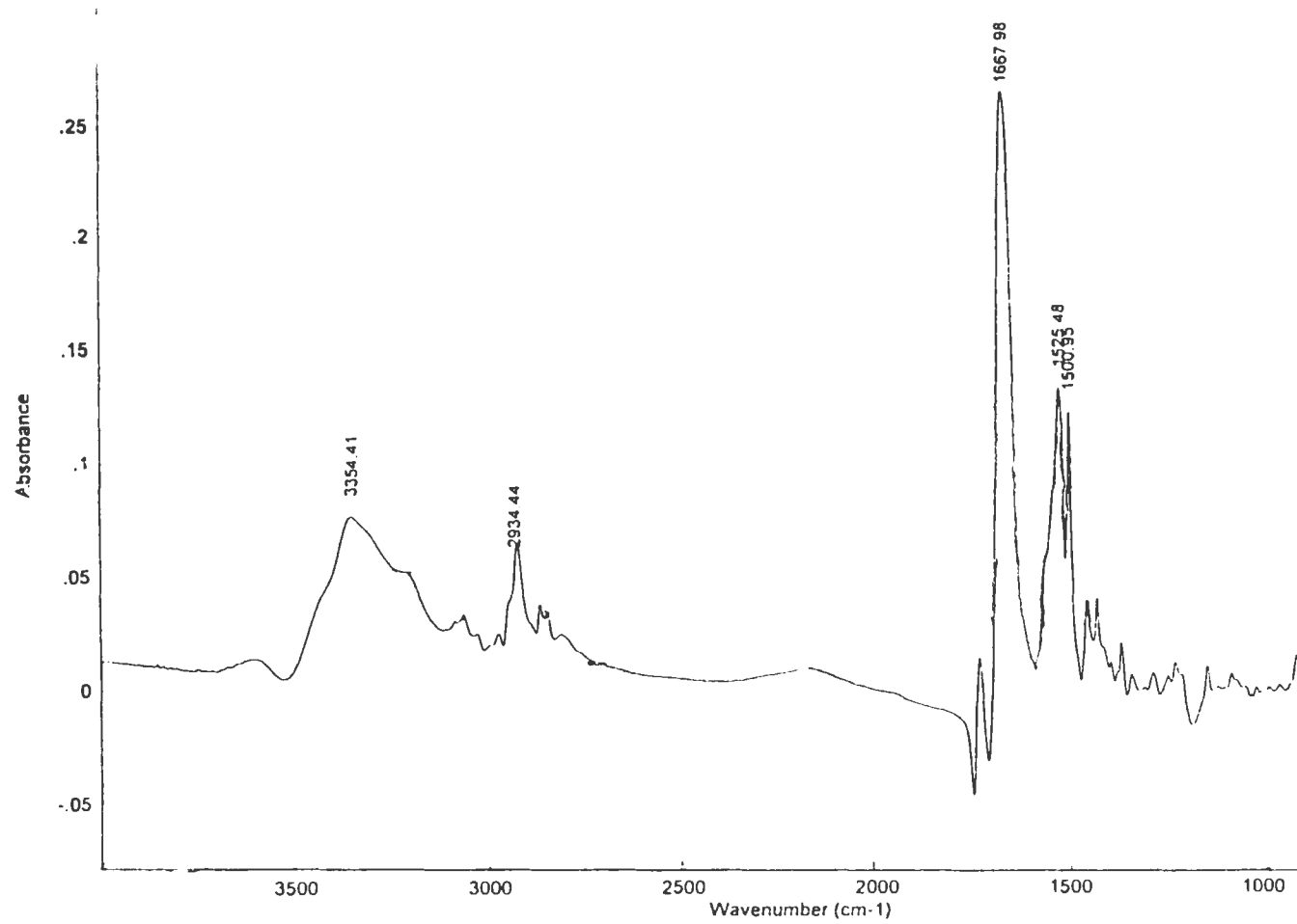


Figure 20 : FT-IR Spectrum of 20% (w/w) DQAIC Solution at 4 cm<sup>-1</sup> Resolution

#### **4.4 CHARACTERISATION OF SOLUTION AFTER SHEAR**

The DQAIC solution in MCM begins to develop gelled cores after being sheared 6 hours at 3000 rpm, and gelled completely within 12 hours turning into an opaque-cremish semi-solid structure. Table VIII summarizes the microscopical changes taking place in the solution during 12 hours shearing and Figure 21 shows the microscopic appearance of the gelled solution.

##### **4.4.1 Rheological Investigations**

A frequency sweep of the gelled solution, Figure 22, showed that all the rheological parameters were increased. The increased elastic modulus ( $G'$ ) is indication of gelling occurred after shear while it was almost zero before shearing of the solution. The system changed from Newtonian to pseudoplastic behavior as indicated by decreasing complex viscosity. The effect of shearing time on  $G''$  of solution and MCM is also shown in Figure 23.  $G''$  or other rheological parameters of the solution increased with time, while  $G''$  of MCM did not change.

**Table VIII: Microscopic and Visual Observation of the Drug Solution During Shear**

<b>Sample</b>	<b>Comments</b>
The drug solution in MCM pre-sheared	Yellow, viscous, clear liquid , clear under the microscope
The drug solution in MCM sheared 3 hr	Yellow, viscous, clear liquid, nothing seen under microscope
The drug solution in MCM sheared 6 hr	Yellow, viscous translucent liquid , clear under the microscope
The drug solution in MCM sheared 9 hr	White, translucent semisolid, cloudy background, extended fibrils
The drug solution in MCM sheared 12 hr	White, opaque semisolid , cloudy background, more distinguished fibrils

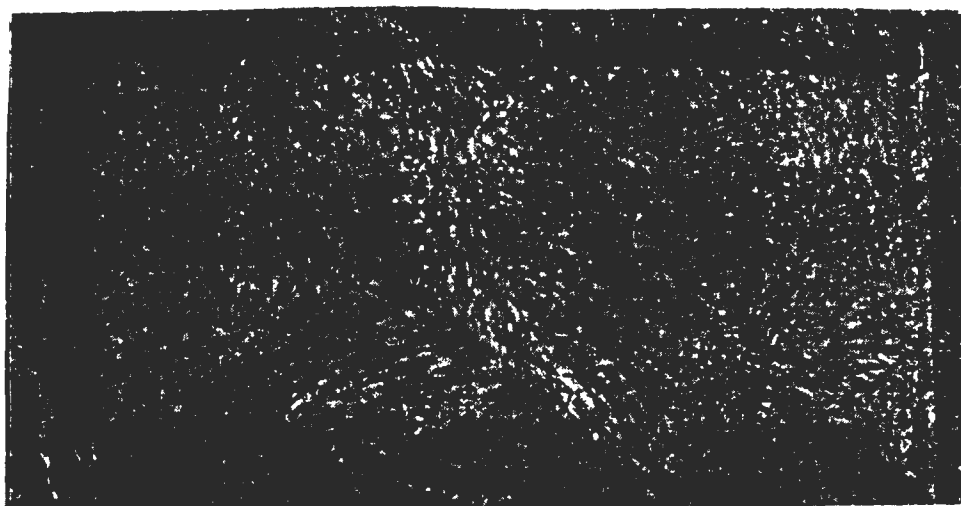


**Figure 21 : Microscopic Image of DQAIC Solution After Shearing 12 hr at 25 x20 Magnification under Cross Polar.**

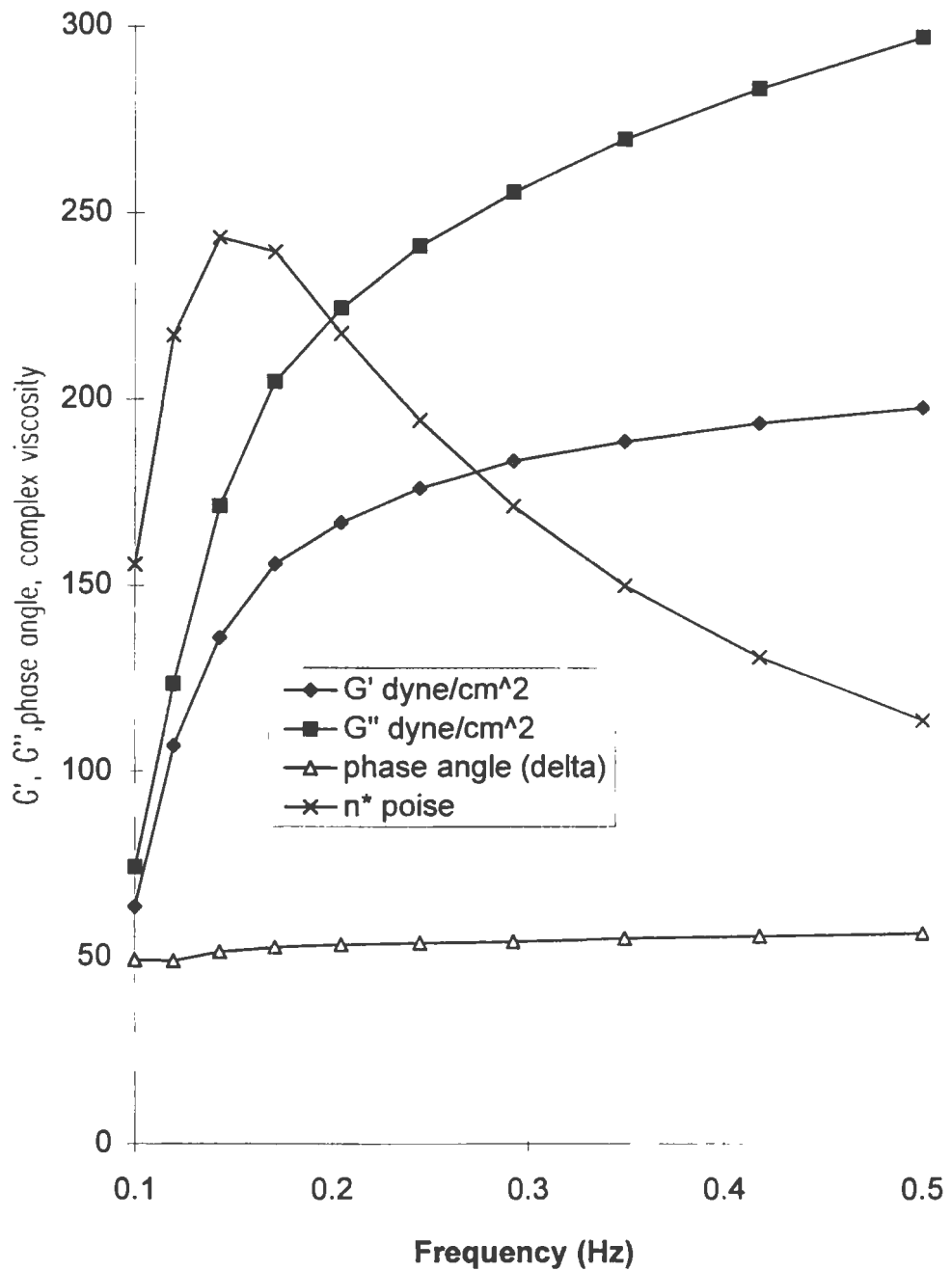


**Figure 22: Frequency Sweep for Sheared Solution with 6 cm Parallel Plate and 1 mm Gap at 25°C**

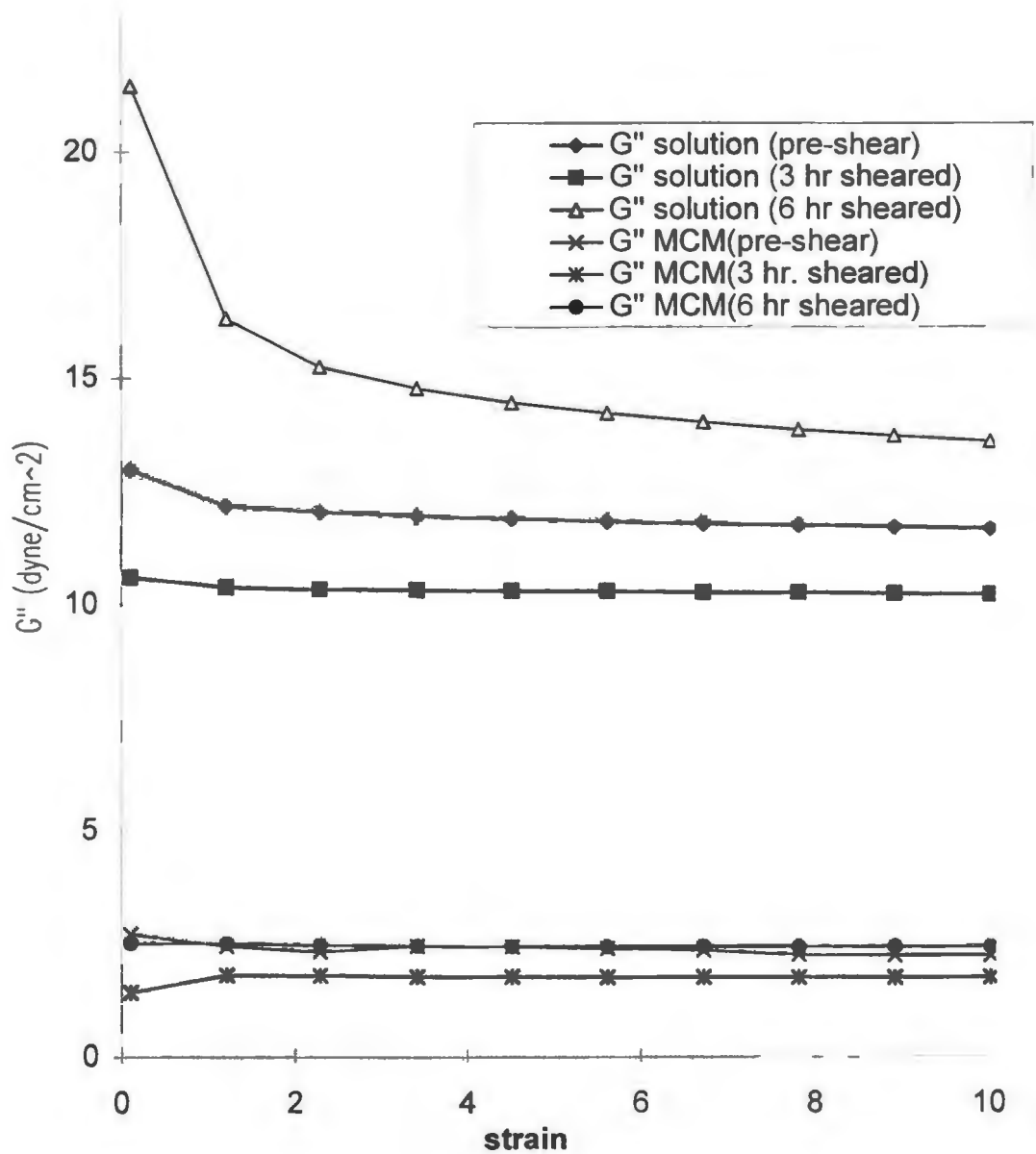


**Figure 23: Effect of Shearing Time on  $G''$  of 20 % (w/w) Drug Solution and MCM with a 6 cm Parallel Plate and 1 mm gap at 25°C**

#### 4.4.2 Morphological and Physicochemical Characterization of the Gelled DQAIC Solution

Tables IX and X demonstrate the DSC traces of the non-sheared and sheared (gelled) sample. The samples were subjected to three heating and cooling cycles. Comparison of enthalpy before and after shear shows an increase in the enthalpies of di- and triglyceride peaks after shearing of the solution. However, disappearance of these differences after second and third heating cycle may be due to moisture uptake during shearing of the solution. Overall, there are no significant differences in DSC results except little shifts appeared in melting point peaks, Figure 24.

Figure 25 shows FT-IR spectra of comparison of non-gelled and gelled samples. The band between  $3600\text{ cm}^{-1}$  and  $3000\text{ cm}^{-1}$  which exhibits an O-H and N-H stretching which is much broader in the spectrum of sheared sample than that of the pre-sheared one. In addition, a shoulder appeared at  $3548\text{ cm}^{-1}$  and an insignificant shoulder at  $3220\text{ cm}^{-1}$  in the non-sheared sample became significantly high in the sheared solution. The other major difference is seen at  $1520\text{ cm}^{-1}$ . This peak is stronger in the pre-sheared sample than in the sheared one. This shows that the shearing causes a decrease in N-H and O-H bending. All other bands are identical in the both spectra. Raman spectrums of the formulation before and after shear were also used for comparison of both samples (Appendix I, 15). However, no shear induced differences were seen in these spectra.

**Table IX: Effect of Shear on the Thermodynamic Properties of the Solution as Determined by Heating Cycles Between -70°C and 150°C**

Peak	First Heating		Second Heating		Third Heating	
	Temperature (°C)	$\Delta H$ (mJ/mg)	Temperature (°C)	$\Delta H$ (mJ/mg)	Temperature (°C)	$\Delta H$ (mJ/mg)
Solution	-26.15	12.7	-25.13	17.0	-24.56	19.1
<i>gel (endo)</i>	<i>-24.24</i>	<i>19.5</i>	<i>-24.56</i>	<i>16.7</i>	<i>-22.52</i>	<i>16.9</i>
Solution	-21.10	-41.2	-17.25	-36.4	-17.67	-37.2
<i>gel (exo)</i>	<i>-18.91</i>	<i>-39.7</i>	<i>-17.03</i>	<i>-43.4</i>	<i>-16.42</i>	<i>-46.6</i>
Solution	-4.52	7.1	-4.86	5.8	-4.82	6.7
<i>gel (endo)</i>	<i>-3.58</i>	<i>10.9</i>	<i>-4.52</i>	<i>4.1</i>	<i>-4.2</i>	<i>4.5</i>
Solution	18.97	12.7	18.69	8.9	18.96	6.6
<i>gel (endo)</i>	<i>19.89</i>	<i>11.5</i>	<i>19.61</i>	<i>9.2</i>	<i>20.55</i>	<i>5.7</i>

**Table X: Effect of Shear on the Thermodynamic Properties of the Solution as Determined by Cooling Cycles Between -70 and 150°C**

	Temperature (°C)	$\Delta H$ (mJ/mg)
First Cooling, solution	-42.45	-30.3
<i>First Cooling, gel</i>	<i>-41.82</i>	<i>-31.0</i>
Second Cooling, solution	-43.10	-29.6
<i>Second Cooling, gel</i>	<i>-42.13</i>	<i>-29.5</i>
Third Cooling, solution	-43.37	-29.5
<i>Third Cooling, gel</i>	<i>-42.21</i>	<i>-30.0</i>



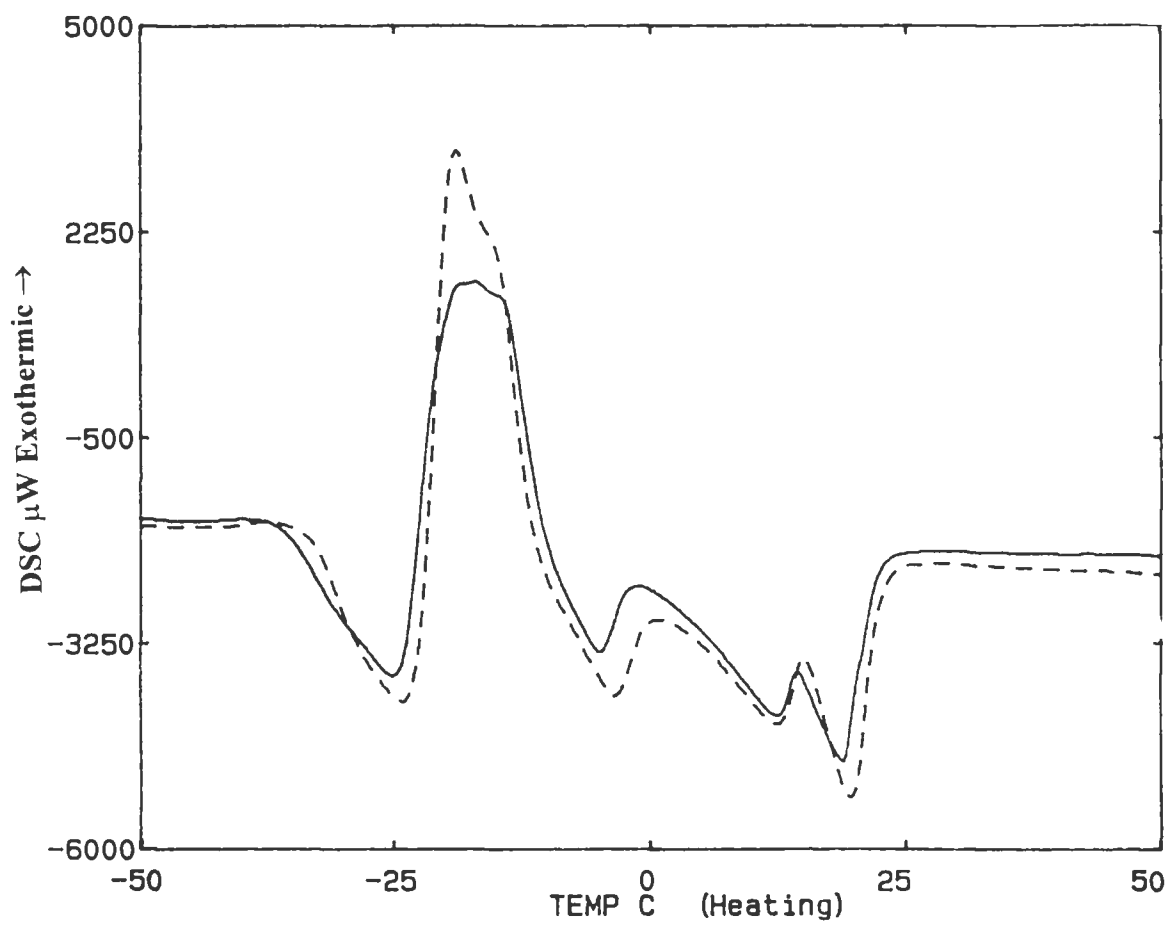


Figure 24: DSC Heating Curves of Non-sheared (—) and Sheared (----) Samples Between -70°C and 150°C

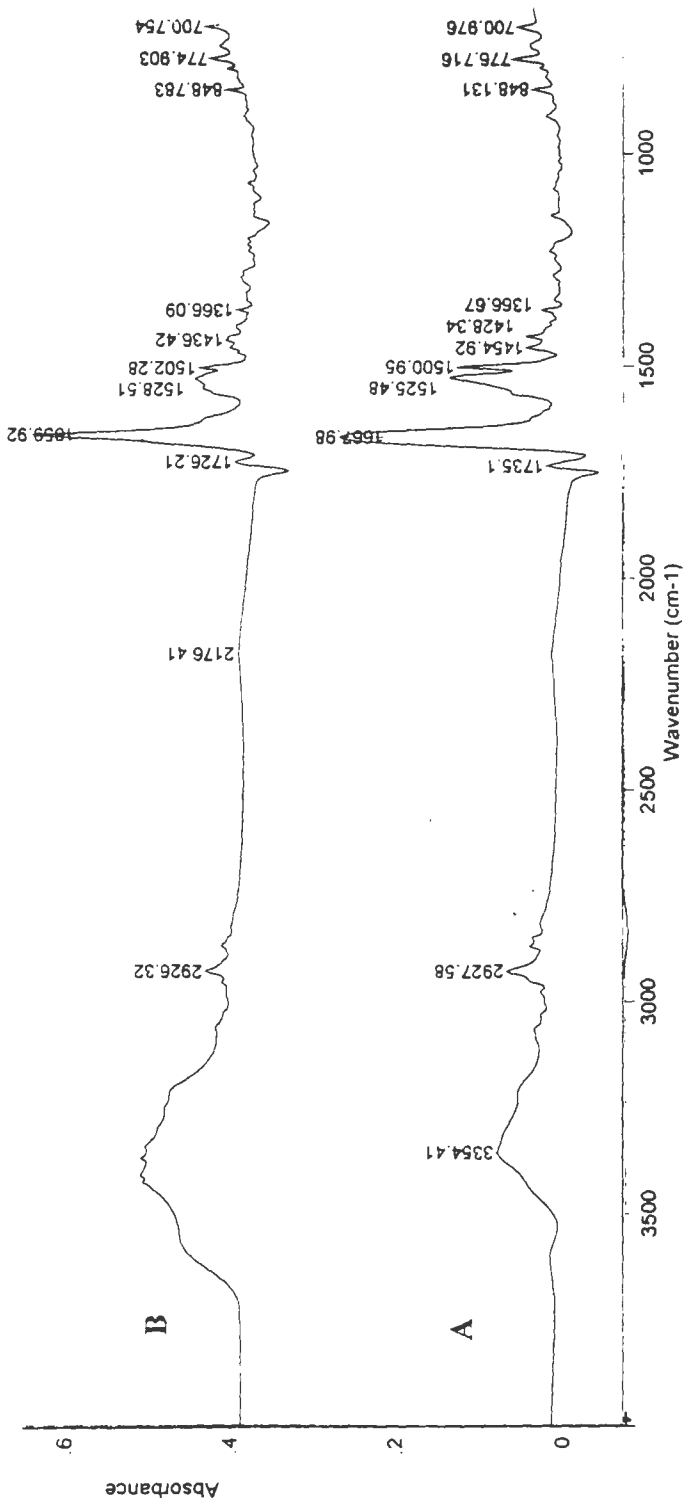
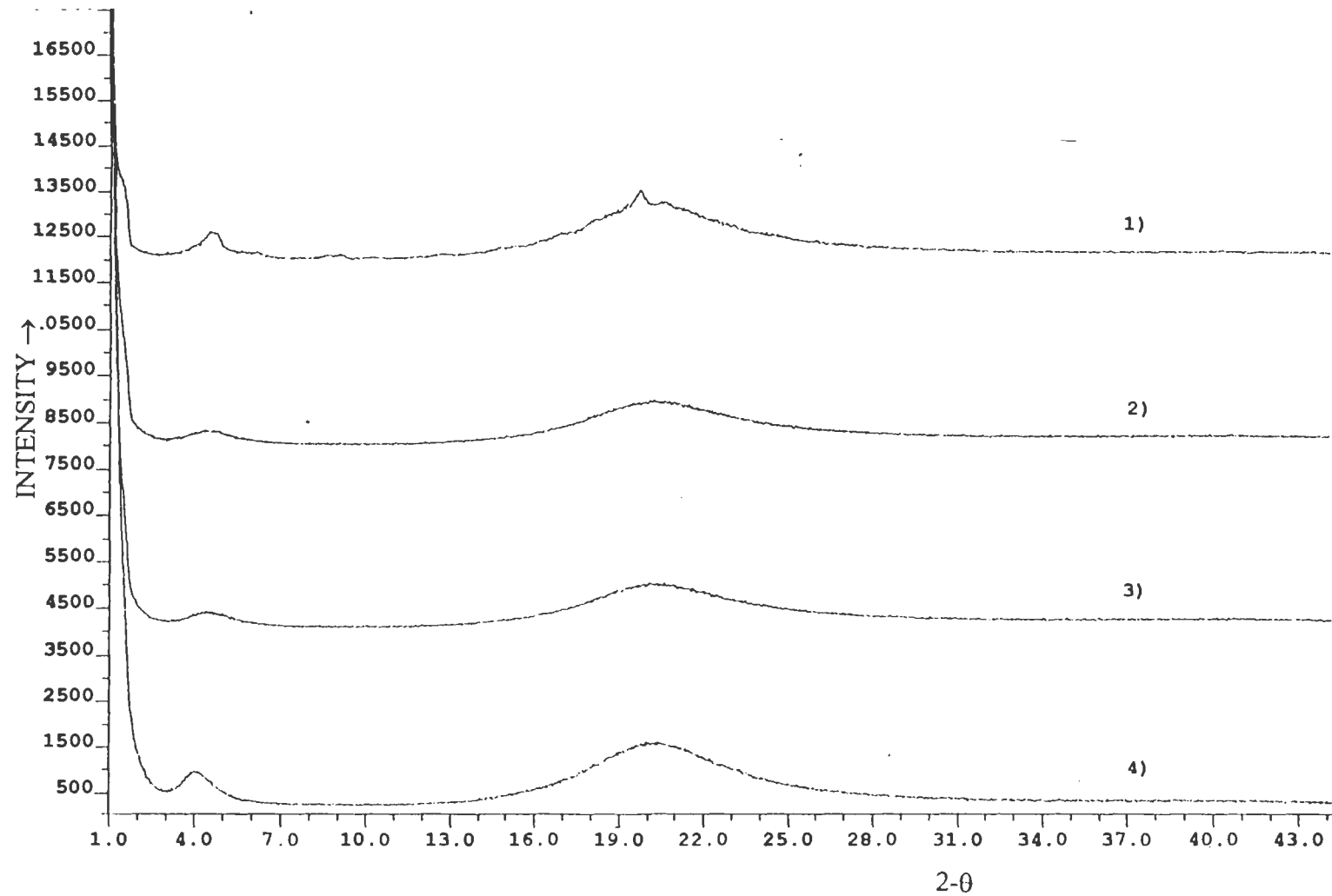


Figure 25 : Comparison of FT-IR Spectra of Non-gelled Sample (A) and Gelled Sample (B) at 4 cm<sup>-1</sup> Resolution

The gelling phenomenon was also followed by the X-ray diffraction, Figure 26, demonstrates those changes. Shearing causes structure development in the system and gel is characterized with a small peak that occurred at  $2\theta$ .

The water content of MCM and the 20% DQAIC solution before and after shear was analyzed. The moisture content of MCM before shearing at 50% RH is  $0.464 \pm 0.024$  % (w/w), which was increased to  $1.664 \pm 0.037$  % (w/w) after shear. The drug solution has  $0.727 \pm 0.025$  % (w/w) moisture content before the shear, which increased  $1.135 \pm 0.024$ % after shearing.

Overall, the increase in O-H, N-H stretching and the decrease in O-H and N-H bending from FT-IR studies shows that there are conformational changes in molecular structure of the system which was conformed further by X-ray studies. Shearing also induced moisture uptake of the solution.



**Figure 26 : X-Ray Diffraction of MCM (4), 20 % DQAIC Solution Before Shear (3),  
After 6 hour Shearing (2) and 12 Hour Shearing (1)**

## **4.5 DETERMINATION OF THE INDIVIDUAL VARIABLES THAT AFFECT ON GELLING**

### **4.5.1 Combined Effects of Shear and Temperature**

In order to investigate the effect of the shear on the gelling properties of the system, the formulation was subjected to 500 rpm, 1500 rpm and 3000 rpm shear rates using Silverson L4R high shear mixer, and the gelling time of the formulation was observed, Table XI. As it can be seen from the results, shear induces gelling phenomenon of the drug solution in MCM. Further the formulations were sheared at 25°C, 40°C, 60°C and 80°C, Table XI. Shearing the formulation at 40°C instead of 25°C induces gelation of the formulation. However, at 60°C the solution gels at longer periods than those sheared at 25°C and 40°C. When the temperature was increased up to 80°C, the solution has not formed a gel but a color change from yellow to brown was observed during shear at this temperature after 24 hours. A chemical reaction or decomposition may occur at this temperature.

### **4.5.2 Effect of Humidity**

The formulation was subjected to shear at 50 % and 30 % Relative humidity (RH) to investigate the effect of the environmental humidity. Little increase observed in the gelling time of the solution at lower humidities, Table XI.

**Table XI: The Variables that Affect on Gelling Time of the Formulation**

<b>Study Conditions</b>	<b>Gelling time (hr)</b>
500 rpm, 25 °C, 50% RH	25.0 ± 2.0
1500 rpm, 25 °C, 50% RH	18.0 ± 2.0
3000 rpm, 25 °C, 50% RH	10.0 ± 2.0
25 °C, 3000 rpm, 50 % RH	10.0 ± 2.0
40 °C, 3000 rpm, 50 % RH	6.0 ± 1.0
60 °C, 3000 rpm, 50 % RH	20.0 ± 2.0
80 °C, 3000 rpm, 50 % RH	did not form a gel
50% RH , 3000 rpm, 25 °C,	10.0 ± 2.0
30 %RH, 3000 rpm, 25°C	12.0 ± 1.0

#### 4.5.4 Effect of Storage Time

The formulation as well as MCM alone was left for a month at different conditions described in Section 3.3.2.6 to investigate gelling tendencies of the formulation upon storage. Viscous modulus was obtained from strain sweep as a representative of a rheological parameter every 7 days after equilibrated for 12 hours at room temperature. Figure 27 shows  $G''$  values vs. time at two different humidity levels (40 % and 60%) at 25°C. As it can be seen from the Figure 27 there is no significant change in  $G''$  values after a month. Figure 28 shows  $G''$  values vs. time for the samples that kept at 4°C , 25°C and 50°C for a month. There is only small amount increase in  $G''$  (from 11.975 dyne/cm<sup>2</sup> to 13.586 dyne/cm<sup>2</sup>) when the sample was kept at 50°C after 4 weeks.

#### 4.5.5 Effect of The Drug Concentrations

Even though formulation studied contains 20% drug, during testing, concentration has been demonstrated a significant effect on the gelling tendencies of the formulation. The effect of drug concentration on the gelling phenomenon was investigated by preparing 0, 2, 5, 7, 10, 12, 15, 17, 20, 22, 25% (w/v) DQAIC solutions and subjecting the solutions to shear as described in Section 3.3.1. The solutions at 15% (w/v) or below concentration did not form a gel after being sheared for 3 days at 3000 rpm, using a Silverson L4R homogenizer.

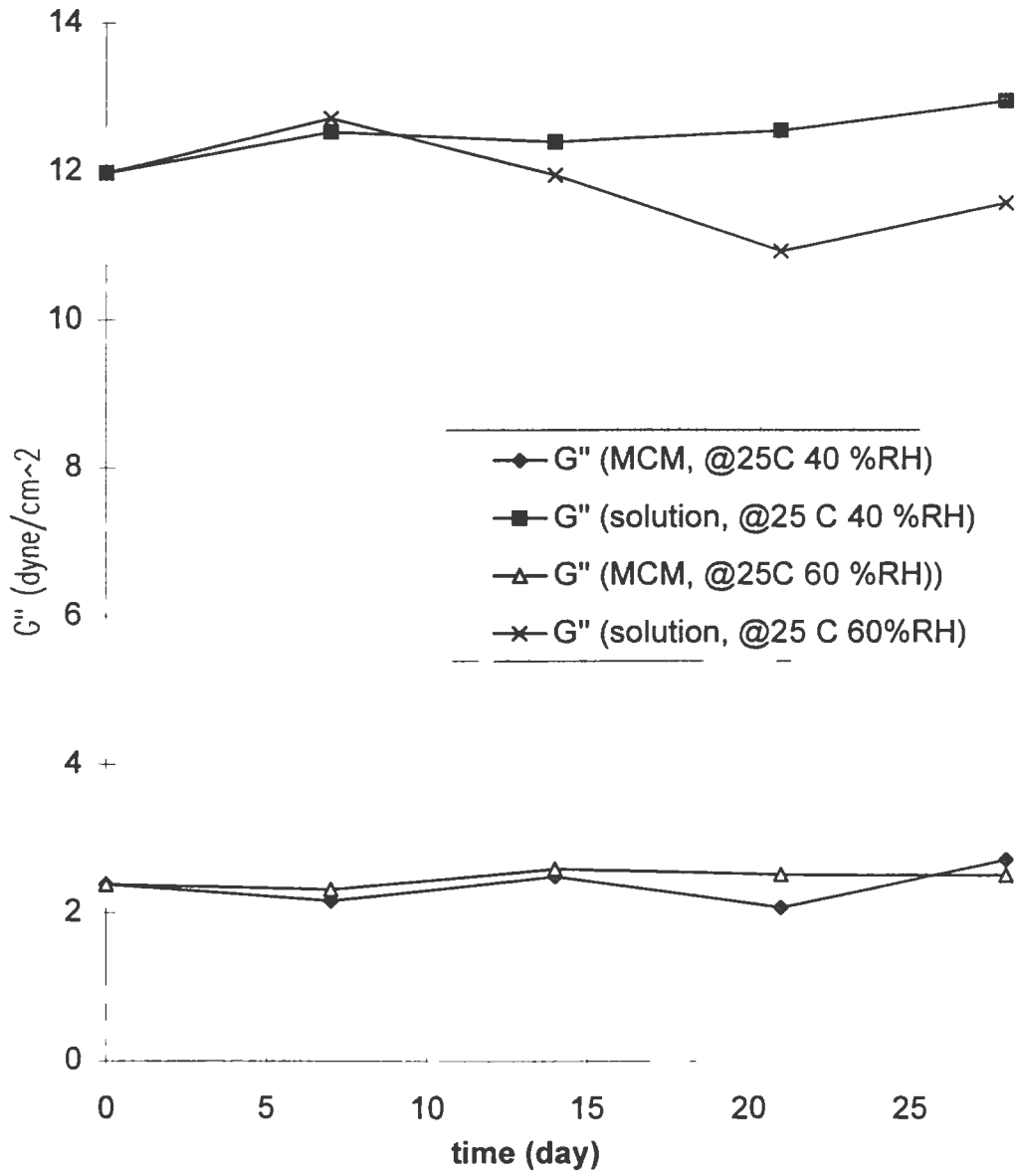


**Figure 27: G'' profiles with time for MCM and 20% (w/w) DQAIC solution at 40 % and 60 % RH 6 cm parallel plate and 1 mm gap**



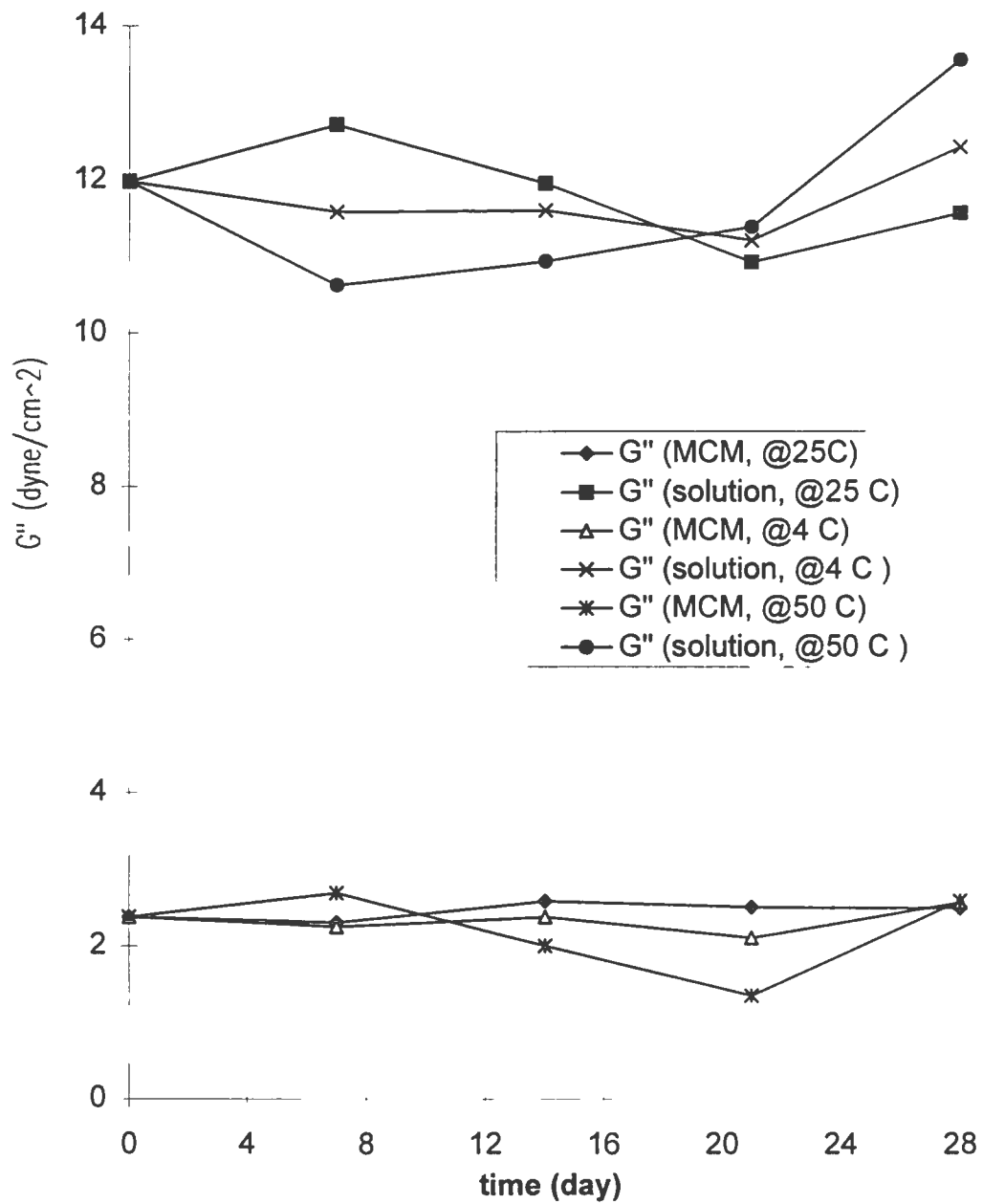


**Figure 28:  $G''$  profiles with time for MCM and 20% (w/w) DQAIC solution at 4°C, 50°C and 25°C obtained with 6 cm parallel plate and 1 mm gap**

In order to evaluate the structure of the system at different concentrations, rheological parameters were measured for each concentration. Zero shear values were obtained at 25°C. Complex viscosity ( $\eta^*$ ) from frequency sweep was accepted as zero shear viscosity and plotted against concentration, Figure 29. Up to 10% (w/v) concentration, the viscosity increases gradually with increasing concentration. Between 10-15% (w/v), viscosity increases more by increasing concentration. This region may be accepted as the region where gelling starts until it reaches the critical concentration (16% w/v) where it becomes entirely shear sensitive.

In order to investigate further, particle size of the solution at each concentration was determined. The vehicle and 2, 5, 7% (w/v) solutions do not have any particles. When the drug concentration is increased up to 10% (w/v), particles begin to appear and particle size increases as the concentration increases, Figure 29 and Table XII. The effect of shearing time on particle size also investigated showed that shear causes particle growth, Figure 30. Before shear, 15% (w/v) solution demonstrated an average particle size of 4.7 nm. This increased to 9.5 nm after 12 hours shearing at 3000 rpm. Similarly the initial particle size of 8.8 nm of 20% (w/v) solution increased to 19.5 nm with shear. Those particles disappear at 80°C whereas they increases at 40°C compared to those measured at 25°C from  $8.8 \pm 0.3$  nm to  $12.5 \pm 0.5$  nm. The increasing particle size with increasing drug concentration may be one of the reasons of gelation.

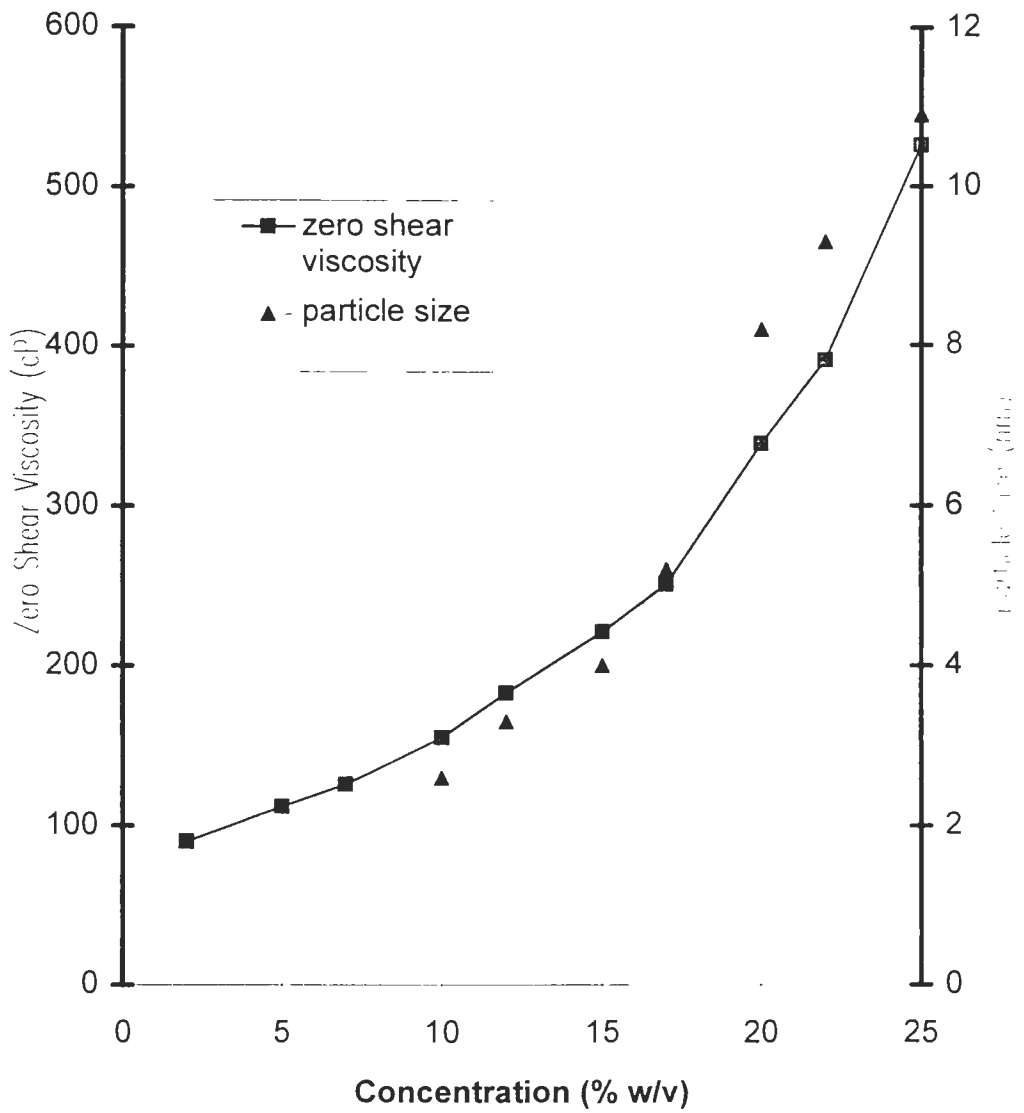


**Figure 29: Effect of the Drug Concentration on Zero Shear Viscosity and Particle Size of the Solution at 25<sup>0</sup>C**

**Table XII: Particle Size Measurements of DQAIC Solution at Different Concentrations at 25°C**

Concentration (% wt/v)	Particle Size (nm)	Polydispersity
10	$2.6 \pm 0.3$	0.509
12	$3.3 \pm 0.4$	0.408
15	$4.0 \pm 0.2$	0.211
17	$5.2 \pm 0.4$	0.383
20	$8.8 \pm 0.3$	0.218
22	$9.3 \pm 0.4$	0.233
25	$10.90 \pm 0.8$	0.373

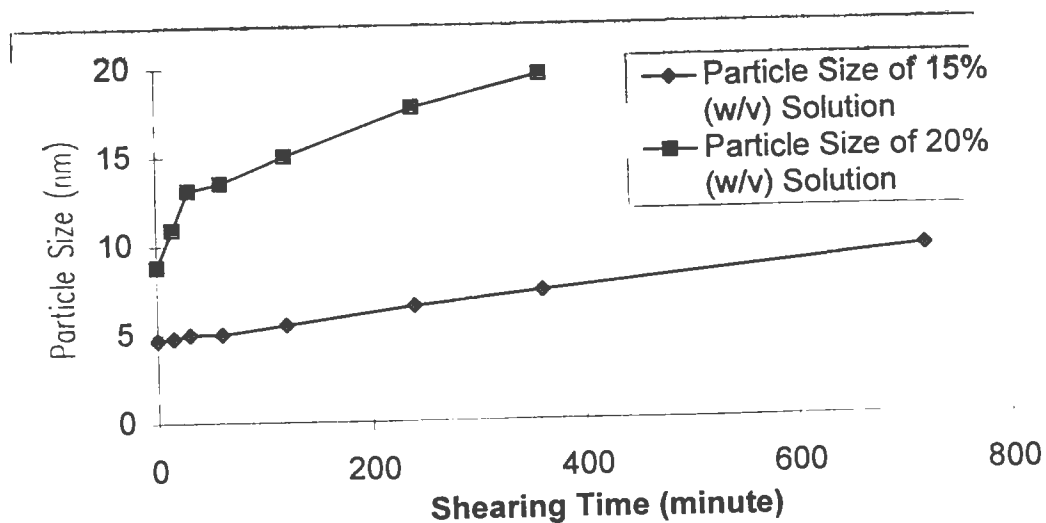


**Figure 30: Effect of Shearing Time on Particle Size of 15% and 20% (w/v) Solutions at 25°C**

DSC of 10 % solution, where gelling does not occur and of 25 % at which gelling occurs were compared, Figures 31 A and B. The enthalpy values of the endothermic and exothermic peak are given in Table XIII. The DSC shows that the melting points of triglyceride components are identical for both solutions. The exothermic peak which is an indicative crystallization of diglyceride has a shoulder which is more distinguished in 25% (w/v) solution. The third peak shifted towards left at 25% (w/v) concentration. It is weakened at this concentration providing enthalpy of 4.7 mJ/mg, half of 10% solution. Insignificant peak of MCM that appeared around at 11°C (Figure 7), was increased as the drug concentration was increased. This became visible in the 20% solution before shear (Figure 19B). The enthalpy of this melting peak was increased from 10% to 25% from 4.4 mJ/mg to 12.44 J/mg, Figure 31. However, shearing has not changed the magnitude of it. It is obvious from Figure 31 A, the drug concentration has significant effect in the presence and magnitude of this peak. These results may indicate that, the drug may interact with one of the vehicle components which is present in a small amount. The interaction between water or glycerin and the drug solution was shown by addition of 2.4% water or glycerin to 20% DQAIC solution. DSC of these mixtures Figures 32 A and B may suggest this possibility.

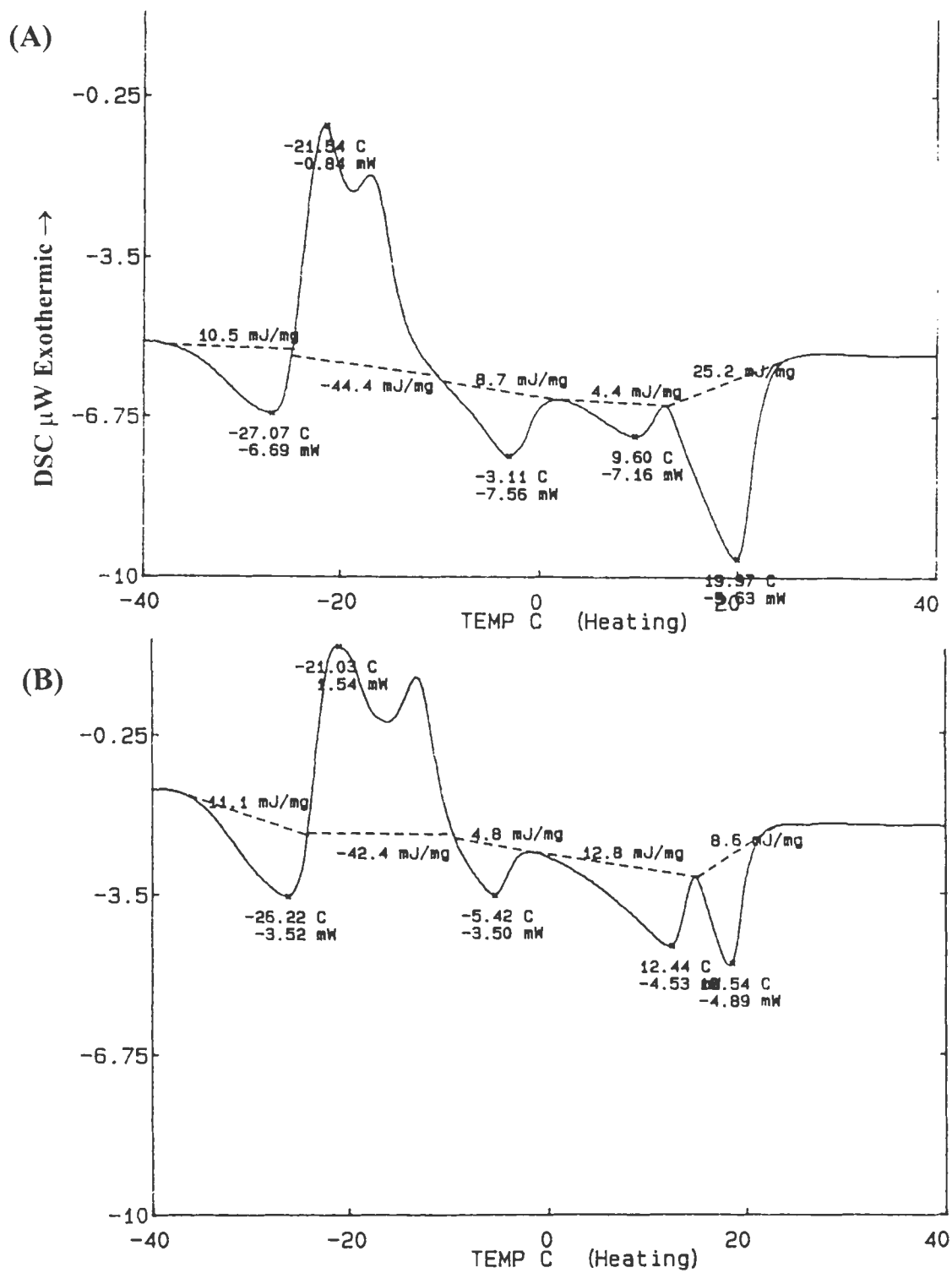


Figure 31: Comparison of DSC heatings of 10% (A) and 25% (B) DQAIC solution in MCM between  $-70^{\circ}$ C and  $150^{\circ}$ C

**Table XIII: DSC Traces During Heating Curve of the Drug Solution in MCM at 10% and 25% (w/v) Concentrations**

<b>Peak*</b>	<b>% (w/v)</b>	<b>Temperature (°C)</b>	<b>Enthalpy (mJ/mg)</b>
1	10	-27.07	10.5
<i>1</i>	25	-26.22	<i>11.1</i>
2	10	-21.54	-44.4
<i>2</i>	25	<i>-21.03</i>	<i>-42.4</i>
3	10	-3.11	8.7
<i>3</i>	25	<i>-5.42</i>	<i>4.8</i>
4	10	9.60	4.4
<i>4</i>	25	<i>12.44</i>	<i>12.8</i>
5	10	19.97	25.2
<i>5</i>	25	<i>18.54</i>	<i>8.6</i>

\* Peaks numbered in *italic* form are for 25% (w/v) solution

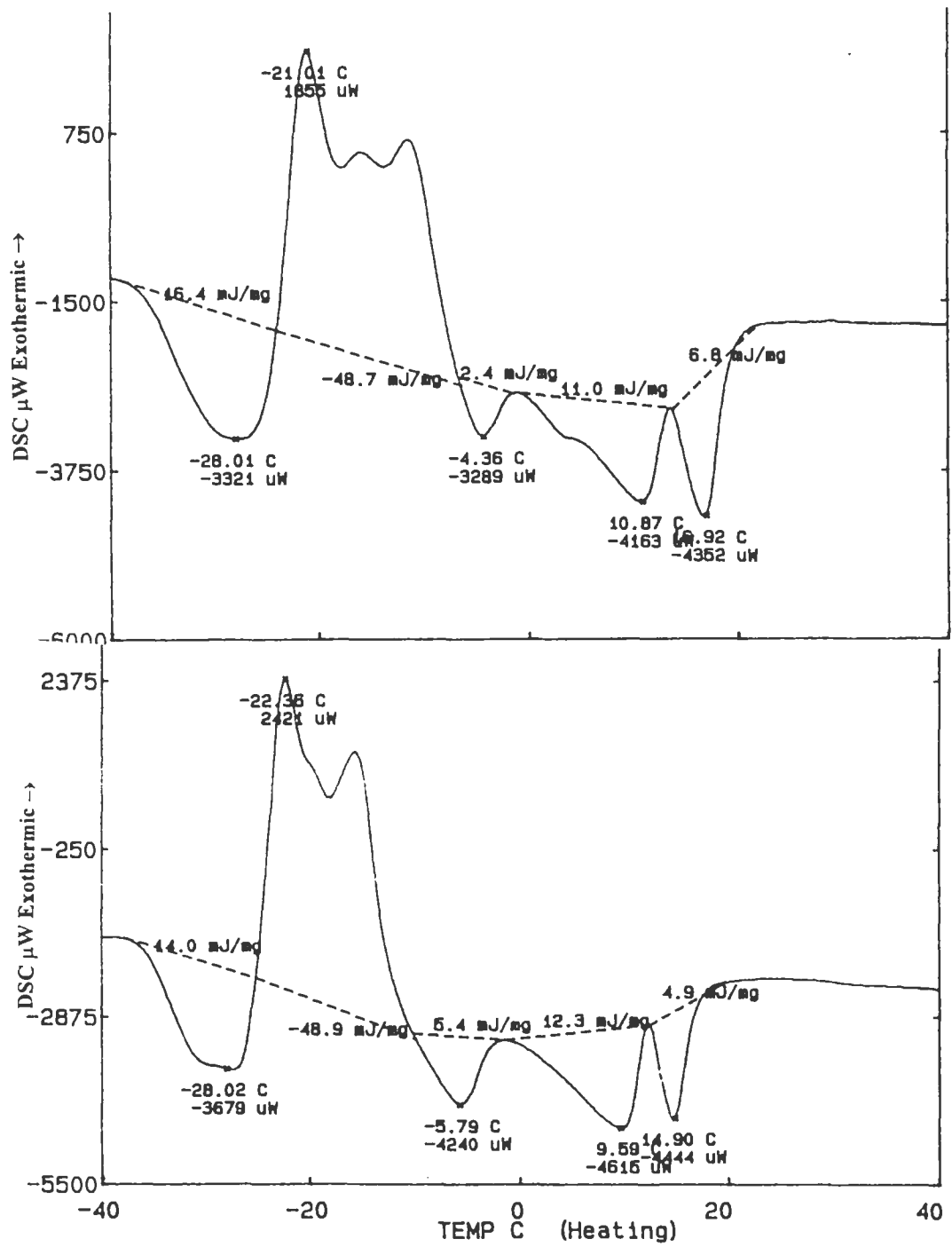
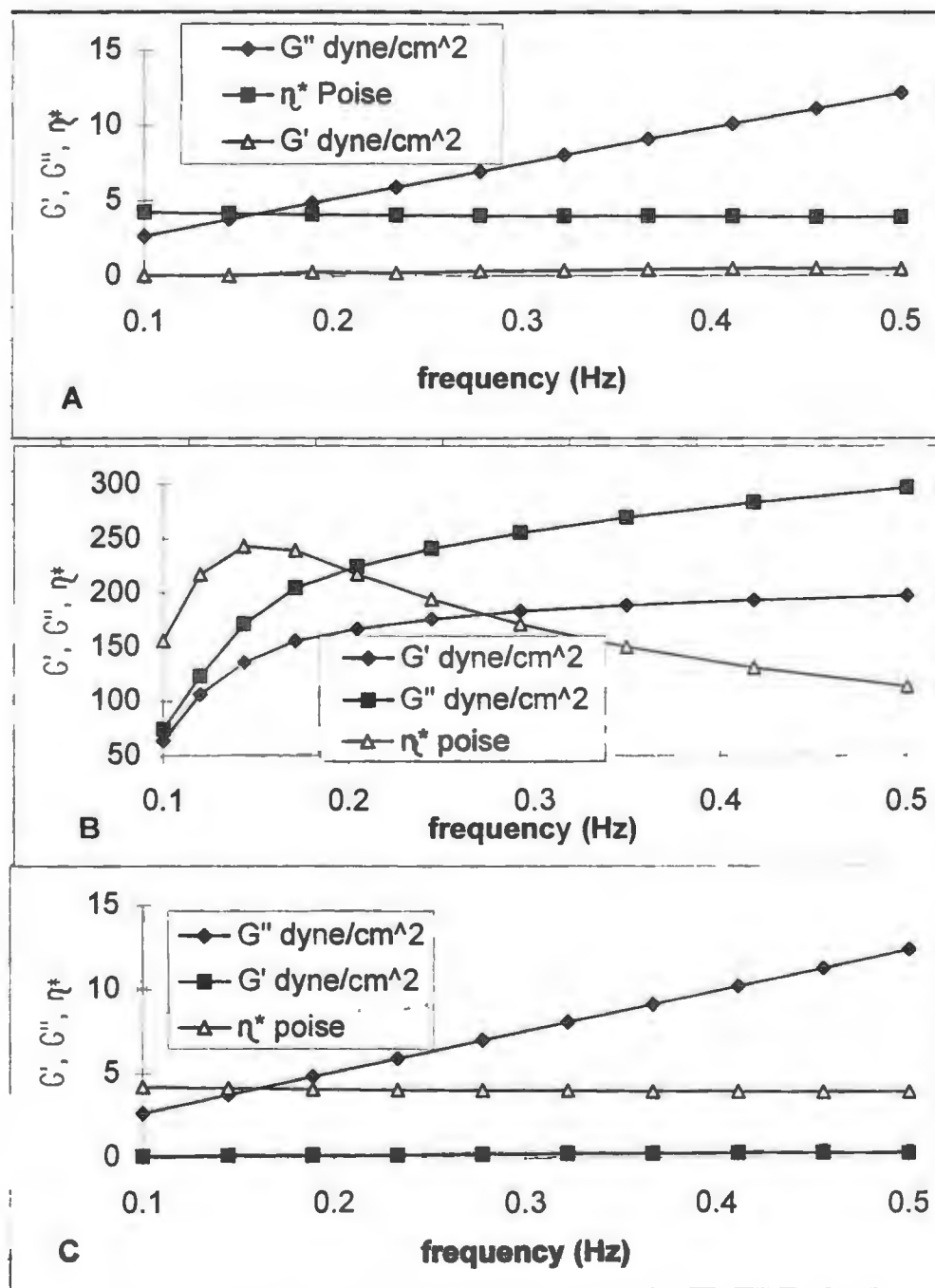


Figure 32: DSC Traces Of 20% DQAIC Solution With 2.4 % Glycerin (A) and 2.4% Water (B) During Heating Between  $-70^{\circ}\text{C}$  and  $150^{\circ}\text{C}$



#### 4.5.6 Reversibility of Gelling Phenomenon

FT-IR spectra revealed that, in the gelled samples slight changes occurred at between  $3000\text{ cm}^{-1}$  and  $3600\text{ cm}^{-1}$  regions indicating that the gelling phenomenon seems to be predominantly physical in nature. The gelled solution was heated up to  $65^{\circ}\text{C}$ , it reverted to a clear solution. FT-IR spectrum and rheological parameters of reverted solution were obtained. Frequency sweep tests showed (Figure 33 A, B, C) that rheological parameters,  $G'$ ,  $G''$  and  $\eta^*$ , of pre-sheared and heated solutions were same, while there is a 25 fold increase in the  $G''$  of sheared sample. FT-IR spectrum (Figure 34) of the sample also shows that there is no differences between pre-sheared sample and heat recovered sample.



**Figure 33: Frequency sweeps of pre-sheared (A), sheared (B) and recovered (C) solutions**

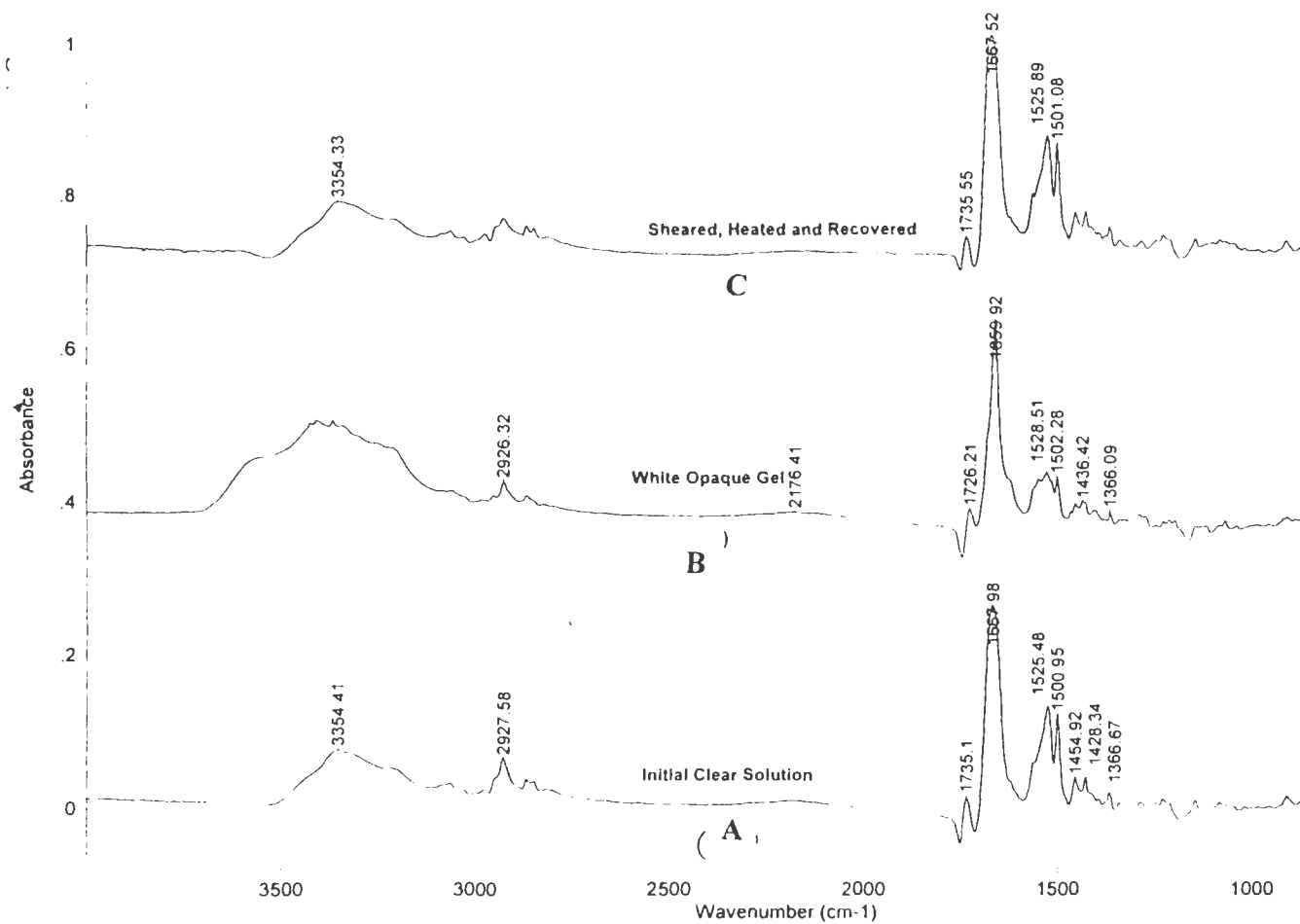


Figure 34: FT-IR spectra of 20 % DQAIC solution before shearing (A), after shearing (B) and recovering at 65°C (C).

#### 4.6 POSSIBLE EXPLANATIONS FOR THE GELATION

Micelles formation and molecular rearrangement were postulated mechanisms for the gelling phenomenon of the formulation. The phenomenon is concentration dependent. The solution reaches saturation at a concentration of 17% (w/v) and addition of drug beyond this level may increase particle formation in presence of impurities such as glycerin and water in the vehicle resulting in drug-drug aggregation. These formed particles can act as gel nuclei. With increased drug concentrations, the particles also become larger providing higher possibility of interaction upon shear. Shear causes particle growth then these particles become continuous phase that may result in phase transition. These particles can be temperature sensitive new metastable form of the drug. Because they become larger at 40°C compare to those at 25°C and disappear at 80°C. Gelling forms faster at 40°C than at 25°C and did not occur at 80°C. These results show that those formed particles can be the reason of gelation.

One other explanation can be given as follow: Since the vehicle has surfactant properties, it can form micelles. At low concentrations of the drug, these micelles may be spherical. However, at high drug concentrations, they may change to stringlike micelles. Long strings may easily entangle upon shear and present structure as seen in Figure 20. The micelle formation can be analyzed further using Deuteriated NMR, short angle X-Ray Scattering and Cryogenic electron microscopy (Cryo-TEM).

These studies also shows that shear somewhat induces the weak hydrogen bonding between the molecules resulting in molecular rearrangement. Therefore, system tries to arrange itself resulting in phase transition.

#### 4.6.1 Studies to Correct Gelling

Different vehicle grades were also evaluated. These grades are namely MCM(D), which contains higher monoglyceride component, and PG-8, containing propylene glycol fatty acid (C<sub>8</sub> - C<sub>10</sub>) esters instead of glyceride. These vehicle grades are explained in section 3.1.1. The same gelling phenomenon was observed with these vehicles. Only the gelling time was delayed (2-3 hr) with MCM(D). Therefore, increasing of mono-ester component has somewhat advantage in terms of minimizing the gelling tendency of the formulation since the solubility of the drug increases as the monoglyceride component increases.

Since gelling is temperature dependent, the effect of temperature on the rheological parameters of these formulation correlated using Arrhenius equation as follows:

$$\ln G'' = \ln A + (E_a/R)1/T.....(5)$$

where G'' is viscous modulus used to replace viscosity, A is a constant depending on the molecular weight and molar volume of the liquid, T is absolute temperature , R is gas constant and E<sub>a</sub> is the activation energy.

According to Arrhenius equation, the slope of  $\ln G''$  vs.  $1/T$  gives  $E_a/R$ . A temperature sweep between 4°C and 80°C was carried out using the rheometer and  $\ln G''$  vs  $1/T$  was plotted for each formulation (Appendix I, Figure 16-18). The slopes were found and the activation energy was tabulated with their gelling time for these formulations, Table XIV and Figure 32. As it can be seen from the results the higher activation energy of a formulation, the longer the gelling time. Therefore, the calculation of activation energy can be helpful to characterizing gelling tendency of a proposed formulation.

**Table XIV: Gelling Time and Activation Energy for 20 % DQAIC Solution with Different Vehicles**

<b>Formulation</b>	<b>Gelling Time (hr)</b>	<b>Activation Energy (cal/mol)</b>
PG-8 + 20 % drug	7± 1.0	8108
MCM + 20% drug	10 ± 2.0	10604
MCM(D) + 20 % drug	11± 2.0	10564
MCM + 20 % drug + PVPK30	15± 1.0	12195

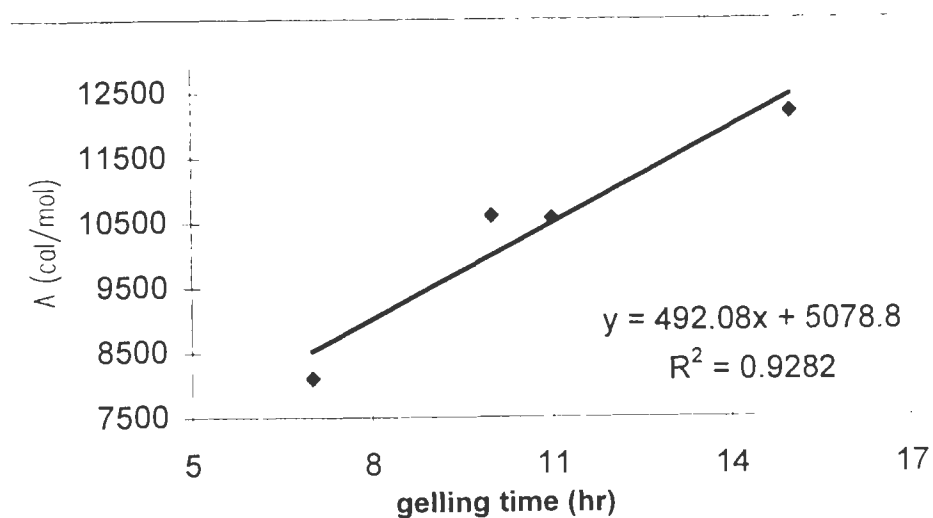


**Figure 32: Correlation Between Activation Energy and Gelling Time of a Formulation**

## V. CONCLUSION

Rheological studies showed that the gelling tendency of the system is related to its molecular rearrangements rather than its flow properties. Viscous modulus ( $G''$ ) among all of the rheological parameters was found to be a good representative of changes occurring in the system. The increased rheological parameters in sheared sample is the sign of structure build up in the system.

Shear induced hydrogen bonding between drug-drug and/or drug-vehicle was demonstrated by a significant increase in absorbance at 3300-3600  $\text{cm}^{-1}$  band region by FT-IR. FT-IR studies also showed that there was no major chemical interaction during shear of the formulation. The slight polymorphic changes detected by X-ray diffraction show that some molecular rearrangement may occur during shearing.

Shear rate used is an important factor. As it increases, the gelling tendency increases. If the shear is combined with other factors such as temperature and humidity, the gelling tendency becomes more critical. Especially, temperature has an important effect on gelling phenomenon. As it increases up to 40°C, gelling occurs faster. If shearing was carried out above 60°C, gelling occurs over a longer time period.

During stability measurements, no time effect was observed at 4°C, 25°C and 50°C and 40% and 60% relative humidities. However, time is an important factor if it is combined



with shear because gelling of DQAIC solution in MCM is a shear induced time dependent behavior.

The gelling tendency of the formulation was also found to be concentration dependent. Placebo and the solutions at 15% (w/v) concentrations and below did not form a gel after shearing for a prolonged period of time. The increased particle size above 10% (w/v) concentrations suggested that the system may not a true solution. These temperature, shear and concentration dependent particles can be a temperature sensitive physical form of the drug which causes gelling.

The gelling were found to be reversible by heating the gelled sample up to 65°C.

In order to minimize the gelling phenomenon, the solution should be prepared at very low shear rates. The energy given by heat should be higher than the energy given by shear, so that gelling can be avoided. If possible, all processing should be conducted at or above 60°C at low humidity levels.

## REFERENCES

- 1) Martin, A.; *Physical Pharmacy*; Lea & Febiger, Malvern, 453-476 (1993)
- 2) Tang, Q; McCarthy, O.J.; Munro, P.A.; *Journal of Dairy Research* 1993, 60: 543-555
- 3) Rector, D.; Matsudomi, N.; Kinsella, J.E.; *Journal of Food Science* 1991, 56(3): 782-788
- 4) Sutananta, W., Craig, D.Q.M., Newton, J.M.; *International Journal of Pharmaceutics*, 111, 51-62 (1994)
- 5) Schrader, B.; *Infrared and Raman Spectroscopy Methods and Applications*; VCH Publishers, New York; 1995: 135- 140
- 6) Skoog D. A.; Leary, JJ.; *Principles of Instrumental Analysis* (4. Edition); Saunders College Publishing; New York; 1992: Chapter 12, 13, 14, 15, 23
- 7) Hiemenz, PC.; Rajagopalan, R.; *Principles of Colloid and Surface Chemistry* (3. Edition); Marcel Dekker, New York 1997: 193-240
- 8) MCM Certificate of Analysis, Abitec Cooperation
- 9) Food and Drug Administration, HHS, 21 CFR Ch. I (4-1-96 Edition): 490-491
- 10) USP 23 NF18, United States Pharmacopeial Convention , Rockville, 1994: 1840-1843

## APPENDIX I

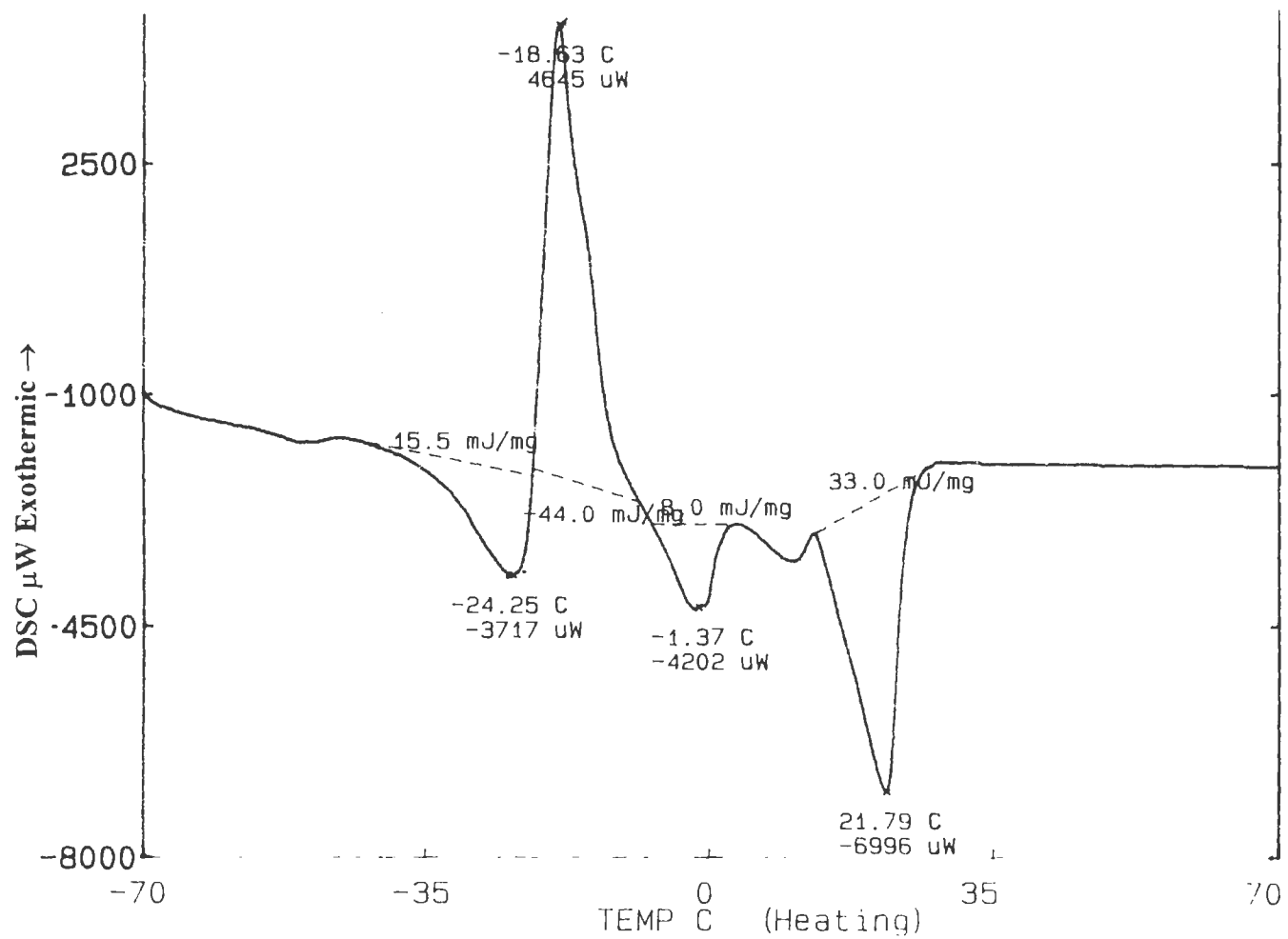


Figure 1: DSC Traces Of MCM During Second Heating Between -70°C And 150°C

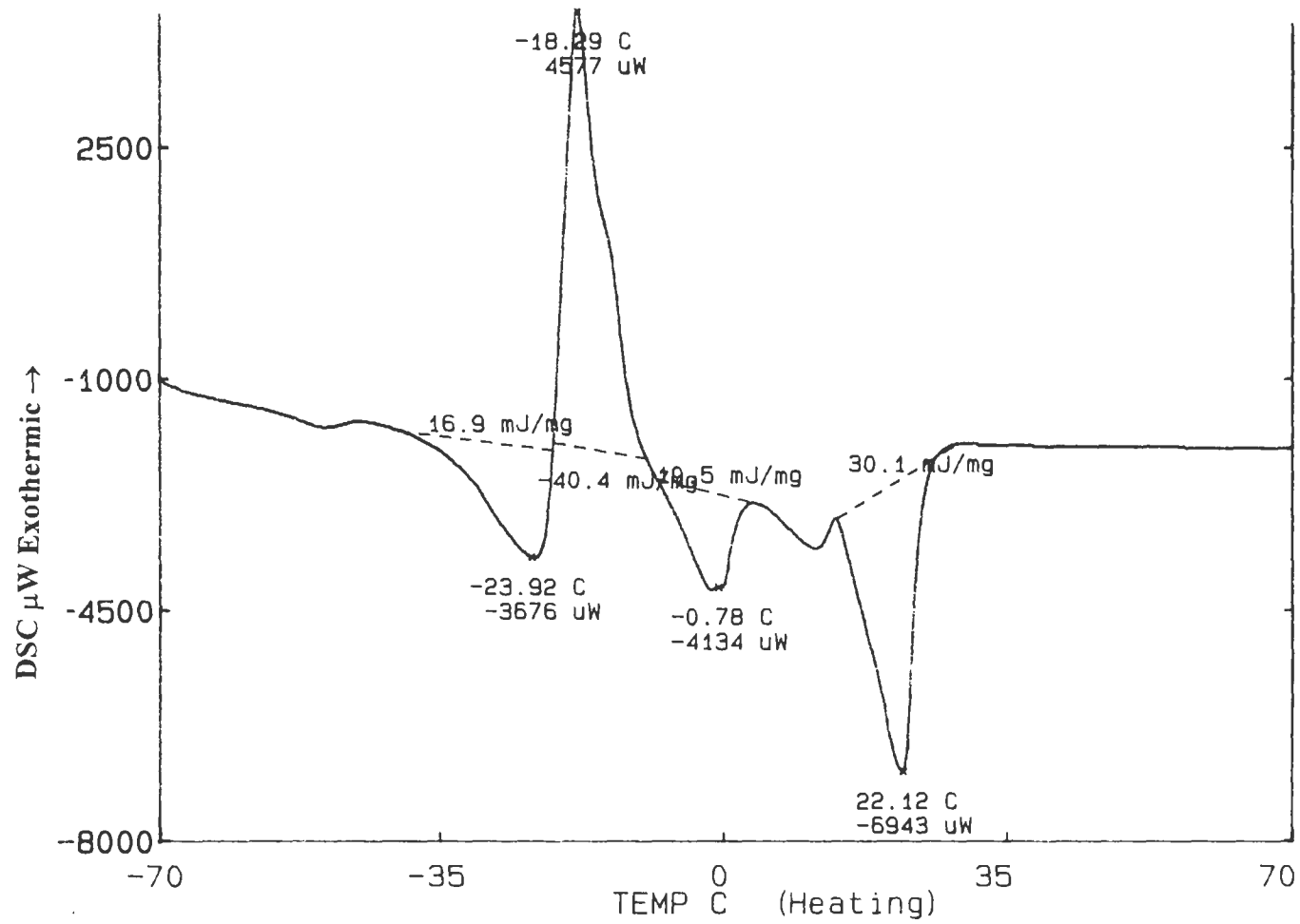


Figure 2: DSC Traces Of MCM During Third Heating Between -70°C And 150°C

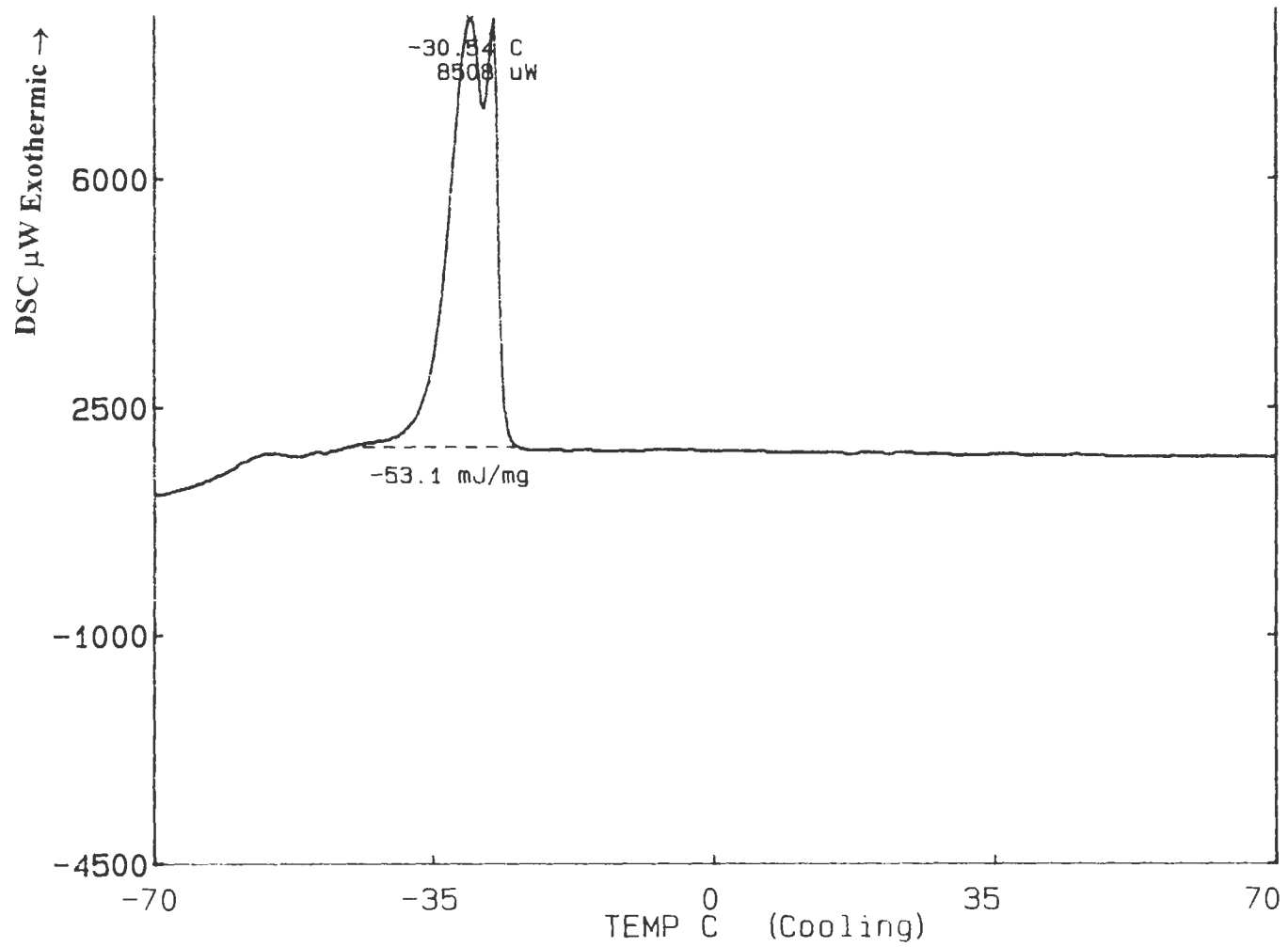


Figure 3: DSC Traces Of MCM During Second Cooling Between -70°C And 150°C

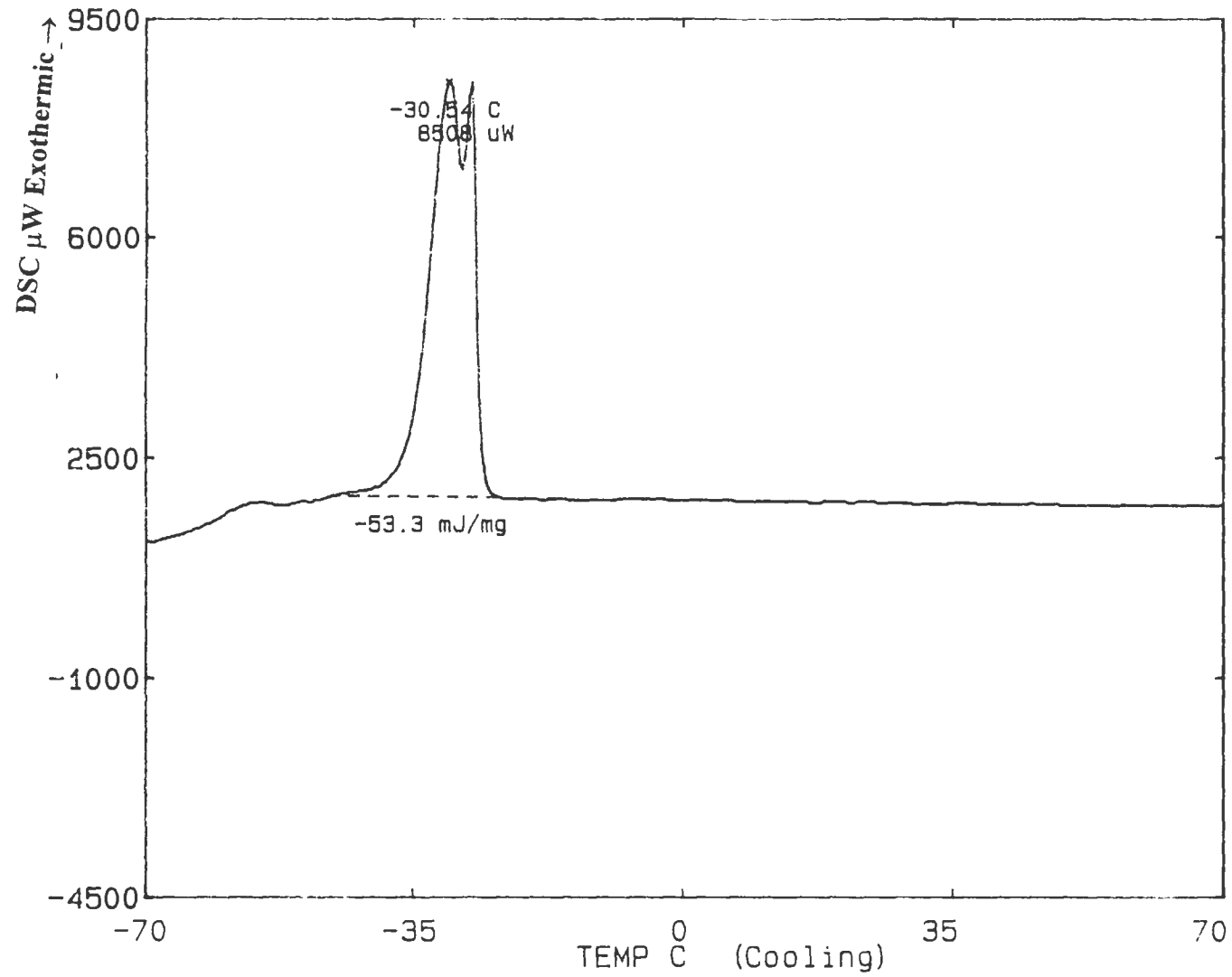


Figure 4: DSC Traces Of MCN During Third Cooling Between  $-70^{\circ}\text{C}$  And  $150^{\circ}\text{C}$

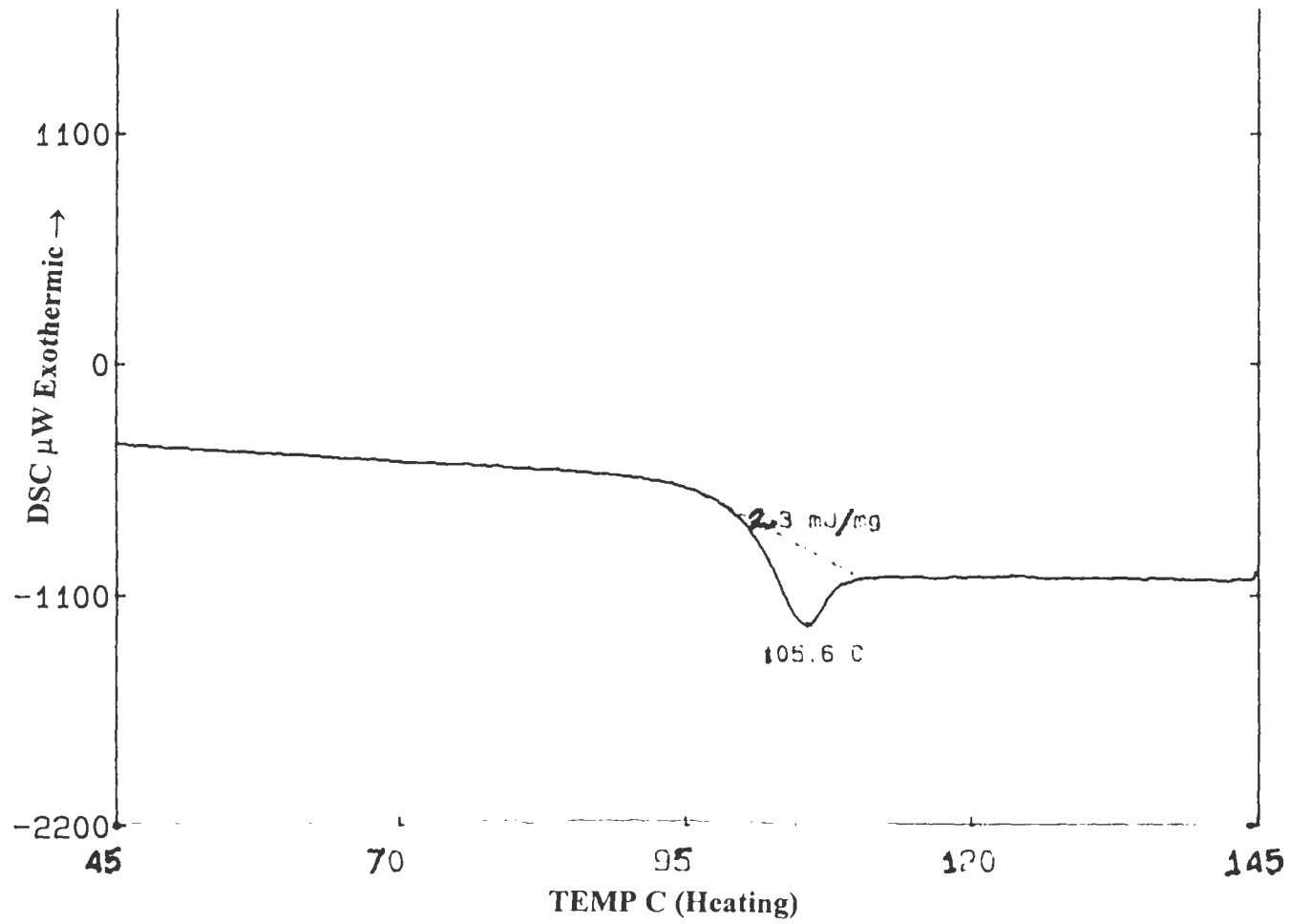


Figure 5: DSC Traces Of DQAIC During Second Heating Between 20°C And 150°C



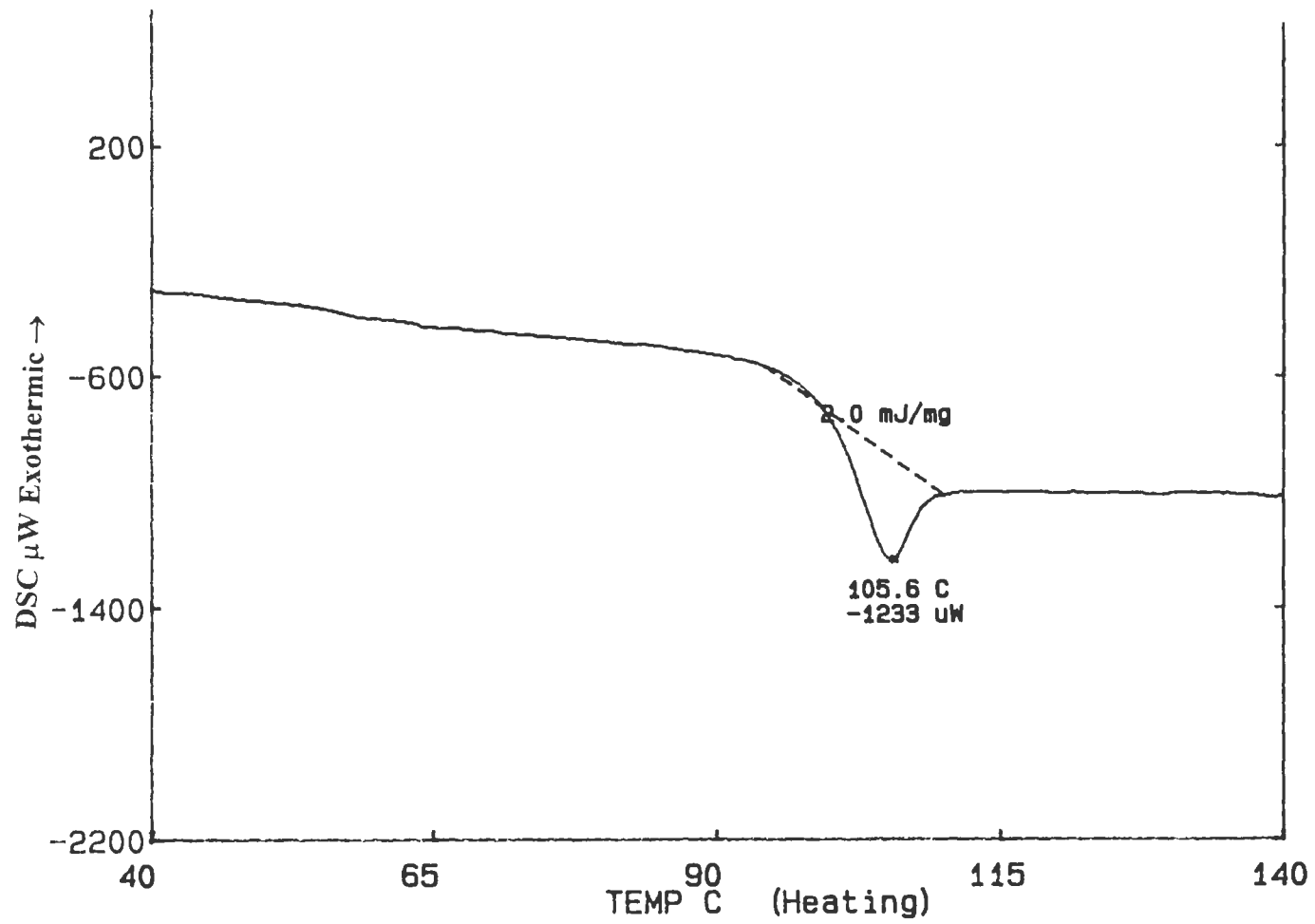


Figure 6: DSC Traces Of DQAIC During Third Heating Between 20 $^{\circ}\text{C}$  And 150 $^{\circ}\text{C}$

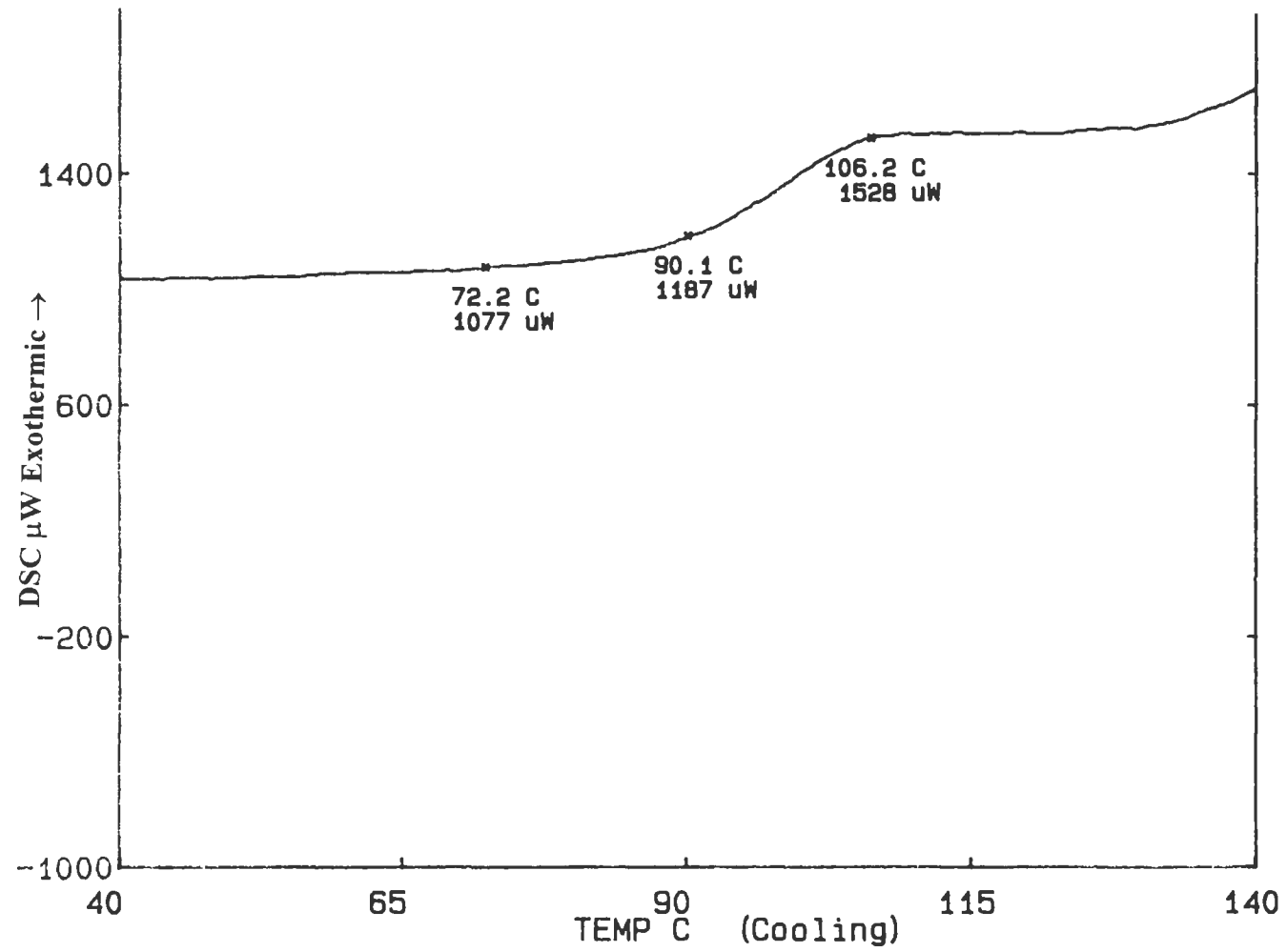


Figure 7: DSC Traces Of DQAIC During Second Cooling Between 20°C And 150°C

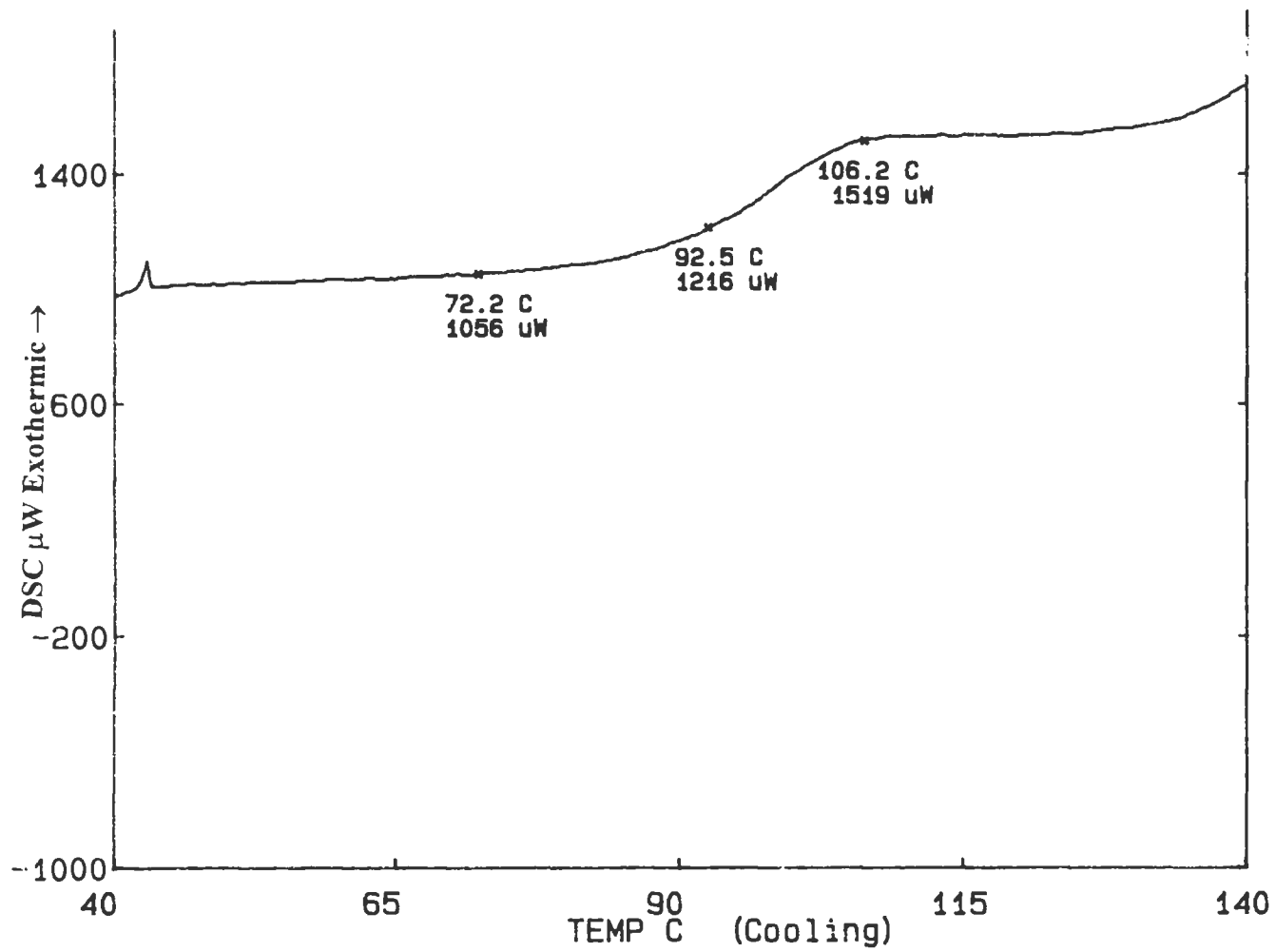
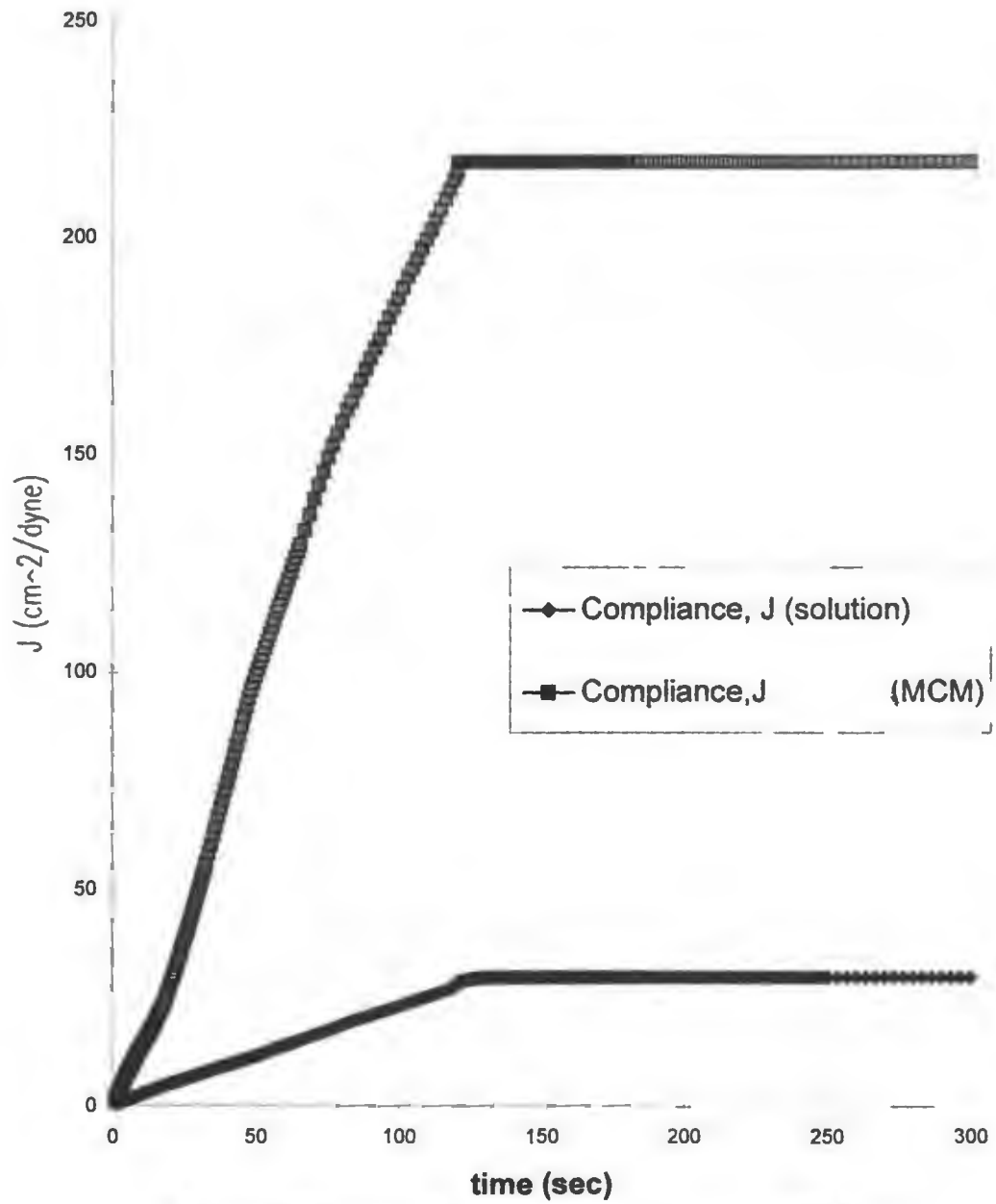
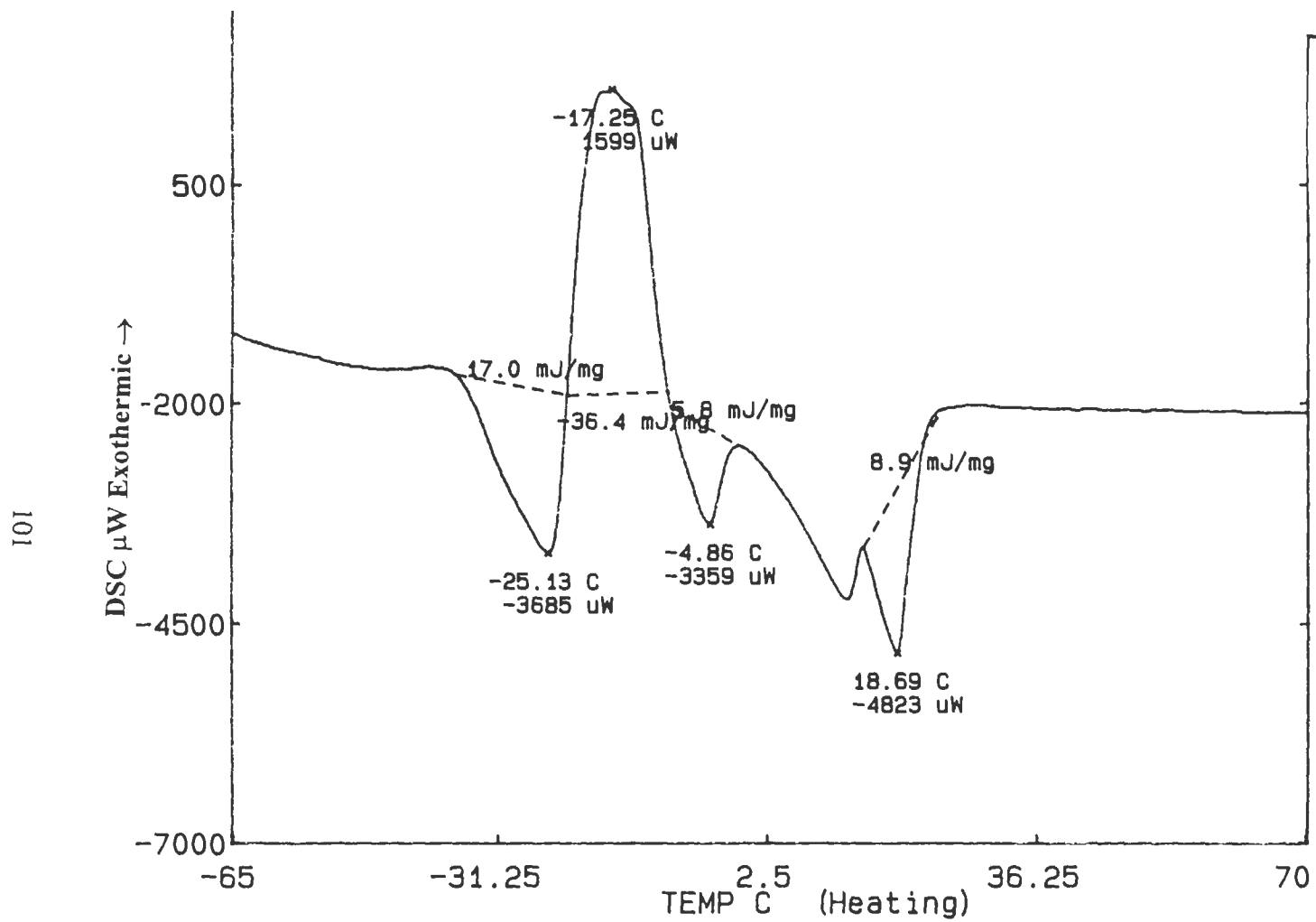


Figure 8: DSC Traces Of DQAIC During Third Cooling Between 20°C And 150°C



**Figure 9: Creep and recovery for MCM and 20 % DQAIC solution with 6 cm parallel plate and 1 mm gap at 25°C**



**Figure 10: DSC Traces Of 20 % DQAIC Solution During Second Heating Between - 70°C And 150°C**

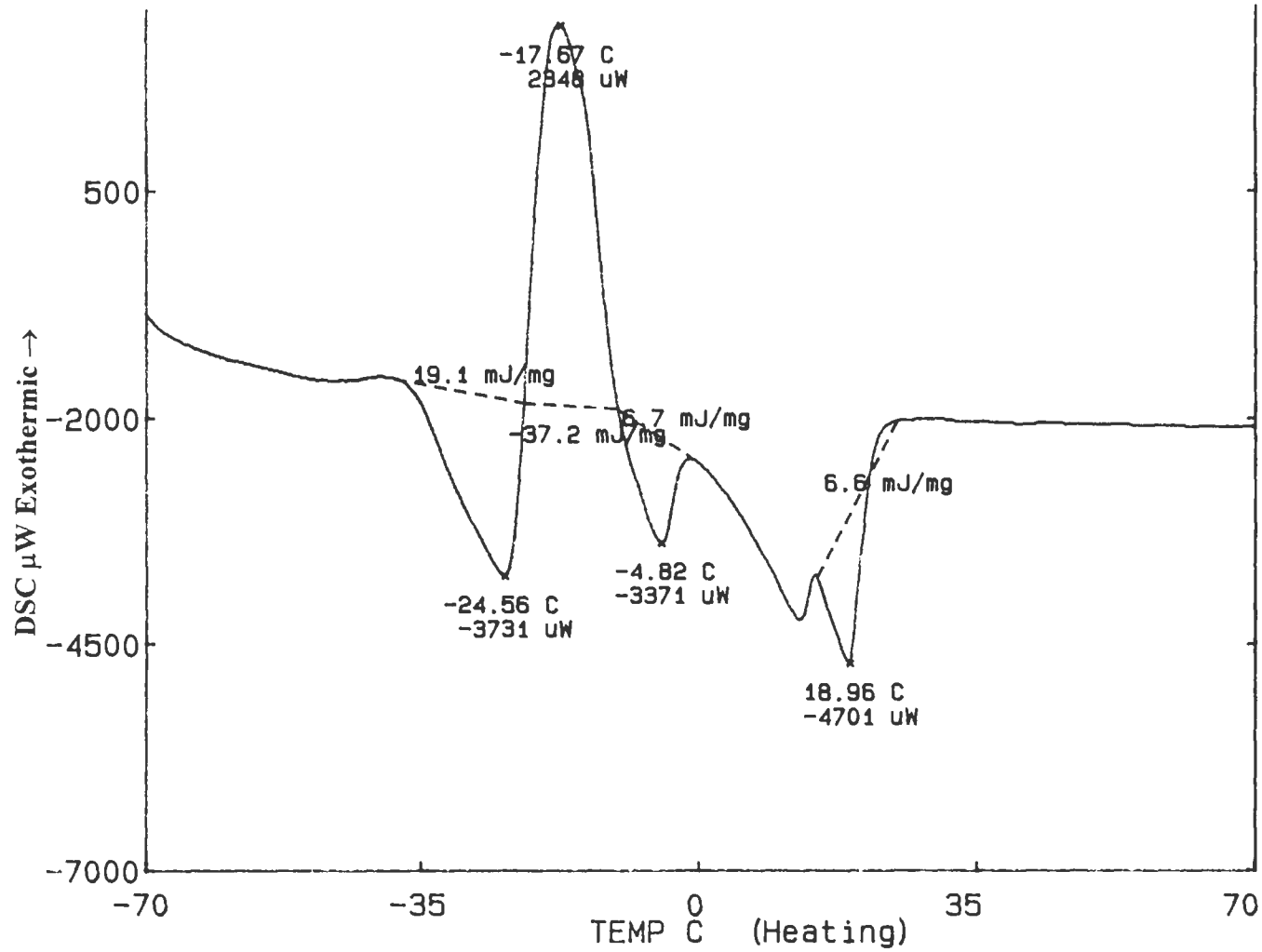


Figure 11: DSC Traces Of 20 % DQAIC Solution During Third Heating Between -  
 $70^{\circ}\text{C}$  And  $150^{\circ}\text{C}$

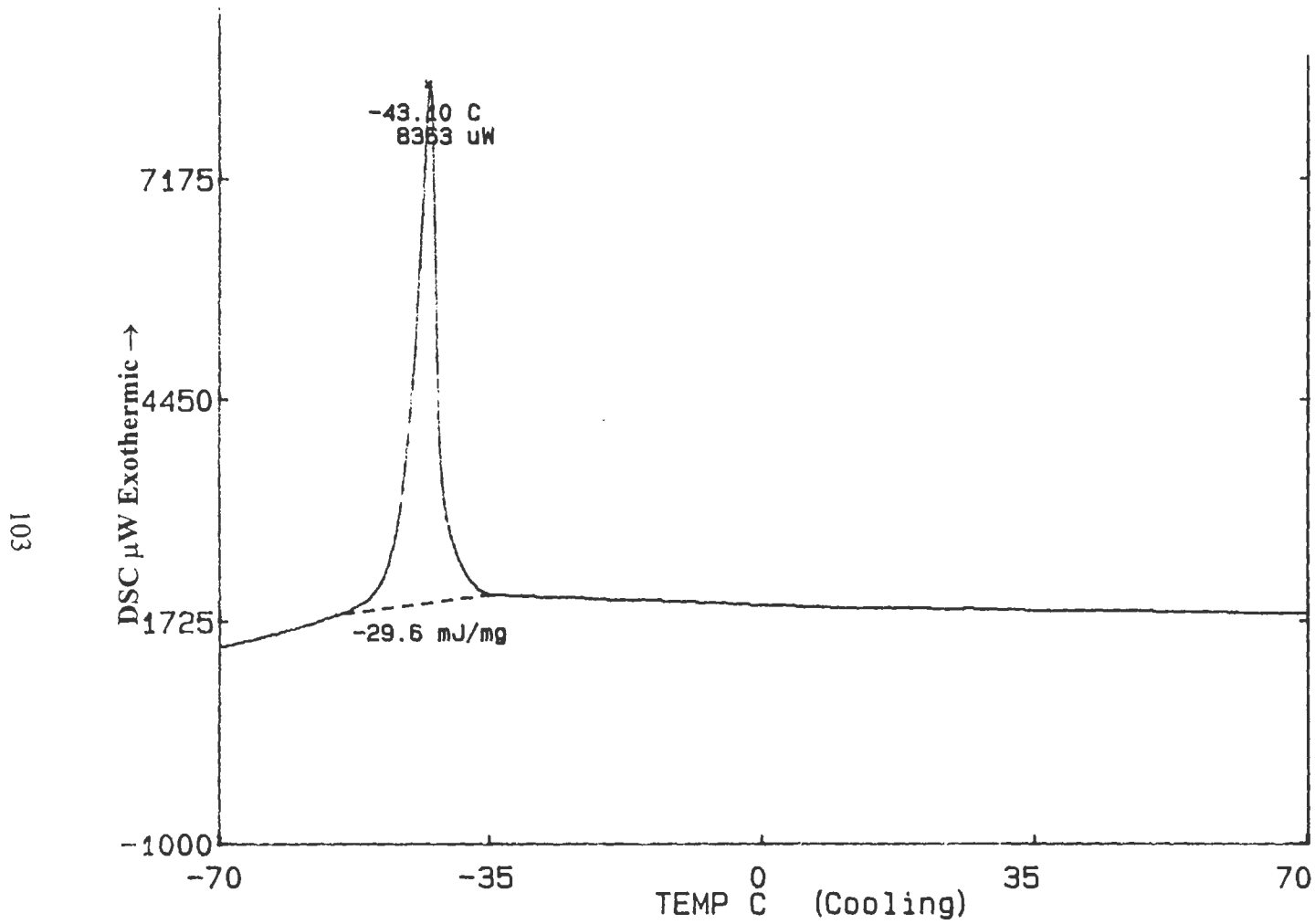


Figure 12: DSC Traces Of 20 % DQAIC Solution During Second Cooling Between -70°C And 150°C

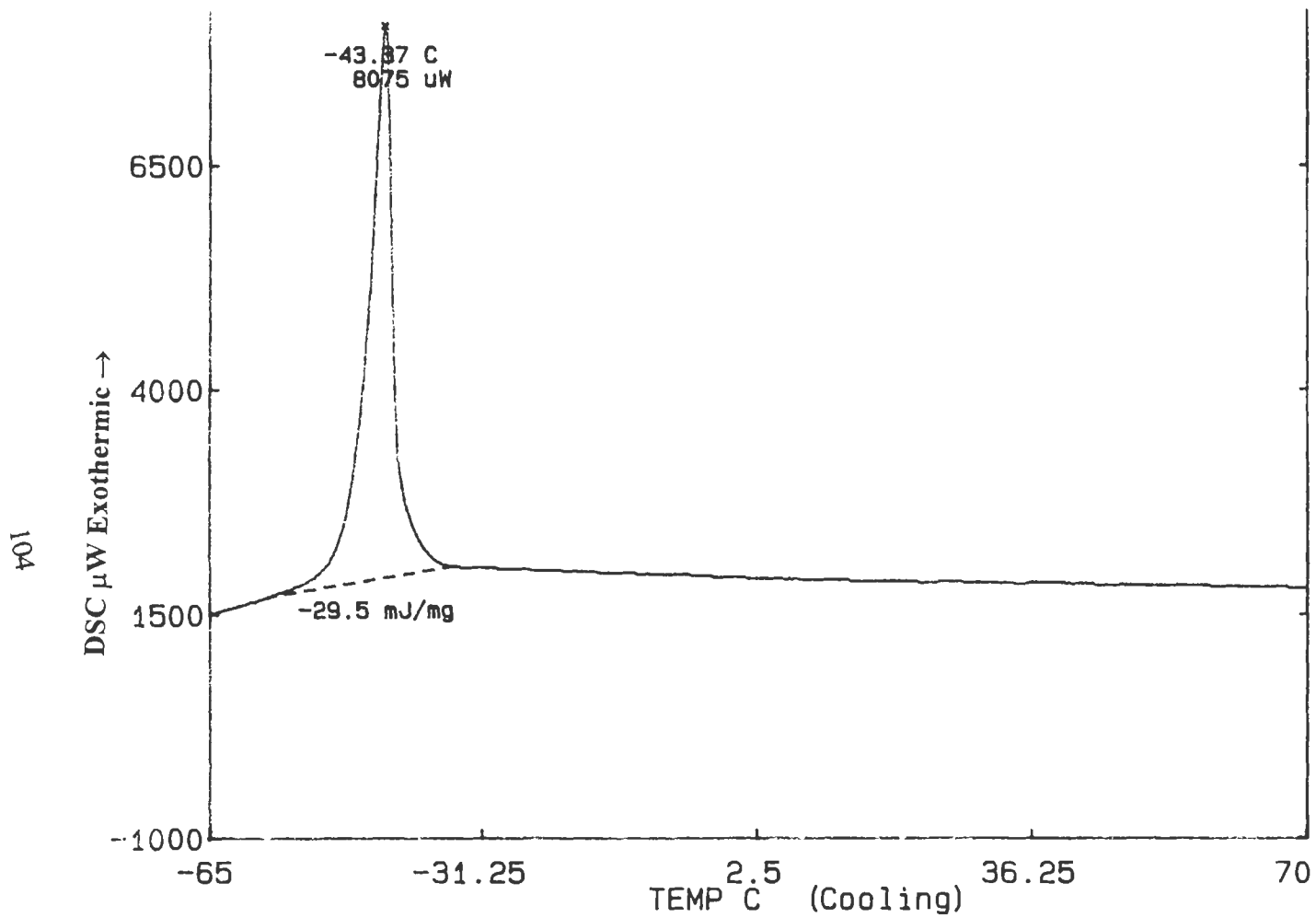


Figure 13: DSC Traces Of 20 % DQAIC Solution During Third Cooling Between -70 $^{\circ}$ C And 150 $^{\circ}$ C



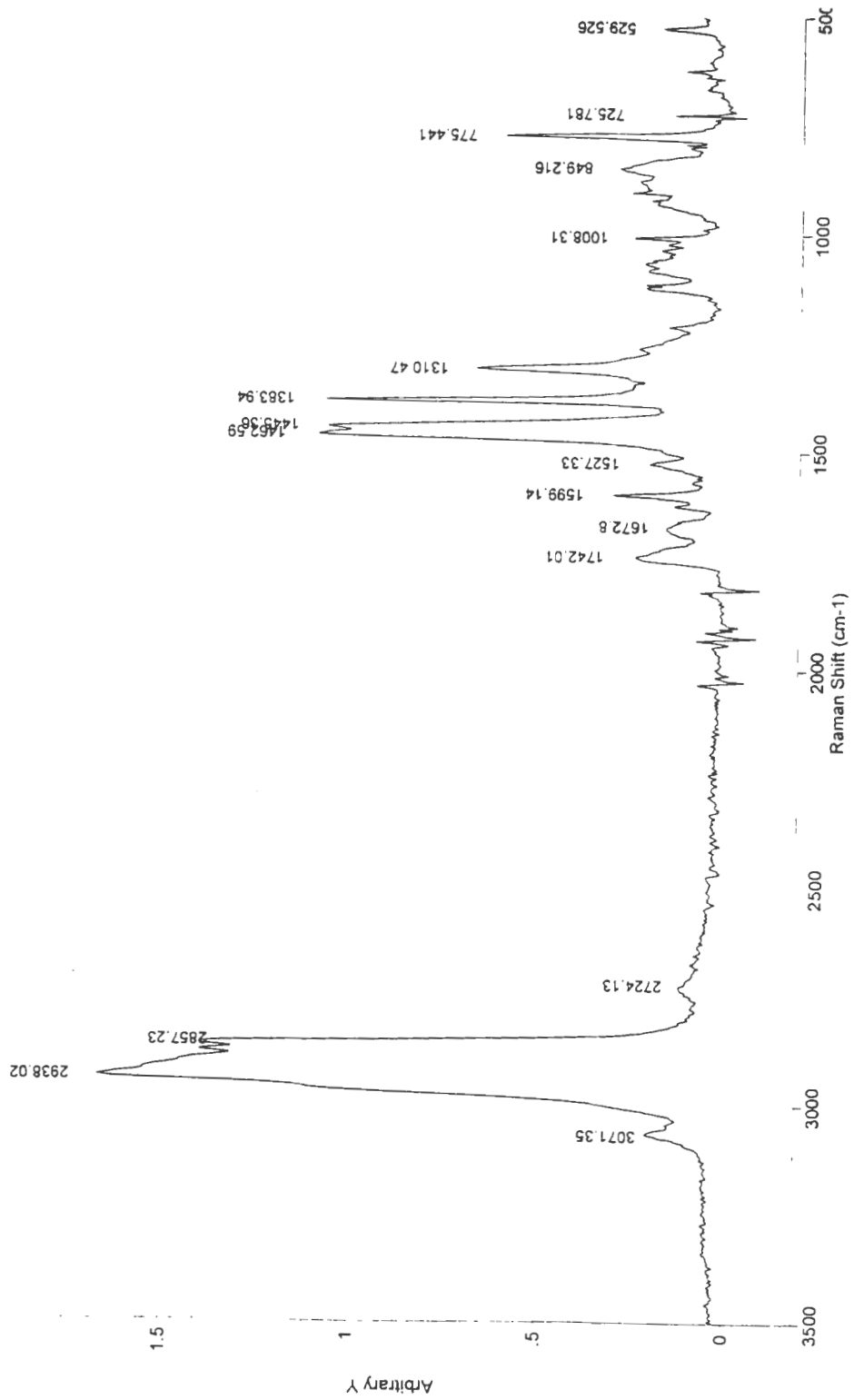
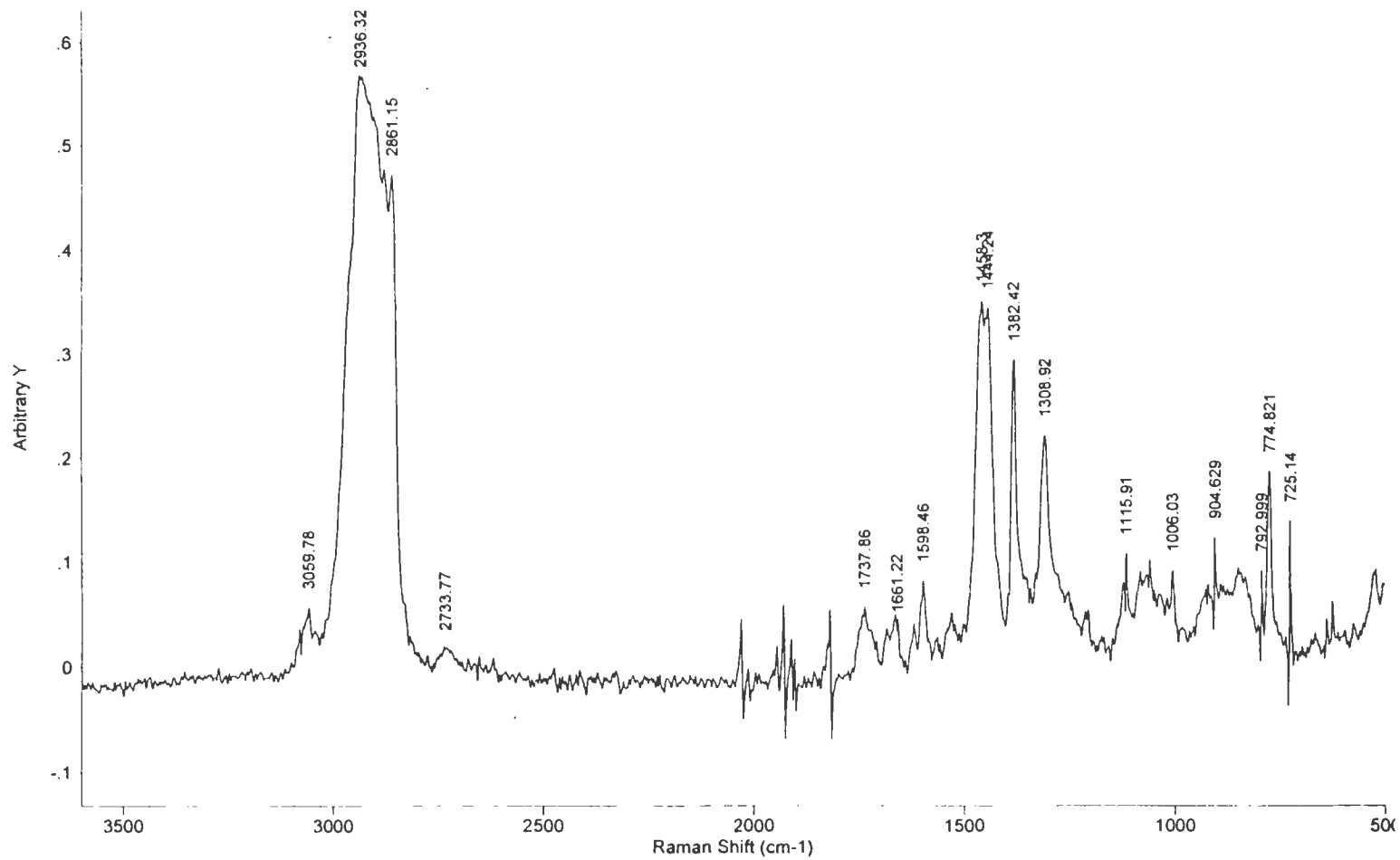
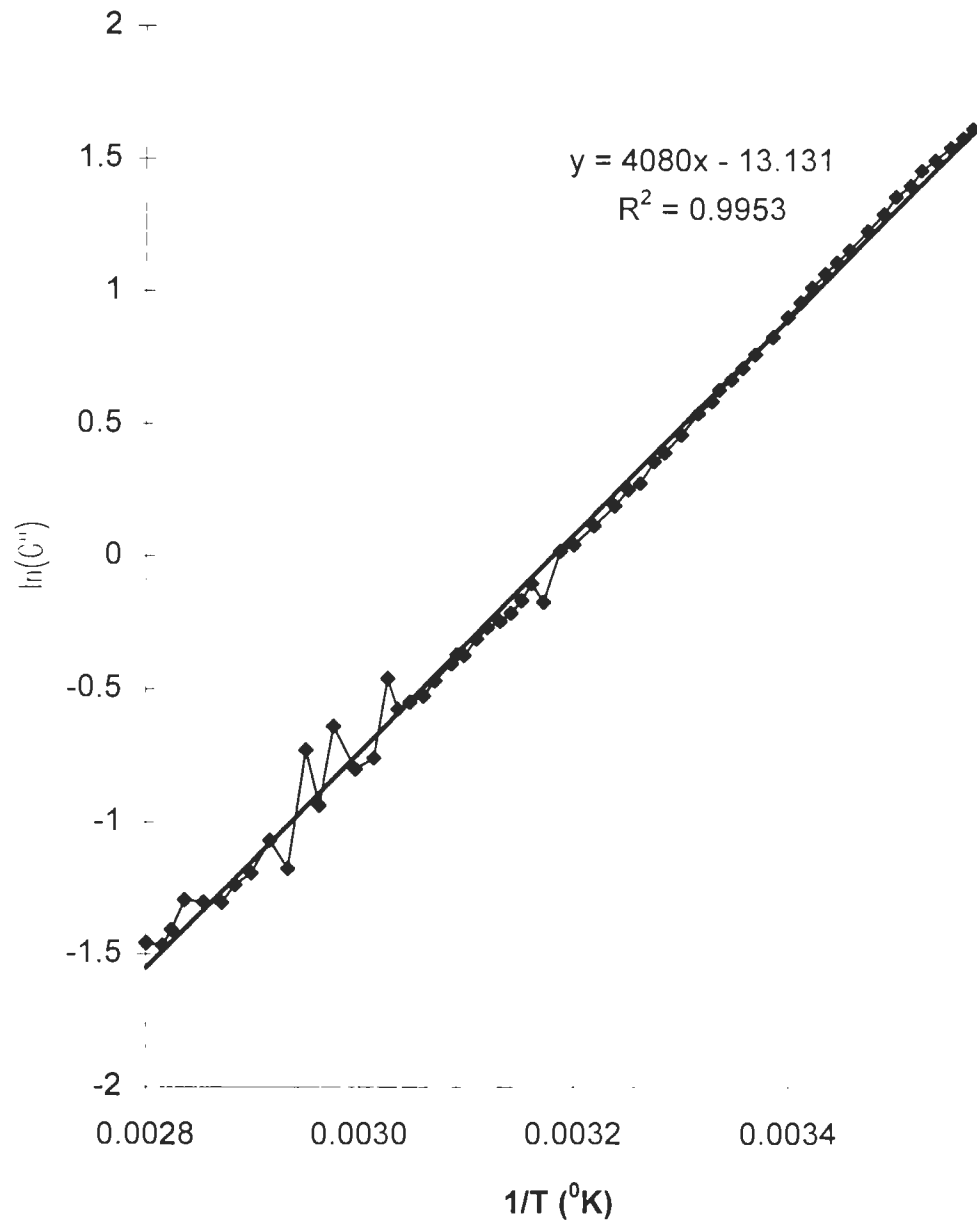


Figure 14 : FT-Raman Spectrum of 20 % DQAIC Solution At 4cm<sup>-1</sup> Resolution



**Figure 15: FT-Raman Spectrum Of 20 % DQAIC Sheared Solution At 4cm<sup>-1</sup> Resolution**



**Figure 16:  $\ln G''$  vs  $1/T$  for the formulation contains PG-8 and 20 % drug obtained with 6 cm Parallel Plate and 1mm gap between  $4^{\circ}C$  and  $80^{\circ}C$**

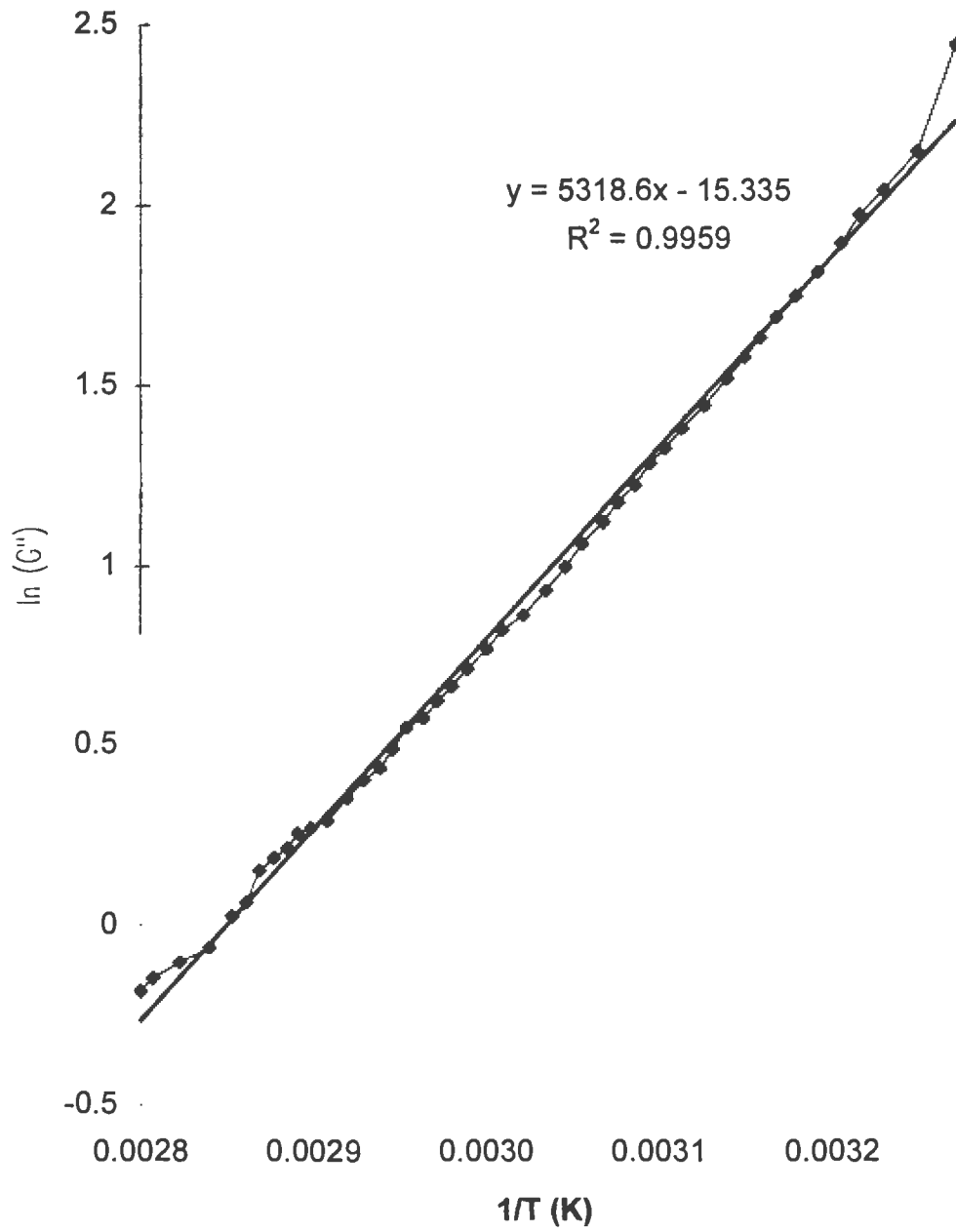


**Figure 17:  $\ln G''$  vs  $1/T$  for the formulation contains MCM (D) and 20 % drug obtained with 6 cm Parallel Plate and 1mm gap between  $4^{\circ}\text{C}$  and  $80^{\circ}\text{C}$**

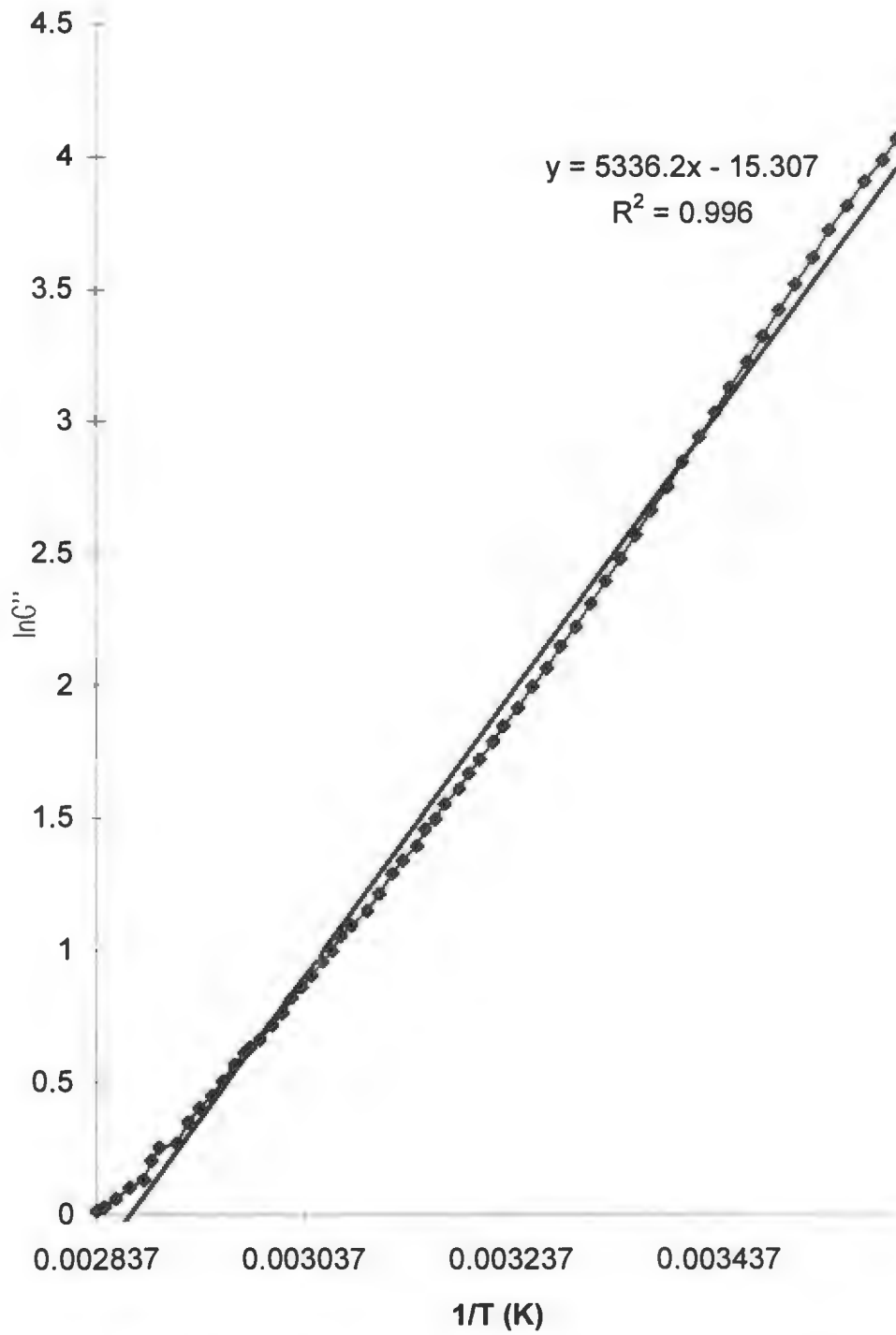


**Figure 18:  $\ln G''$  vs  $1/T$  for the formulation contains MCM and 20 % drug obtained with 6 cm Parallel Plate and 1mm gap between  $4^{\circ}\text{C}$  and  $80^{\circ}\text{C}$**

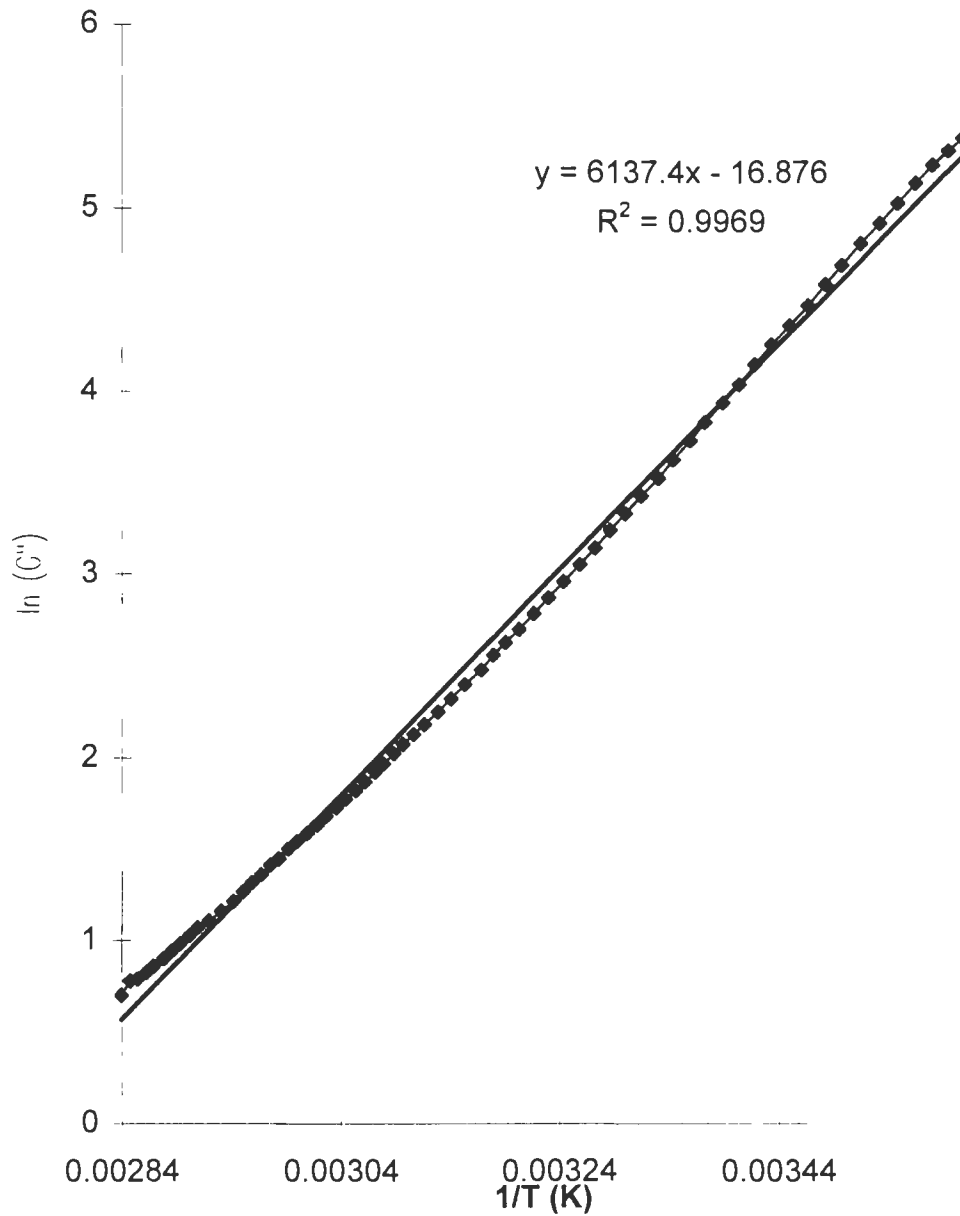


**Figure 19:  $\ln G''$  vs  $1/T$  for the formulation contains 20 % drug, MCM and 3 % PVP K30 obtained with 6 cm Parallel Plate and 1mm gap between 4<sup>0</sup>C and 80<sup>0</sup>C**

## BIBLIOGRAPHY

Beveridge, T., Jones, L., Tung, M.A., Progel and Gel Formation and Reversibility of Whey, Soybean, and Albumen Protein Gels, *Journal of Agricultural and Food Chemistry*, 32, 307-313 (1984)

Boersma, W.H., Laven, J., Stein, H., Viscoelastic Properties of Concentrated Shear Thickening Dispersions, *Journal of Colloid and Interface Science*, 149, 10-22 (1992)

Burley, S.K., Wang, A.H., Votano, J.R., Rich, A., Antigelling and Antisickling Bisphenyl Oligopeptides and Peptide Analogues Have Similar Structural Features, *Biochemistry*, 26, 5091-5099 (1987)

Costantinides, P.P., Scalart, J.P., Formulation and Physical Characterization of Water-in-oil Microemulsions Containing Long- versus Medium Chain Glycerides, *International Journal of Pharmaceutics*, 158, 57-68 (1997)

Costantinides, P.P., Scalart, J.P., Lancaster, C., Marcello, J., Marks, G., Formulation and Intestinal Absorption Enhancement Evaluation of Water -in Oil Microemulsions Incorporating Medium-Chain Glycerides, *Pharmaceutical Research*, 11, 1385-1390 (1994)

Davis, S.S., Is Pharmaceutical Rheology Dead?, *Pharmaceutica Acta Helveticae*, 49, 161-168 (1974)

Doxsee, M.K., Chang, R.C., Chen, E., Crystallization of Solid-State Materials in Nonaqueous Gels, *Journal of American Chemical Society*, 120, 585-586, (1998)

- Engstrom, S., Drug Delivery from Cubic and Other Lipid Water Phases, *Lipid Technology*, 2, 42-45 (1990)
- Fennema, R. O., Food Chemistry, *Principles of Food Science* (3. Edition), Marcel Dekker Inc., New York (1996)
- Ferry, J.D., *Viscoelastic Properties of Polymers*, John Wiley & Sons, Inc., New York (1980)
- Food and Drug Administration, HHS, 21 CFR Ch. I (4-1-96 Edition), 490-491 (1996)
- Fukuoka, E., Makita, M., Nakamura, Y., Glassy State of Pharmaceuticals. IV. Studies on Glassy Pharmaceuticals by Thermomechanical Analysis, *Chemical and Pharmaceutical Bulletin*, 37, 2782-2785 (1989)
- Hamad, N., Robinson, R.R, Power, J.J., Influence of Monoglycerides on Gelling of Canned Beans and Starch Extracted from Beans, *Food Technology*, 226, 124-130 (1965)
- Hancock, B.C., Zografi, G., Molecular Mobility of Amorphous Pharmaceutical Solids Below Their Glass Transition Temperatures, *Pharmaceutical Research*, 11, 471-477 (1994)
- Hancock, B.C., Zografi, G., The Relationship Between the Glass Transition Temperature and the Water Content of Amorphous Pharmaceutical Solids, *Pharmaceutical Research*, 11, 471-477 (1993)
- Hiemenz, PC., Rajagopalan, R., *Principles of Colloid and Surface Chemistry* (3. Edition), Marcel Dekker, New York (1997)



- Izuka, A., Winter, H., Hashimoto, T., Molecular Weight Dependence of Viscoelasticity of Polycaprolactone Critical Gels, *Macromolecules*, 25, 2422-2428 (1992)
- Izuka, A., Winter, H.H., Temperature Dependence of Viscoelasticity of Polycaprolactone Critical Gels, *Macromolecules*, 27, 6883-6888 (1994)
- Kamata, Rector, D., Kinsella, J.E., Influence of Temperature of Measurement on Creep Phenomena in Glycinin Gels, *Journal of Food Science*, 53, 589-591 (1988)
- Kato, A., Ibrahim, H.R., Tagaki, T., Kobayashi, K., Excellent Gelation of Egg White Preheated in the Dry State Is Due to the Decreasing Degree of Aggregation, *Journal of Agricultural and Food Chemistry*, 38, 1868-1872 (1990)
- Ker, Y.C., Toledo, R.T., Influence of Shear Treatments on Consistency and Gelling Properties of Whey Protein Isolate Suspensions, *Journal of Food Science*, 57, 82-90 (1992)
- Koike, A., Nemoto, N., Watanabe, Y., Osaki, K., Dynamic Viscoelasticity and FT-IR Measurements of End-Crosslinking  $\alpha$ ,  $\omega$ -Dihydroxyl Polybutadiene Solutions Near the Gel Point in the Gelation Process, *Polymer Journal*, 28 (11), 942-950 (1996)
- Kuhn, P.R., Foegeding, A.E., Mineral Salts Effects on Whey Protein Gelation, *Journal of Agricultural and Food Chemistry*, 39, 1013-1018 (1991)
- Li, G., Chang, K.C., Viscosity and Gelling Characteristic of Sunflower Pectin As Affected by Chemical and Physical Factors, *Journal of Agricultural and Food Chemistry*, 45, 4785-4789 (1997)
- Maa, Y., Hsu, C., Effect of Shear on Proteins, *Biotechnology and Bioengineering*, 51, 458-465 (1996)

- Martin, A., *Physical Pharmacy*, Lea & Febiger, Malvern, 453-476 (1993)
- MCM Certificate of Analysis, Abitec Cooperation (1998)
- Mehanna, A., Abraham, J.D., Comparison of Crystal and Solution Hemoglobin Binding of Selected Antigelling Agents and Allosteric Modifiers, *Biochemistry*, 29, 3944-3952 (1990)
- Mine, Y., Laser Light Scattering Study on the Heat-Induced Oval Albumin Aggregates Related to Its Gelling Property, *Journal of Agricultural and Food Chemistry*, 44, 2086-2090 (1996)
- Moore, D.J., Mendelsohn, R., Role of Ceramides II and IV In the Structure of the Stratum Corneum Lipid Barrier, 20<sup>th</sup> IFSCC Congress, Cannes, 1998
- Moynihan, C.T., Easteal, J.A., Wilder, J., Tucker, J., Dependence of Glass Transition Temperature on Heating and Cooling Rate, *The Journal of Physical Chemistry*, 78 (26), 2673-2677 (1974)
- Nonaka, M., Li-Chan, E., Nakai, S., Raman Spectroscopic Study of Thermally Induced Gelation Of Whey Proteins, *Journal Of Agricultural And Food Chemistry*, 41, 1176-1181 (1993)
- Pena, E.L., Lee, L.B., Stearns, J.F., Structural Rheology of a Model Ointment, *Pharmaceutical Research*, 11, 875-881 (1994)
- Powel, D., Swrbrick, J., Banker, G.S., Effects of Shear Processing and Thermal Exposure on the Viscosity Stability of Polymer Solutions, *Journal Of Pharmaceutical Sciences*, 55, 601-605 (1966)

Rector, D., Matsudomi, N., Kinsella, J.E., Changes in Gelling Behavior of Whey Protein Isolate and  $\beta$ -Lactoglobulin During Storage: Possible Mechanism(s), *Journal of Food Science*, 56, 782-788 (1991)

Rosen, S.L., *Fundamental Principles of Polymeric Materials*, John Wiley & Sons, Inc., New York (1993)

Schrader, B., *Infrared and Raman Spectroscopy Methods and Applications*, VCH Publishers, New York (1995)

Skoog D.A., Leary, J.J., *Principles of Instrumental Analysis* (4. Edition), Saunders College Publishing, New York (1992)

Sutananta, W., Craig, D.Q.M., Newton, J.M., The Effect of Aging on the Thermal Behavior and Mechanical Properties of Pharmaceutical Glycerides, *International Journal of Pharmaceutics*, 111, 51-62 (1994)

Tang, Q., McCarthy, O.J., Munro, P., Oscillatory Rheological Comparison of the Gelling Characteristics of Egg White, Whey Protein Concentrations, Whey Protein Isolate, and  $\beta$ -Lactoglobulin, *Journal of Agricultural and Food Chemistry*, 42, 2126-2130 (1994)

Tang, Q., McCarthy, O.J., Munro, P., Oscillatory Rheological Study of the Effects of pH and Salts on Gel Development in Heated Protein Concentrated Solutions, *Journal of Dairy Research*, 62, 469-477 (1995)

Tang, Q., McCarthy, O.J., Munro, P.A., Oscillatory Rheological Study of the Gelation Mechanism of Whey Protein Concentrate Solutions: Effect of Physicochemical Variables on Gel Formation, *Journal of Dairy Research*, 60, 543-555 (1993)

Tano, T., Umemure, J., Gel to Liquid Crystalline Phase Transition of Black Lipid Films in Air as Studied by FT-IR Spectroscopy, *Chemistry Letters*, 801-802 (1996)

*USP 23 NF18*, United States Pharmacopeial Convention, Rockville, 1840-1843 (1994)

Westesen, K., Siekmann, B., Investigation of the Gel Formation of Phospholipid-Stabilized Solid Lipid Nanoparticles, *International Journal of Pharmaceutics*, 151, 35-45 (1997)